CRANFIELD INSTITUTE OF TECHNOLOGY

COLLEGE OF AERONAUTICS

AIRCRAFT DESIGN DIVISION

Ph.D Thesis

Academic Year 1985 - 86

R. I. WATKINS

Multilevel Optimum Design of Large Laminated composite structures

Supervisor: Prof. A. J. Morris

August 1986

97

SUMMARY

A general method for the optimal design of large laminated composite structures, that allows full design variable (ply thickness and orientation) freedom, has been developed. The number of variables and constraints, and hence the problem size, being dealt with at any given moment in the optimization process is kept within reasonable bounds by using a multilevel optimization scheme.

The optimization process is split into a system level and an element level. At the system level the entire structure is considered and the individual laminae thicknesses (not ply angles) are sized so as to minimize the total structural weight within the constraints placed on the system. These constraints can include strain, displacement, buckling and gauge limits. Once the design has converged at this level the optimization process then switches to the element level. The objective function at the element level combines a weight function and a strain energy change function into a utility function which is minimized and in which the relative importance of each part is reflected by weighting coefficients. Minimizing the change in strain energy ensures load path continuity when switching between the two levels of optimization, and so decouples the problems at the two levels. Continuous lamina thickness and ply-angle variation is used to minimize the element level objective function while satisfying strain, buckling and gauge

constraints. In this way optimum use is made of the material in each element, without changing the the load paths in the overall structure and thereby ensuring that the constraints at the system level are still satisfied. The procedure switches between the two levels until overall convergence has been achieved.

Structures representative of straight, forward swept and delta wings are used to illustrate the effectiveness of the system and to show that the optimal designs produced are feasible and realistic, and compare favourably with designs obtained by more conventional and intuitive methods.

ACKNOWLEDGEMENT

I am most grateful to the National Institute for Aeronautics and Systems Technology in South Africa for their sponsorship and support during this work, and for providing me with the opportunity to futher my studies and broaden my knowledge.

I wish to express my gratitude to my supervisor, Prof. Alan Morris, for the valuable advice, guidance and encouragement given to me throughout the course of this Doctoral research programme.

My thanks are also due to Dr. Les Oswald, the computer manager at the College of Aeronautics, for so willingly providing me with advice and assistance in the development of the software associated with this thesis.

My special thanks are due to my wife Sally, whose love, care and unwavering support have made possible the fruition of this work - and to my doting daughter Andrea, for providing the joys of life.

Finally I thank my parents and relatives whose continued support and good wishes have been a great source of inspiration and encouragement.

CONTENTS

LIST OF FIGURES

NOTATION

a - constant or plate length.

A - membrane terms in the laminate rigidity matrix

b - constant or plate width

B - strain/displacement matrix

B - coupling terms in laminate rigidity matrix

c - functions or constants

C - variable

D - bending terms in the laminate rigidity matrix

E - elastic (Young's) modulus

f - function or function value

F - force

g - constraint function at element level

G - shear modulus or constraint function at system level

k - element stiffness matrix

K - global stiffness matrix

L - number of lamina/layers

m - number of half wave lengths of buckle

M - a 3x5 matrix defined in Appendix C

n - number of half wave lengths of buckle

N - number of deformation modes of the plate

N - number of load cases

P - load vector

q - objective function weighting coefficients, or if in matrix form then the lamina stress-strain relations

Q - transformed lamina stress-strain relations

$\bar{Q}$ - reduced stiffness properties of lamina

r - matrices of lamina invariant properties

R - laminate rigidity matrix (A,B,D)

t - lamina/layer thickness

T - strain transformation matrix

u - deflection in the x-direction

U - lamina invariant properties or strain energy

v - deflection in the y-direction

V - strain energy

w - element/component weight

w - deflections in z-direction

W - total weight of the structure, or work done

x - variables

z - distance from plate midsurface to the lamina centroid

Greek symbols

γ - shear strain

δ - deflections/deflection vector

Δ - change (of parameter)

ε - strain

θ - lamina/ply layup angle

κ - plate midsurface curvature

ν - Poisson's ratio

ρ - material density

σ - direct stress

τ - shear stress

Φ - a 5xL matrix - function of ply angles

Superscripts

L - lower bound

T - transpose of a matrix

U - upper bound

° - optimum value, or midsurface values when applied to plate strains

′ - reduced set, or transformed axis set

Subscripts

a - linearization point in element optimization

crit- critical buckling load

j - lamina/layer number

l - lamina (generally used in strain expressions)

L - longitudinal direction (of the fibres)

m - number of half wave lengths of buckle

n - number of half wave lengths of buckle

pl - plate (generally used in strain expressions)

T - transverse direction (of the fibres)

x - x-direction

xy - x-y plane

y - y-direction

z - z-direction

CHAPTER 1

1 INTRODUCTION

1.1 Rationale

The use of composite materials, and in particular fibre reinforced plastics, is expanding rapidly in the aircraft industry and the last decade has seen the range of applications of these materials expand from mere aircraft trimmings and fittings to secondary structure such as cabin floors, flaps and rudders, and even primary structure eg. the Harrier GR5 wing.

The advantages of these materials when compared to aluminium or titanium, are numerous, but those traditionally highlighted are:-

a) the potential reductions in structural weight (see figure 1.1) due to their high specific strength (figure 1.2) and excellent fatigue properties (figure 1.3) and,

b) the potential for reductions in the production and life cycle costs, primarily due to the reduced number of parts and fasteners required (figure 1.1) so needing less less labour, and the improved fatigue life leading to fewer inspection and maintainance requirements.

	Aileron structure		Vertical fin structure	
	Aluminium	Composite	Aluminium	Composite
Weight (lbs)	139.9	107.4	858	642
% Composite weight	5.8	61.9	0	76
Weight saved (lbs)	-	32.5	-	216
% Weight saved	-	23.2	-	25.2
No. of parts (excl. fastners)	398	205	716	201

Figure 1.1 Alumnium and composite structure comparison

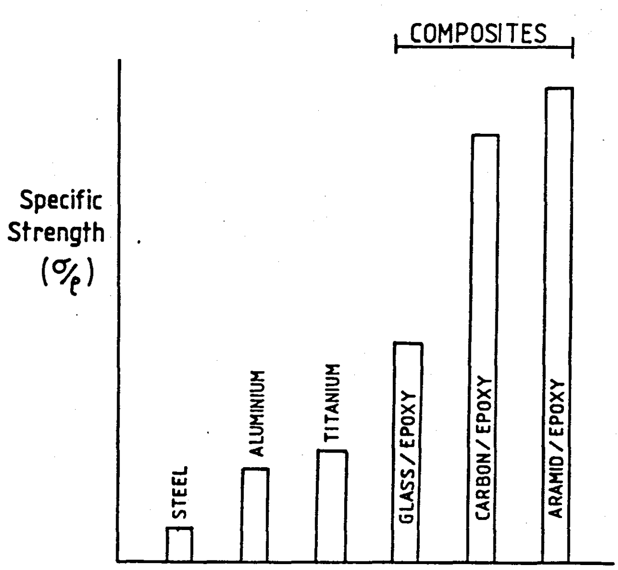

Figure 1.2 Material specific strength

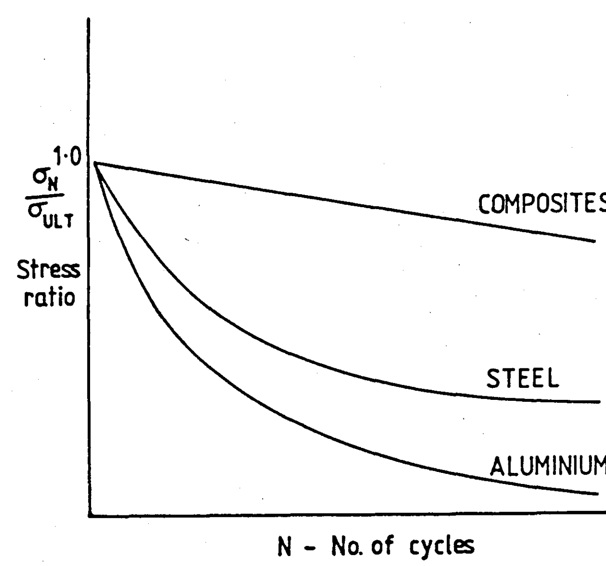

Figure 1.3 Relative fatigue strength

Another potentially major advantage of composite materials is the ability to "tailor" the laminated material in such a way that certain desired structural behaviour can be induced i.e. the designer has the power to "design" the material, as well as the structure.

This additional design flexibility that these materials allow, stems from the highly directional properties of the fibres (typically glass, carbon or aramid types). Simply by laying fibres at various prescribed angles and sequences, a material (laminate) can be built that has certain desired strengths and stiffnesses in specfic directions. Suitable manipulation of these properties can lead to the design of plates which behave quite differently to isotropic (eg. aluminium) plates eg. a plate can be made to bend or twist when loaded in tension.

The analysis of the interaction of these layers of fibres (lamina) and their effect on the overall stuctural behaviour is, however, a very complex and tedious process. Furthermore, many of the common design constraints such as stress and strain limits are highly non-linear functions of the design variables (lamina thickness and fibre orientation (ply angle)). As a result there are no simple formulae for proper sizing of laminates and design intuition cannot be considered a reliable guide in these circumstances. This has, in the past, limited designers to using relatively simple fibre layups whose behavior is easily understood and so in many cases the full potential of these materials has not been realized.

The use of modern mathematical optimization techniques combined with some composite structural analysis method, in a computer based design system is an attractive solution to the problem. Non-linear optimization techniques have advanced a great deal over the last 20 years and can now provide a sound, reliable basis for laminate sizing. Modern computers also have the powerful processing capability required to analyse large laminated composite structures and the interaction of their elements and laminae.

1.2 Literature Survey

The potential for applying optimization techniques to the design of composite structures has not escaped the attention of other researchers. Numerous publications on various aspects of optimum composite structures have appeared since the late 1960's. The early papers on this subject essentially reported on the feasiblity of the concept (Ref. [2], [3]) and it was not until after 1973, when Khot et al. (Ref. [4]) and Schmit and Farshi (Ref. [5]) published their work, that research in this field became more widespread.

The work by Khot and Schmit showed that optimization techniques could be used successfully in the design of realistic optimum composite structures. Their papers, interestingly, reported on two different aspects of optimum composite design, with Khot describing design methods for large structures using the finite element method of analysis, while Schmit's work concentrated on the optimum design of individual panels. Practically all the subsequent literature on optimum composite design can readily be classified as dealing with either one of these aspects and are catergorized accordingly in this survey. The two catergories are discussed separately.

A selected list of some of the work published on the optimum design of individual composite structural elements or components is given in the references (Refs. [6]-[16]). The comparatively large number of published works that falls into this catergory, can probably be attributed to the fact that the problem size dealt with here is, generally, significantly smaller (in terms of the number of desgn variables) than that dealing with multi-element structures. These problems can thus often be solved using only desktop computers eg Refs. [6] and [7], or even if a large computer has to be used, only a limited memory size and storage capacity is required.

Much of the work presented in this catergory is very similar in nature (minimum weight design of symmetric laminated panels) and only really differs in detail and in the solution method chosen. Massard (Ref. [6]) describes a method that includes strength constraints, bending and inplane loads, and that varies the number of layers and ply angles (within a prescribed set) to achieve an optimum.

Flanagan (Ref. [7]) gives a method using a derived gradient technique to size a laminate subject to inplane loads only, varying either the ply ratios or ply angles, while Park (Ref. [8]) varies the ply thickness and angle to design minimum weight panels subject to inplane loads and strength and stiffness constraints. Buckling constraints (as well as strength and stiffness constraints) are included in Schmit and Farshi's work (Ref. [9]), setting it slightly apart from the former 3 papers. They use the method of inscribed hyperspheres to ensure that feasible designs are acheived after each design iteration but limit the work to considering only inplane loading, and vary only the lamina thickness (ply angles remain fixed) when sizing a laminated panel.

Tauchert and Adibhatla have investigated different types of optimum composite panels and have derived methods for designing symmetric laminated plates for maximum stiffness (Ref. [10]) and bending strength (Ref. [11]), by varying the lamina thicknesses and ply angles using a quasi-Newton method. The weight of the panel was not taken into consideration but an upper limit was placed on the total plate thickness.

The work published by Stroud et al. (Refs. [12]-[13]) on minimum weight design of composite panels under combined loads was the ground work that lead to the computer program PASCO. This (publically available) program is intended for use on uniaxially stiffened composite panels subjected to combined inplane loads. Non-linear mathematical programming techniques (method of feasible directions) are used to acheive an optimum design by varying the lamina thickness and ply-angle and stiffener spacing, width and depth.

Work on other aspects of optimum composite panel design has been published by McKeown (Ref. [14]) who established an upper bound on the number of layers in optimal (plane-stress) composite sheets, and Adali who developed techniques for design sensitivity analysis (Ref. [15]) and multi-objective (minimizing the dynamic deflection and maximizing the natural frequencies) design methods (Ref. [16]) for antisymmetric angle-ply laminates.

Published literature indicates that only a small number of structural synthesis systems for large multi-element laminated composite structures have been developed in the past. One of the few of these that is publically available in documented form is the program OPTCOMP developed by Khot (Ref. [17]). The program is based on an optimality criterion method which assumes that the strain energy density is equal for all ply groups as the laminate approaches minimum thickness (i.e. minimum weight). An iterative redesign procedure for adjusting the number of plies is derived from this optimality condition. The ply thicknesses and angles remain fixed. The program includes approximate buckling constraints and uses a finite element code to reanalyse the structure at each iteration and update the stress state.

The above report (and program) was preceeded by a number of papers by Khot and his colleagues in which the basic theory (with stress and displacement constraints) was developed (Ref. [18]) and twist constraints for aeroelastic tailoring of wings were included (Ref. [19]). This work was all based on the philosophy of using the number of plies (of prescibed thicknesses and angles) as the design variables rather than altering the actual ply thickness or angle.

McKeown was also active in this field in the mid 1970's and published two papers (Refs. [20]-[21]) describing a novel approach to the optimum composite design problem. He proposed reformulating the problem into one in which the primary variables were the nodal deflections of the finite element model. This leads to a multilevel problem (or "inner and outer subproblems") which he shows to be a convenient approach to solving the non-linear mixed integer problem involved, and allows the optimal number of layers, layer thickness and ply angles to be determined simultaneously. The usefulness of the method is, however, somewhat restricted by the need to express all the constraints in terms of the nodal deflections, which may lead to very complex and computationally inefficient (and possibly unreliable) expressions for some constraints.

Starnes and Haftka (Ref. [22]) modified an existing structural optimization program (WIDOWAC - by the same authors) to include composites. The design variables considered were lamina thicknesses (at fixed angles) and penalty functions were used to introduce the strength, displacement, twist, buckling and gauge constraints, with the search algorithm being a Newton method. Their work included interesting comparisons of the optimum designs acheived in composites and aluminium.

A computational procedure for sizing composite airframe structures developed by NASA in the late 1970's is descibed by Sobieski (Ref. [23]). The procedure includes a finite element analysis and mathematical optimization technique and allows the variation of the layer thicknesses and ply angles so as to satisfy stress and deflection constraints, while optimizing individual elements. The method described apparently allows great flexibility in terms of the design variables, material selection, combinations and construction, but since individual panels are optimized separately, the resulting design will only be near, but not generally at, the minimum total mass design.

The results of an interesting multilevel approach to the optimum composite design problem were presented by Schmit and Mehrinfar (Ref. [24]). They demonstrated stable convergence of the procedure when applying it to the design of composite wing box structures that were subject to strength, deflection and both panel and local buckling constraints. A key feature of the method was the selection of the change of stiffness (rather than weight) as the element (or lower) level objective function to be minimized. The potential versatility of the method was, however, restricted by allowing only the lamina thicknesses to vary while the ply angles remained fixed.

Finally, a paper by Stroud (Ref. [25]) illustrates some of the potential problems associated with optimized structures. He emphasizes the sensitivity of optimized composite structures to off-design conditions and imperfections and the resulting need to ensure that absolutely all load cases are considered in the design process.

1.3 Objective Of This Work

The aim of this work can broadly be defined as the development of a structural synthesis system for laminated composite structures that will ensure the most efficient use of material in the structure, within the bounds prescibed by the designer. The most efficient use of material essentially implies a design that uses a minimum volume or weight of material to perform a given function.

This system is to act as a tool for the design engineer, performing all the tedious, complex and repetitive calculations required to produce an optimum structural design. It is to be an effective and versatile design tool free of the various limitations imposed on structural complexity or design variables that have restricted the usefulness of previously published work (see section 1.2).

1.4 Scope And Presentation Of This Work

In order to make the most efficient use of the special properties of composite materials, full design variable freedom (for thickness and ply angle variation) must be allowed in the design/optimization procedure. This can, however, rapidly lead to an unweildly problem with an inordinately large number of variables as the number of elements in the finite element model increases. In the past many researches (see section 1.2) have limited the problem size by working with fixed ply angles and allowing only the laminae thicknesses to vary. Design variable linking has also been used to limit the number of variables by ensuring symmetry of the laminates and by defining certain elements (in the finite element model) as being of the same laminate type.

In this work, however, a general method for optimal design of composite structures is developed that does allow full variable (thickness and ply angle) freedom, and includes design variable linking and the ability to keep ply angles and/or thicknesses fixed as an design option rather than a limitation. This is achieved, while keeping the problem being dealt with at any given moment in the optimization process a feasible size, by using a multilevel optimization scheme.

The optimization process is split into a system (or upper) level and an element (or lower) level. At the system level the entire structure is considered and the individual laminae thicknesses (not ply angles) are sized so as to minimize the total structural weight within the constraints placed on the system. These constraints can include strain, displacement, buckling and minimum gauge limits. Once the design has converged at this level the optimization process then switches to the element level. At the element level full design variable freedom is allowed such that the weight of the individual element may be minimized. In order to decouple the problems at the two levels, and to maintain the stiffness distribution (and hence the load paths, displacements, etc.) established in the system level optimization, the stiffness change of the individual elements is kept to a minimum while carrying out the element level optimization. This is achieved by setting up a multi-criteria objective function in which both element weight and stiffness change are minimized. In this way optimum use is made of the material in each element, without changing the load paths in the overall structure and thereby ensuring that the constraints at the system level are still satisfied. The procedure switches between the two levels until overall convergence has been achieved.

The results obtained using this multilevel optimization scheme were very satisfactory and demonstrated both the viability and effectiveness of the method. Structures representative of straight, forward swept and delta wings were used as test examples and were optimized using full design variable freedom (ply thickness and angle) to satisfy strain, buckling and displacement constraints. The final designs produced were all feasible and realistic, comparing very favourably with designs obtained by more conventional and intuitive methods. Convergence of the overall procedure was generally obtained after 4 to 5 iterations of the overall (ie. both levels) optimization procedure.

The concept and philosophy of applying a multilevel optimization system to the problem of optimal design of laminated composite structures has been shown, in this work, to work well and to warrant futher development work to fully exploit its potential. To this end recommendations for futher development and enhancement of the basic system have been made.

The development of the theory, the methods employed in the cuurent work and the results obtained are addressed in detail in the subsequent chapters. In chapter 2 futher motivation for the use of a multilevel optimization scheme is given, together with a detailed description of the problem formulation. Chapters 3, 4 and 5 concentrate on aspects of the element level optimization, starting with the description of the objective function and constraints at that level (chapter 3), and going on to an explanation of the optimization algorithm chosen (a sequential LP method) and the ways of linearizing the constraint and objective functions (chapter 4). This is followed by some examples illustrating the effectiveness of the element optimization scheme in chapter 5. In chapters 6, 7 and 8 the same topics are covered as in chapters 3, 4 and 5 respectively, but for the system level optimization scheme. Chapter 9 contains a discussion of the results of the overall multilevel scheme, and is followed by the conclusions drawn from this work as well as suggestions for future research and development work in this line, in chapter 10.

The appendices contain much of the material and information that forms the theoretical and mathematical base for this work, but which would not have been relevant to include in the main body of the text. The appendices dealing with theory (A - D) are followed by one (E) describing some of the problems encountered with the computer implemetation of the theory presented in the following chapters, and then there are two appendices (F and G) giving brief descriptions of the programs developed for the element and system level optimization processes.

CHAPTER 2

2 PROBLEM FORMULATION

The methods commonly used in structural optimization cannot be easily or readily applied to the optimum composites design problem. The primary reasons for this are the inordinately large number of design variables (and related constraints) associated with laminated composite structures, and the high degree of interdependence of these variables. This leads to problems that are generally too large to deal with realistically on existing computers, and that may also tend to be unstable i.e. the optimization scheme may not converge.

In order to overcome these obstacles an approach needs to be adopted where the number of design variables under consideration at any point should be kept as low as posssible. Futhermore to avoid the potential convergence problem, full design variable freedom should only be allowed when optimizing small substructures which are well defined in terms of constraints and loading.

The use of multi-level optimization is particularly suitable in this case as it can be used to satisfy both of the above requirements. In this work the upper level (or system level) of optimization is performed considering the entire structure and using only the layer thicknesses of the laminated structural components as the design variables i.e. the ply angles and the number of layers is kept fixed. The number of design variables can be further limited by defining an upper bound of 6 on the number of layers at the optimum (see Appendix C for the derivation thereof). The maximum number of design variables at the upper optimization level is then 6xN (where N is the number of structural elements) and the problem size, although large, is thus still in the same order of magnitude as the more common, isotropic material, structural optimization problems.

The lower level (or element level) of optimzation considers only individual elements where the major constraint is that the change of stiffness of the element should be kept to a minimum as weight is reduced. This ensures that the stiffness, and hence the load paths, in the overall structure do not change substantially, so preserving the continuity when switching back to the upper level of optimization. The system and element level problems are effectively decoupled in this manner, and the loads in any given element can thus be assumed to remain the same irrespective of the change in the design variables during the lower level of optimization. This constraint together with strain, buckling and gauge constraints leads to a well defined problem at the element level and so full freedom of the design variables (layer thickness and ply angle) can be allowed. The maximum number of variables at this level is always likely to be small as there are only two variables per layer. The number of variables at this level can obviously limited to 12, if 6 is used as the upper bound on the number of layers at the optimum.

The multilevel approach is also attractive in terms of dealing with buckling constraints. The inclusion of local buckling constraints in addition to the usual strain, stiffness and gauge limits presents difficulties in regular optimization methods because their meaningful representation requires that consideration be given to the detail design of the many individual components which make up the structural system. This problem is avoided by dealing with the higher modes of panel buckling at the element level optimization, where closed form solutions can be effectively used, and with panel buckling constraints at the system level, where rigorous solutions may have to used for areas of complex structural geometry.

The multilevel concept therefore appears to be a sound basic approach to the optimum design of laminated composite structures, especially if the constraints include buckling, strength and stiffness limits.

A schematic description of the multilevel approach adopted in this work is given in figure 2.1 where t_i and θ_i represent the thickness and ply orientations respectively. The formulation employed here represents an intuitive decomposition of the primary problem statement into a system design problem and a set of uncoupled element level problems. Results are obtained by iterating between system and element level problems.

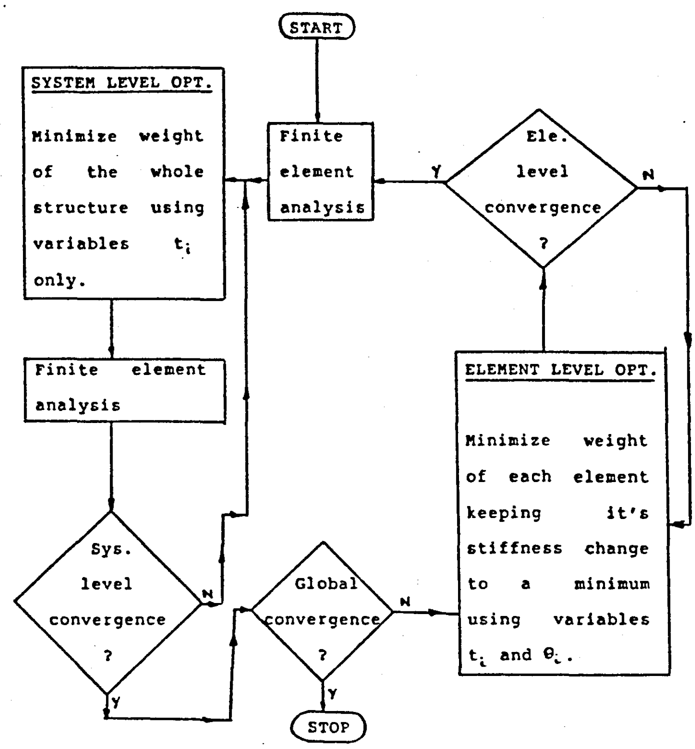

Figure 2.1 Multilevel design logic

Expressed more formally, the composite structure optimization problem can be written in general terms as:-

$$\min \; W(t)$$

subject to:- i) $c(\theta,t) \leq 0$

ii) $\theta^L \leq \theta \leq \theta^u$

iii) $t^L \leq t \leq t^u$

where

$W(t)$	is the total structural weight (proportional to variable t)
$c(\theta,t)$	are the constraints (dependent on the variables and t)
θ,t	are the ply angle and thickness variables respectively, associated with each lamina
L,U	superscripts indicating the lower and upper bounds respectively

When expressed in the multilevel optimization way used in this work, it can be written as:-

System level:

Find t such that

$$\min W(t)$$

subject to:- i) $G(t) \leqslant 0$

ii) $t^L \leqslant t \leqslant t^U$

and

Element level:

Find θ and t such that

$$\min w(t)$$

subject to:- i) $\Delta k \rightarrow 0$

ii) $g(\theta,t) \leqslant 0$

iii) $\theta^L \leqslant \theta \leqslant \theta^U$

iv) $t^L \leqslant t \leqslant t^U$

where

$G(t)$ are constraints applicable at system level

(t is the only variable)

$g(\theta, t)$ are constraints applicable at element level

(θ and t are variables)

Δk is the stiffness change of the element

$w(t)$ is the element weight

The other symbols are the same as in primary problem statement.

CHAPTER 3

3 ELEMENT LEVEL OPTIMIZATION

3.1 Objective Function At Element Level

In order to obtain stable convergence of the overall design procedure, the behaviour of the structure, and the resultant load paths within it, should not be altered significantly when switching from one optimization level to another. This can be achieved by requiring that the stiffness change at the element level optimization be kept to a minimum.

The stiffness change of the element can thus be used as a constraint (with relatively tight move limits) at the lower level of optimization or alternatively can be used as the objective function to be minimized. The latter method has been used very succesfully in Refs. [24] and [26].

The use of stiffness change alone, however, as the objective function will not generally be sufficient to drive the design to an optimum. This is particularly well illustrated in the case where the element satisfies all the constraints (buckling and strain), as there is then no incentive to change the design (and so reduce the volume of material), since the stiffness change will then be zero i.e. a minimum. Stiffness change and weight should thus be combined in a multi-objective function that is to be minimized. The inclusion of weight as a part of the objective function ensures that both layer thicknesses and layup angles wil be used such that a design will be obtained that achieves a good compromise of minimized weight and stiffness change, while satisfying all the constraints.

The various multi-objective optimization methods that have been developed over the years are described in Refs. [27],[28] and [29] in detail. Many of these methods require the user to have some knowledge of the constrained optimum values of each objective function individually, and use these values in the optimization process. In this design problem, however, it is not known what the optimum element weight will be. The basic, weighted objectives method of combining objective functions, descirbed in Ref. [27], is an extension of the utility function techniques and does not require information on the individual optima, and is thus chosen for this work. The method is briefly described below.

The basis of the weighted objectives method consists of adding all the objective functions together using different weighting coefficients for each. The multi-objective optimization problem is thereby transformed to a scalar optimization problem by creating one function of the form

$$f(x) = \sum_{i=1}^{k} q_i f_i(x) \qquad (3.1.1)$$

where $f_i(x)$ are the original objective functions

x are the variables

q_i are the weighting coefficients representing the relative importance of the criteria (q 0)

It is usually assumed that $\sum_{i=1}^{k} q_i = 1$. Note that the weighting coefficients do not reflect proportionally the relative importance of the objectives but are only factors, which when varied, would locate different points in the design space.

The location of these points depends not only on the values of q_i but also on the units in which the functions are expressed. The q_i can, however, be made to reflect closely the importance of the objective functions if all the functions are expressed in units of approximately the same numerical values. Thus eqn. (3.1.1) can be changed to the form

$$f(x) = \sum_{i=1}^{k} q_i f_i(x) c_i \qquad (3.1.2)$$

where

c_i are constant multipliers.

According to Ref. [27] the best results are usually obtained if $c_i = 1/f_i^o$, where f_i^o is the ideal optimum of the objective function f_i within the bounds of the prescribed constraints.

Now in the element level optimization $f_i^o = 0$ for the stiffness change part of the objective function. This leads to $c_i = \infty$ which is obviously not acceptable, since the solution would then be totally dominated by this part of the multi-objective function. Furthermore, the calculation of the f_i^o value for the weight function involves a complete optimzation scheme in its own right and the additional computational effort required for this does not seem justified.

These problems are overcome in this work by assuming the f_i^o value for the weight function is merely the element weight obtained in the system level optimization iteration immediately prior to the element level optimization, while the f_i^o value for the stiffness change function is taken to be the element stiffness upon entry into the element level optimization. Experience has shown these to be suitable values in that they allow the weighting coefficients q to represent proportionately the relative importance of the various parts of the objective function when varied in the range 0 to 1.

The total objective function thus has the form

$$f(x) = q_1 f_1(x)/W + q_2 f_2(x)/\Delta k \qquad (3.1.3)$$

where W and Δk are the f_i^o values for the weight and stiffness change as described above. This form of eqn. (3.1.2) ensures that the separate objective functions are dimensionless and will have similar numerical values and thus neither should dominate the solution, unless vastly differing weighting coefficients are assigned to the two parts.

3.2 Constraints At The Element Level

The constraints to be considered at the element level of optimization are buckling (to be prevented), strain (with upper (tension) and lower (compression) bounds), minimum lamina thickness and bounds on the layup angles. These can, respectively, be written as:-

Buckling:-

$$(F_X)_{crit}/F_X \geq 1/C_1$$
$$(F_Y)_{crit}/F_Y \geq 1/C_2 \qquad (3.2.1)$$
$$(F_{XY})_{crit}/F_{XY} \geq 1/C_3$$

where $F_X + F_Y + F_{XY} = F_{TOT}$

and $F_X/F_{TOT} = C_1$; $F_Y/F_{TOT} = C_2$; $F_{XY}/F_{TOT} = C_3$

Strain:- (per layer)

$$\varepsilon_L^L \leq \varepsilon_L \leq \varepsilon_L^u$$
$$\varepsilon_T^L \leq \varepsilon_T \leq \varepsilon_T^u \qquad (3.2.2)$$
$$\varepsilon_{LT}^L \leq \varepsilon_{LT} \leq \varepsilon_{LT}^u$$

Thickness:-

$$t^L \leq t \leq t^u \qquad (3.2.3)$$

Angle:-

$$\theta^L \leq \theta \leq \theta^u \qquad (3.2.4)$$

Note that the constraints (3.2.1) applies to the element as a whole whereas the constraints (3.2.2) - (3.2.4) are applicable to the individual lamina in the element.

The variables F_x, F_y and F_{xy} in the buckling constraint equations are the forces in the x, y and shear directions respectively, and the subscipt "crit" denotes the buckling load in that direction. The constraints are here written in a way which approximates very closely the well known form of the buckling constraint equation

$$F_x/(F_x)_{crit} + F_y/(F_y)_{crit} + (F_{xy}/(F_{xy})_{crit})^2 \leq 1 \qquad (3.2.5)$$

Eqn. (3.2.5) can be written in the form

$$\alpha + \beta + \gamma \leq 1 \qquad (3.2.6)$$

where α, β and γ can take on any value as long as the inequality is satisfied. If it is specified that $\alpha = C_1$, $\beta = C_2$ and $\gamma = C_3$ (which is the same as the buckling constraint eqns. (3.2.1)) the inequality (3.2.6) is still satisfied since by eqns. (3.2.1) $C_1 + C_2 + C_3 = 1$. The constraint eqns. (3.2.1) thus satisfy the generalized buckling constraint eqn. (3.2.5) but impose the additional individual limits on $F_x/(F_x)_{crit}$, $F_y/(F_y)_{crit}$ and $F_{xy}/(F_{xy})_{crit}$.

The advantage of writing the buckling constraints in the form of eqns. (3.2.1) as opposed to eqn. (3.2.5) is that the design variables (which occur in the "crit" terms) may be dealt with directly rather than the inverse design variables and so helps to simplify the optimization algorithm. It should be noted, however, that this form of the buckling constraint can be extremely conservative. (Experience with using this form has shown that in the interest of a more optimal solution it would probably be better to use eqn. (3.2.5) despite the extra mathematical complexity).

The derivation of the formulae for calculating the buckling loads is given in section 3.2.1.

The strain constraints used are the lamina strains in the longitudinal (ε_L), transverse (ε_T) and shear (ε_{LT}) directions. (The method for transformation of the element strains into lamina strains is given in section 3.2.3.) The superscripts L and U indicate the lower and upper bounds applicable, with the same notation being applied to the thickness (t) and ply-angle (θ) limits. The maximum strain criteria is used in preference to the Tsai-Hill failure criteria say, because:- (i) of the more direct relation between its strain components and the design variables (thereby probably making the convergence more stable and providing more understandable sensitivity information if required), and (ii) experienced composite designers regularly use strain limits in practice and thus have grown accustomed to them.

A further possible "constraint" is the application of an upper limit of 6 on the number of lamina per element. The reason for this is that 6 is the established upper bound for the number of layers in an optimum design laminate. Setting the upper bound on the number of lamina also has very distinct computational advantages in that the total problem size is then well contained and can be predetermined. It, futhermore, then helps to avoid the complexity of the integer programming problems associated with having a variable number of lamina. The derivation of this bound is given in Appendix C. It may be argued that this low limit does not allow for the incremental type stacking frequently used by designers to limit interlaminar shear and edge stresses. The detail analysis of these effects is, however, very complex and cannot therefore realistically be included in a design optimization package of the type descibed here. If these effects are of concern to the designer, the optimization package can still be used to produce a fundamentally sound design which can then be refined to suit the specfic requirements.

3.2.1 <u>Calculation Of The Buckling Loads For Composite Plates</u>

The derivation of buckling loads for a specially orthotropic laminate (see Appendix A for definition thereof) is relatively straightforward and can be found in most texts on the subject. In this section, however, only the condition of symmetry about the midplane is imposed i.e. there need not necessarily be a lamina at $-\theta$ for each lamina at $+\theta$. This implies that there may be coupling between direct and shear in-plane loads and between bending and twisting moments, but there is no coupling between in-plane loads and bending/twisting moments.

A completely unbalanced, unsymmetric layup does generally imply coupling between in-plane loads and moments i.e. a plate would bend under any in-plane loading. This added complexity normally precludes the use of closed form solutions for the buckling analysis, and an eigen solution has to be done. This type of layup is, however, very seldom used in practice as it can lead to major design and manufacturing problems such as high residual stresses and warping, due to the thermal expansion and contraction of the lamina induced by the curing process. The buckling analysis of these layups is therefore not considered in this work.

Now from Ref. [30], the strain energy of an anisotropic plate due to bending (with no midsurface extensions) is

$$V_{SE} = 0.5\iint[D_{11}(\partial^2 w/\partial x^2)^2 + 2D_{12}(\partial^2 w/\partial x^2)(\partial^2 w/\partial y^2) + D_{22}(\partial^2 w/\partial y^2)^2 + 4D_{33}(\partial^2 w/\partial x\partial y)^2 + 4(D_{13}(\partial^2 w/\partial x^2) + D_{23}(\partial^2 w/\partial y^2))(\partial^2 w/\partial x\partial y)]dxdy \quad (3.2.1.1)$$

where $D_{11}, D_{12}, \ldots, D_{33}$ represent the bending stiffness components of the plate (as derived in Appendix A).

If the plate is assumed to be simply supported on all the edges a deflection function of the following form can be used:-

$$w = \sum_{m=1}^{\infty} \sum_{n=1}^{\infty} a_{mn} \sin \frac{m\pi x}{a} \sin \frac{n\pi y}{b} \qquad (3.2.1.2)$$

Thus

$$\begin{aligned}
\partial w/\partial x &= \sum_m \sum_n a_{mn} (m\pi/a) \cos(m\pi x/a) \sin(n\pi y/b) \\
\partial w/\partial y &= \sum_m \sum_n a_{mn} (n\pi/b) \sin(m\pi x/a) \cos(n\pi y/b) \\
\partial^2 w/\partial x &= -\sum_m \sum_n a_{mn} (m\pi/a) \sin(m\pi x/a) \sin(n\pi y/b) \qquad (3.2.1.3) \\
\partial^2 w/\partial y &= -\sum_m \sum_n a_{mn} (n\pi/b) \sin(m\pi x/a) \sin(n\pi y/b) \\
\partial^2 w/\partial x \partial y &= \sum_m \sum_n a_{mn} (nm\pi^2/ab) \cos(m\pi x/a) \cos(n\pi y/b)
\end{aligned}$$

Substituting eqns. (3.2.1.3) into eqn. (3.2.1.1) then gives, for a plate of length a and width b,

$$\begin{aligned}
V_{SE} = 0.5 \int_0^b \int_0^a [& D_{11} \left(\sum_m \sum_n a_{mn} (m\pi/a)^2 \sin(m\pi x/a) \sin(n\pi y/b)\right)^2 + \\
& 2D_{11} \left(\sum_m \sum_n a_{mn} (nm\pi^2/ab) \sin(m\pi x/a) \sin(n\pi y/b)\right)^2 + \\
& D_{22} \left(\sum_m \sum_n a_{mn} (n\pi/b)^2 \sin(m\pi x/a) \sin(n\pi y/b)\right)^2 + \\
& 4D_{33} \left(\sum_m \sum_n a_{mn} (nm\pi^2/ab) \cos(m\pi x/a) \cos(n\pi y/b)\right)^2 - \\
& 4(D_{13} \left(\sum_m \sum_n a_{mn} (m\pi/a)^2 \sin(m\pi x/a) \sin(n\pi y/b)\right) + \\
& D_{23} \left(\sum_m \sum_n a_{mn} (n\pi/b)^2 \sin(m\pi x/a) \sin(n\pi y/b)\right)) \\
& \left(\sum_m \sum_n a_{mn} (nm\pi^2/ab) \cos(m\pi x/a) \cos(n\pi y/b)\right)] dxdy
\end{aligned}$$

Intergrating this with respect to x and evaluating it over the limits 0 to a gives,

$$
\begin{aligned}
V_{SE} = 0.5 \int_0^b [& \sum_m \sum_n a_{mn}^2 (m\pi/a)^4 (a/2)\sin^2(n\pi y/b)) + \\
& 2D_{12} (\sum_m \sum_n a_{mn}^2 (nm\pi^2/ab)^2 (a/2)\sin^2(n\pi y/b)) + \\
& D_{22} (\sum_m \sum_n a_{mn}^2 (n\pi/b)^4 (a/2)\sin^2(n\pi y/b)) + \\
& 4D_{33} (\sum_m \sum_n a_{mn}^2 (nm\pi^2/ab)^2 (a/2)\cos^2(n\pi y/b))]dy
\end{aligned}
$$

and then intergrating this with respect to y and evaluating over the limits gives

$$
\begin{aligned}
V_{SE} = (\pi^4/8)ab[& D_{11} \sum_m \sum_n a_{mn}^2 (m/a)^4 + 2(D_{12} + 2D_{33}) \\
& (\sum_m \sum_n a_{mn} (nm/ab)^2) + D_{22} (\sum_m \sum_n a_{mn} (n/b)^4)] \qquad (3.2.1.4)
\end{aligned}
$$

It is interesting to note that the terms coupling bending and twisting (D_{13} ,D_{23}) do not appear in the final expression of the bending strain energy. It may be argued that this is a function of the deflection form (eqn. (3.2.1.2)) that was chosen. It can, however, be shown that any equation that satisfies the boundary conditions for a simply supported plate i.e. w = 0 at all the edges, will always produce the same result. The assumption of a simply supported plate (rather than the deflection function chosen) thus implies that the coupling terms are of no significance in the buckling calculations.

Now the work done by the compression force F (force per unit width) during buckling is

$$W_x = 0.5(F_x)\int_0^b\int_0^a (\partial w/\partial x)^2\,dxdy$$
$$= 0.5(F_x)\int_0^b\int_0^a \sum_m\sum_n a_{mn}(m\pi/a)^2 \cos^2(m\pi x/a)\sin^2(n\pi y/b)$$
$$= (\pi^2 b/8a)F_x\sum_m\sum_n a_{mn}^2 m^2 \qquad (3.2.1.5)$$

and similarly in the y-direction the work done is

$$W_y = 0.5(F_y)\int_0^b\int_0^a (\partial w/\partial y)^2\,dxdy$$
$$= (\pi^2 a/8b)F_y\sum_m\sum_n a_{mn}^2 n^2 \qquad (3.2.1.6)$$

Considering the load in the x-direction only the critical buckling load is given by equating eqns. (3.2.1.4) and (3.2.1.5) giving

$$(\pi^2 b/8a)F_x\sum_m\sum_n a_{mn}^2 m^2 = (\pi^4/8)ab[D_{11}\sum_m\sum_n a_{mn}^2(m/a)^4 + 2(D_{12} + 2D_{33})(\sum_m\sum_n a_{mn}^2(nm/ab)^2) + D_{22}(\sum_m\sum_n a_{mn}^2(n/b)^4)]$$

Asumming that only the first coefficient of a_{mn} is relevant, the above equation can be written as

$$F_x m^2 = a^2\pi^2[D_{11}(m/a)^4 + 2(D_{12} + 2D_{33})(nm/ab)^2 + D_{22}(n/b)^4]$$

or

$$(F_x)_{crit} = (\pi a/m)^2[D_{11}(m/a)^4 + 2(D_{12} + 2D_{33})(nm/ab)^2 + D_{22}(n/b)^4]$$

Clearly $(F_x)_{crit}$ is minimum for n = 1 i.e. a one half sine wave deflection in the y-direction.

Thus

$$(F_x)_{crit} = (\pi a)^2 [D_{11} (m/a^2)^2 + (2/(ab)^2)(D_{12} + 2D_{33}) + D_{22}/(m^2 b^4)] \tag{3.2.1.7}$$

For a minimum value of F_x, the value of m which satisfies $dF_x/dm = 0$ has to be found.

Thus

$$dF_x/dm = (\pi a)^2 [2D_{11} m/(a^4) - 2D_{22}/(m^3 b^4)] = 0$$

leading to

$$m = (a/b)((D_{22}/D_{11})^{0.25}) \tag{3.2.1.8}$$

The plate can only buckle into an integer number of half sine waves and hence if m is not an integer value, the lowest buckling load calculated using the nearest integer values on either side of m is taken to be the critical load.

Now similarly for $(F_y)_{crit}$ equating eqns. (3.2.1.4) and (3.2.1.6) leads to

$$F_y = (\pi b/n)^2 [D_{11} (m/a)^4 + 2(D_{12} + 2D_{33})(nm/ab)^2 + D_{22}(n/b)^4]$$

This is obviously a minimum for m = 1, thus

$$(F_y)_{crit} = (\pi b)^2 [D_{11}/(n^2 a^4) + (2/(ab))(D_{12} + 2D_{33}) + D_{22}(n^2/b^4)) \tag{3.2.1.9}$$

For a minimum find the value of n for $dF_Y/dn = 0$.

$$dF_Y/dn = (\pi b)^2 [-2D_{11} /(n^3 a^4) + 2D_{22}/(nb^4)] = 0$$

leading to

$$n = (b/a)((D_{11} /D_{22})^{0.25}) \qquad (3.2.1.10)$$

or the next higher integer.

The calculation of the critical shear load for buckling is done in a similar manner. The work done by the shear force F_{XY} is defined as

$$W_{XY} = F_{XY}\int_0^b\int_0^a (\partial w/\partial x)(\partial w/\partial y)dxdy \qquad (3.2.1.11)$$

Using the deflection function (3.2.1.2) again, eqn.(3.2.1.11) becomes

$$W_{XY} = F_{XY}\int_0^b\int_0^a (\sum_m\sum_n\sum_p\sum_q a_{mn}\, a_{pq}\, (mq\pi^2/ab)\cos(m\pi x/a)\sin(n\pi y/b)$$
$$\sin(p\pi x/a)\cos(q\pi y/b))dxdy$$

Now noting that

$$(\cos(m\pi x/a)\sin(p\pi x/a))dx = 0 \quad \text{if } m \pm p \text{ is an even number}$$

and

$$(\cos(m\pi x/a)\sin(p\pi x/a))dx = (2a/\pi)(m/(m^2-p^2))$$
$$\text{if } m \pm p \text{ is an odd number}$$

then

$$W_{XY} = 8F_{XY}\sum_m\sum_n\sum_p\sum_q a_{mn}\, a_{pq}\, (mnpq/((m^2-p^2)(q^2-n^2))) \qquad (3.2.1.12)$$

where m,n,p and q are such integers that $m \pm p$ and $n \pm q$ are odd numbers.

Equating eqns. (3.2.1.4) and (3.2.1.12) an expression for F_{XY} is obtained as follows:-

$$F_{XY} = (\pi^4 ab/64)(D_{11} \sum_m \sum_n a^2_{mn}(m/a)^4 + 2(D_{12} + 2D_{33})(\sum_m \sum_n a^2_{mn}(nm/ab)^2) + D_{22}(\sum_m \sum_n a^2_{mn}(n/b)^4))/(\sum_m \sum_n \sum_p \sum_q a_{mn} a_{pq}(mnpq/((m^2-p^2)(q^2-n^2)))) \quad (3.2..1.13)$$

Now it is necessary to select such a system of constants a_{mn} and a_{pq} as to make F_{XY} a minimum.

The solution at this stage becomes very tedious and involves the solving of a number of simultaneous equations. Suffice it to say therefore that the remainder of the mathematical manipulation required to solve for $(F_{XY})_{crit}$ can be found in Refs. [30],[31] or [32] and only the final result will be presented here.

A very convenient form of writing the expression for $(F_{XY})_{crit}$ is given in Ref. [12], and it repeated below.

Defining the parameter C as

$$C = (D_{11} D_{22})^{0.5}/(D_{12} + 2D_{33})$$

then for $C \geq 1$

$$(F_{XY})_{crit} = (2/b)^2 (D_{11} D^3_{33})^{0.25} \quad (8.125 + 5.05/C)$$

and for $C < 1$

$$(F_{xy})_{crit} = (2/b)^2 (D_{22}(D_{12}+2D_{33}))^{0.5}(11.7+0.532C+0.938C^2)$$

3.2.2 Calculation Of The Lamina Strains

Laminated plate theory is based on certain hypotheses (see Appendix A) which simplify the analysis without really restraining the generality of the theory. The most important of these is the assumption that the strains are linear functions in the thickness direction of the laminate, that is to say that they are equal in the case of in-plane loads and proprotional to the thickness in the case of bending loads.

This assumption implies that there is no damage inside the laminate, such as delaminations or cracks which would allow the strain field to become discontinuous. The assumptions of laminated plate theory would no longer be valid under such conditions, and therefore the strain constraints should be specified in a manner that ensures that all the lamina remain intact under all the various loading conditions applied to the laminate.

Failure of individual lamina in a composite structural element may not necessarily lead to complete failure of that element but will almost certainly act as a point from which further failure or cracks may propogate, and for this reason as well the strains in each lamina need to be kept within acceptable limits.

In this section it is shown how the individual lamina strains can be derived from the overall plate strains and curvatures. The derivation is based on the diagrams in figure 3.2.2.1 and the notation used is consistent with that in the diagram and Appendix A.

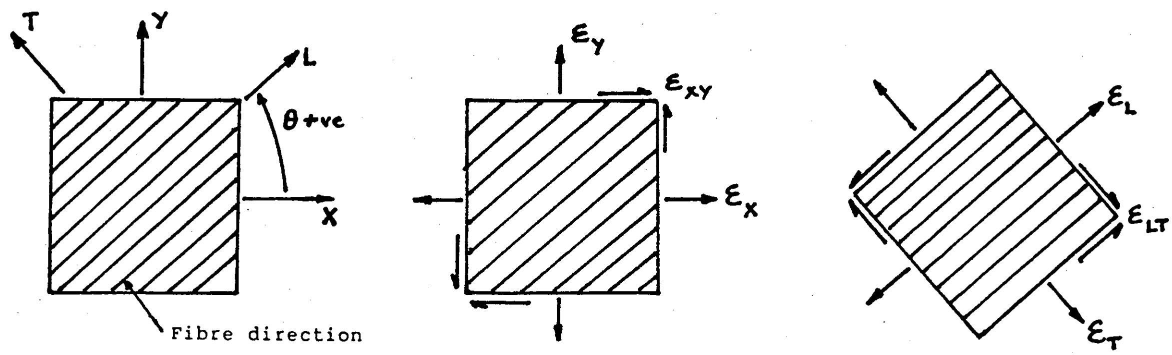

Figure 3.2.2.1 Strain transformation

The notation in figure 3.2.2.1 indicates the use of the x-y axes system for the "off-axis" or global axis system, and the L-T axes for "on-axis" or local lamina axis system. It is also worth noting that strain is non-dimensional and purely geometric, so involving no material properties or balance of forces.

Now the strain-displacement relations are

$$\varepsilon_L = \partial u/\partial L \quad ; \quad \varepsilon_T = \partial v/\partial T \quad ; \quad \varepsilon_{LT} = \partial u/\partial T + \partial v/\partial L$$

where u and v are displacements in the L and T directions respectively. The quantities u,v,L and T are vectors and hence the relative values in any new axis system, say L′-T′, can be defined by

$$L = L'\cos\theta + T'\sin\theta$$

$$T = -L'\sin\theta + T'\cos\theta$$

or

$$L' = L\cos\theta - T\sin\theta$$

$$T' = L\sin\theta + T\cos\theta \qquad (3.2.2.1)$$

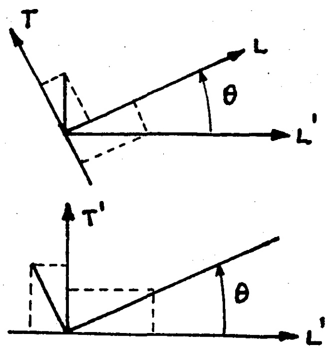

From eqn. (3.2.2.1)

$$\partial L'/\partial L = \cos\theta \; ; \; \partial L'/\partial T = -\sin\theta$$

$$\partial T'/\partial L = \sin\theta \; ; \; \partial T'/\partial T = \cos\theta \qquad (3.2.2.2)$$

Now the relations between the displacements (as opposed to the strains) in the primed and unprimed co-ordinates are the same as those given in eqn. (3.2.2.1) because all quantities are vectors.

Thus

$$u = u'\cos\theta + v'\sin\theta \qquad (3.2.2.3)$$

$$v = -u'\sin\theta + v'\cos\theta$$

or

$$u' = u\cos\theta - v\sin\theta \qquad (3.2.2.4)$$

$$v' = u\sin\theta + v\cos\theta$$

Now since $\varepsilon_L = \partial u/\partial L$, by chain differentiation it can be written as

$$\varepsilon_L = (\partial u/\partial L')(\partial L'/\partial L) + (\partial u/\partial T')(\partial T'/\partial L)$$

Substituting into this eqns. (3.2.2.2) and (3.2.2.3), gives

$$\varepsilon_L = ((\partial u'/\partial L')\cos\theta + (\partial v'/\partial L')\sin\theta)\cos\theta + ((\partial u'/\partial T')\cos\theta + (\partial v'/\partial T')\sin\theta)\sin\theta$$

Thus

$$\varepsilon_L = \varepsilon_X\cos^2\theta + \varepsilon_Y\sin^2\theta + \varepsilon_{XY}(\sin\theta\cos\theta) \quad (3.2.2.5)$$

where

$$\varepsilon_X = \varepsilon'_L = \partial u'/\partial L'$$
$$\varepsilon_Y = \varepsilon'_T = \partial v'/\partial T'$$
$$\varepsilon_{XY} = \varepsilon'_{LT} = \partial u'/\partial T' + \partial v'/\partial L'$$

Similarly it can be shown that

$$\varepsilon_T = \varepsilon_X\sin^2\theta + \varepsilon_Y\cos^2\theta - \varepsilon_{XY}(\sin\theta\cos\theta) \quad (3.2.2.6)$$

$$\varepsilon_{LT} = -2\varepsilon_X\sin\theta\cos\theta + 2\varepsilon_Y\sin\theta\cos\theta + \varepsilon_{XY}(\cos^2\theta - \sin^2\theta) \quad (3.2.2.7)$$

Now eqns. (3.2.2.5) - (3.2.2.7) can be written in matrix form as

$$\begin{Bmatrix}\varepsilon_L\\ \varepsilon_T\\ \varepsilon_{LT}\end{Bmatrix} = \begin{bmatrix}\cos^2\theta & \sin^2\theta & \sin\theta\cos\theta\\ \sin^2\theta & \cos^2\theta & -\sin\theta\cos\theta\\ -2\sin\theta\cos\theta & 2\sin\theta\cos\theta & (\cos^2\theta - \sin^2\theta)\end{bmatrix}\begin{Bmatrix}\varepsilon_X\\ \varepsilon_Y\\ \varepsilon_{XY}\end{Bmatrix}$$

$$\{\varepsilon_\ell\} = [T]\begin{Bmatrix}\varepsilon_X\\ \varepsilon_Y\\ \varepsilon_{XY}\end{Bmatrix} = [T]\{\varepsilon'_\ell\} \quad (3.2.2.8)$$

where eqn. (3.2.2.8) is true for each lamina.

Note that the values ε_X, ε_Y and ε_{XY} in eqn. (3.2.2.8) are the sum of strains due to in-plane and bending stresses. These strains can be written as

$$
\begin{aligned}
\varepsilon_x &= \varepsilon_x^{\circ} + \kappa_x z \\
\varepsilon_y &= \varepsilon_y^{\circ} + \kappa_y z \\
\varepsilon_{xy} &= \varepsilon_{xy}^{\circ} + \kappa_{xy} z
\end{aligned}
\qquad (3.2.2.9)
$$

where

z is the distance from the plate midsurface

ε° is the membrane (midsurface) strain

κ is the midsurface curvature

CHAPTER 4

4 OPTIMIZATION METHOD AT THE ELEMENT LEVEL

4.1 Optimization Algorithm

Linear programming (LP) methods have been the subject of a large proportion of the work done on optimization methods to date. This has resulted in very efficient algorithms being developed that have a high degree of reliability and a sound theoretical basis. In view of these successes, it is not surprising that some of the methods commonly used for solving general constrained nonlinear problems (laminated composite element optimization is such a problem) exploit the LP techniques.

The general, nonlinear problem can be converted to a linear constrained problem by linearizing the constraints and the objective function. These linear approximations permit the solution of the general problem by the LP or simplex LP methods in a recursive, or sequential manner.

The nonlinear functions $f(t,\theta)$ can be approximated in the vicinity of a point (t_α,θ_α) by Taylors expansion,

$$f(t,\theta) = f(t_\alpha,\theta_\alpha)+(t-t_\alpha)(\partial f(t,\theta)/\partial t)_\alpha+(\theta-\theta_\alpha)(\partial f(t,\theta)/\partial \theta)_\alpha$$

where the higher order terms of the expansion have been ignored, as is usually done.

The point $(t_\alpha, \theta_\alpha)$ is called the linearization point. It should be recognized that the linearization is in many instances a gross approximation, and as such must be treated with caution. It is, nonetheless, an approximation that is widely used, and can give excellent results if it is sensibly applied.

The type of recursive LP method used in this work is commonly refered to as approximation programming (Refs. [34] and [35]) and is described briefly below.

The objective function and the constraints are linearized by taking the first terms of the Taylor expansion about the current point $(t_\alpha, \theta_\alpha)$. This is done for each iteration and no part of the preceeding problem is retained (one of the major differences when compared to other sequential LP methods). The original nonlinear problem is thus locally approximated by linear terms, permitting the solution of nonconvex problems. To ensure the approximation is adequate, however, move limits are placed on the t_α and θ_α i.e. the permissible variation of t and θ are limited.

To solve a problem a starting point $(t_\alpha, \theta_\alpha)$ is chosen and the objective function and constraints are linearized in the neighbourhood of $(t_\alpha, \theta_\alpha)$. The LP problem is then solved and the solution is taken to be the starting point for the next iteration. The nonlinear functions are relinearized about the new (t_a, θ_a) and the process is repeated until either no significant improvement occurs in the solution, or successive solutions start to oscillate between the vertices of the feasible region. In the latter event the move limits may be reduced and the solution process continued. Computational efficiency, however, requires that these move limits be kept as large as possible so as not to slow down the convergence to the optimum.

Convergence is assumed if the change in objective function value for two successive LP subproblems is smaller than a desired value and the nonlinear constraints are satisfied within the desired tolerance.

The method of approximation programming is attractive in that it is applicable to nonconvex problems and produces feasible or nearly feasible intermediate solutions with good accuracy (Ref. [35]). Futhermore, it is well suited to development work since by the very nature of a LP problem, the progress of the solution can easily be tracked thereby allowing relatively easy identification of problem areas.

Finally it worth noting that the combination of infeasible (or nearly feasible) design points, about which the constraint functions for the next LP problem are linearized, and highly non-linear constraints (such as buckling constraints) can in some cases result in a design space with no feasible region being produced. This can effectively be overcome by scaling the design into the (non-linear) feasible design region before the linearization process is initiated. This particular problem and the scaling procedures are discussed in Appendix E.

4.2 Linearization Of The Objective Function

In section 3.1 the form of the objective function was given (eqn. (3.1.3)) as

$$f(t,\theta) = q_1 f_1(t,\theta)/W + q_2 f_2(t,\theta)/\Delta k \qquad (4.2.1)$$

Now, before this function can be linearized it is necessary to define the functions $f_1(t,\theta)$ and $f_2(t,\theta)$ in a proper mathematical form.

The first function, $f_1(t,\theta)$, is the weight of the element. This is directly proportional to the density and thickness of the individual lamina, but not the ply angle. It can thus be written as

$$f_1(t,\theta) = \sum_{j=1}^{L} \rho_j t_j \qquad (4.2.2)$$

where

ρ is the desity of lamina j

t is the thickness of lamina j

The second function, $f_2(t,\theta)$, is the stiffness change in an element and is dependent on the change in angle and thickness of each lamina. There are numerous ways of choosing to evaluate (and so assign a numerical value to) the stiffness change of an element. In Refs. [24] and [26] the stiffness change (the only function to be minimized at the lower level) is expressed as

$$\Delta R = \left(\sum_m \sum_n (R_{mn} - R^*_{mn})^2 \right)^{0.5}$$

where R_{mn} are the terms of the laminate rigidity matrix (see Appendix A) and * denotes the value upon entry to this level of optimization. This form of expression for stiffness change was tried initially in conjunction with weight in a multi-criteria objective function. The optimization results (and the convergence rates) were found to be very sensitive to other input parameters (load cases, weighting coefficients etc) and the degree of compromise between the two "minimized" objectives unpredictable. The change in element strain energy was then used as a means of expressing stiffness change in the element, and provided much more satisfactory results. This was also thought to provide a more accurate gauge of the load continuity at the upper optimization level, since both element strains and stiffness are taken into account.

Eqn. (4.2.1) can thus be re-written as

$$f(t,\theta) = q_1 f_1(t,\theta)/W + q_2 f_2(t,\theta)/\Delta U \qquad (4.2.3)$$

where ΔU represents the change in strain energy in the element. The actual element strain energy is evaluated as

$$U = \{\varepsilon_{pl}\}^T [R]\{\varepsilon_{pl}\} \qquad (4.2.4)$$

where $\{\varepsilon_{pl}\}$ is the vector of element strains and [R] the rigidity matrix as defined in Appendix A.

The strain energy change part of the objective function can be expressed as

$$f_2(t,\theta) = (U - U^*)^2 = (\{\varepsilon_{pl}\}^T [R]\{\varepsilon_{pl}\} - U^*)^2 \qquad (4.2.5)$$

where $\{\varepsilon_{pl}\}$ is the vector of plate strains and curvatures (see Appendix A), [R] is the plate rigidity matrix and U^* the strain energy of the element on entry to this level of optimization.

The linearized form of eqn. (4.3), using a Taylor series expansion is thus

$$f_2(t,\theta) = (U-U^*)_a^2 + \sum_{j=1}^{L} (t-t_a)_j (\partial f_2(t,\theta)/\partial t_j)_a + (\theta-\theta_a)_j (\partial f_2(t,\theta)/\partial \theta_j)_a \qquad (4.2.6)$$

where subscript "a" denotes that these values are evaluated at the point of linearization, and

$$\partial f_2(t,\theta)/\partial t_j = 2(U-U^*)(\{\partial \varepsilon_{pl}/\partial t_j\}^T [R]\{\varepsilon_{pl}\} + \{\varepsilon_{pl}\}^T [\partial R/\partial t_j]\{\varepsilon_{pl}\} + \{\varepsilon_{pl}\}^T [R]\{\partial \varepsilon_{pl}/\partial t_j\}) \qquad (4.2.7)$$

A similar expression can be written for $\partial f_2(t,\theta)/\partial\theta$.

The derivatives $\partial R/\partial t$ and $\partial R/\partial\theta$ of the rigidity matrix [R] are given in Appendix B.

The methods for evaluating $\partial\varepsilon/\partial t$, $\partial\varepsilon/\partial\theta$, are given in the section 4.3.

The above equations (4.2.5)-(4.2.7) are only valid for single load cases. If multiple load cases are to be considered these can be re-written respectively as

$$f_2(t,\theta) = \sum_{n=1}^{NL} (U_n - U_n^*)^2 \tag{4.2.8}$$

(in this case ΔU becomes $\sum_{n=1}^{NL}(\Delta U)$)

where NL is the number of load cases, and

$$f_2(t,\theta) = \sum_{n=1}^{NL} (U_n - U_n^*)^2 + \sum_{j=1}^{L}((t-t_a)_j \sum_{n=1}^{NL}(\partial f_2(t,\theta)/\partial t_j)_a + (\theta-\theta_a)_j \sum_{n=1}^{NL}(\partial f_2(t,\theta)/\partial\theta_j)_a) \tag{4.2.9}$$

where

$$\partial f_2(t,\theta)/\partial t_j = 2\sum_{n=1}^{NL}(U-U^*)(\{\partial\varepsilon_{pl}/\partial t_j\}^T[R]\{\varepsilon_{pl}\} + \{\varepsilon_{pl}\}^T[\partial R/\partial t_j]\{\varepsilon_{pl}\} + \{\varepsilon_{pl}\}^T[R]\{\partial\varepsilon_{pl}/\partial t_j\}) \tag{4.2.10}$$

and a similar expression for $\partial f_2(t,\theta)/\partial\theta$.

4.3 Linearization Of The Lamina Strain Constraints

The relationship between the plate strains and the loads applied to the plate (derived in Appendix A, eqn. (A.10)) can be written as

$$\{F\} = \left[\begin{array}{c|c} A & B \\ \hline B & D \end{array}\right] \{\varepsilon_{pl}\}$$

$$= [R]\{\varepsilon_{pl}\} \qquad (4.3.1)$$

At the element level of optimization it is assumed that the applied loads do not change when the design variables are varied. The derivatives of eqn. (4.3.1) with respect to the design variables t_j can thus be written as

$$\{\partial F/\partial t_j\} = [\partial R/\partial t_j]\{\varepsilon_{pl}\} + [R]\{\partial \varepsilon_{pl}/\partial t_j\} = 0$$

leading to

$$\{\partial \varepsilon_{pl}/\partial t_j\} = -[R]^{-1}[\partial R/\partial t_j]\{\varepsilon_{pl}\} \qquad (4.3.2)$$

A similar expression for the derivative with respect to the design variables θ_j (ply angles) can be written

$$\{\partial \varepsilon_{pl}/\partial \theta_j\} = -[R]^{-1}[\partial R/\partial \theta_j]\{\varepsilon_{pl}\} \qquad (4.3.3)$$

In eqn. (4.3.2) the derivative of the rigidity matrix [R] is

$$[\partial R/\partial t_j] = \left[\begin{array}{c|c} \partial A/\partial t_j & \partial B/\partial t_j \\ \hline \partial B/\partial t_j & \partial D/\partial t_j \end{array}\right]$$

with a similar expression for $\partial R/\partial \theta_j$. These derivatives (of the rigidity matrix) are given in Appendix B.

Now the individual lamina strains can be expressed in terms of the plate strains (see section 3.2.2) as

$$\{\varepsilon_l\} = [T]\{\varepsilon_l'\} \qquad (4.3.4)$$

where

[T] = strain transformation matrix (eqn. (3.2.2.8))

$$\{\varepsilon_l'\} = \begin{Bmatrix} \varepsilon_x^\circ + \kappa_x \; z \\ \varepsilon_y^\circ + \kappa_y \; z \\ \varepsilon_{xy}^\circ + \kappa_{xy} \; z \end{Bmatrix} \qquad \text{(eqn. (3.2.2.9))}$$

and where the ε° and κ are the plate midsurface strains and curvatures respectively. Equation (4.3.4) can thus be written in the following form

$$\{\varepsilon_l\} = [T]_j [e_1]\{\varepsilon_{pl}\} + [T]_j z_j [e_2]\{\varepsilon_{pl}\} \qquad (4.3.5)$$

where z_j is the distance from the centre of the plate to the centroid of lamina j, and

$$[e\ ] = \begin{bmatrix} 1 & 0 & 0 & 0 & 0 & 0 \\ 0 & 1 & 0 & 0 & 0 & 0 \\ 0 & 0 & 1 & 0 & 0 & 0 \end{bmatrix}$$

$$[e\ ] = \begin{bmatrix} 0 & 0 & 0 & 1 & 0 & 0 \\ 0 & 0 & 0 & 0 & 1 & 0 \\ 0 & 0 & 0 & 0 & 0 & 1 \end{bmatrix}$$

Differentiating eqn. (4.3.5) with respect to the lamina thickness variable t_i gives

$$\{\partial \varepsilon_l/\partial t_i\}_j = [T]_j [e_1]\{\partial \varepsilon_{pl}/\partial t_i\} + [T]_j z_j [e_2]\{\partial \varepsilon_{pl}/\partial t_i\} \quad (4.3.6)$$

Substituting eqn. (4.3.2) into eqn. (4.3.6) gives

$$\{\partial \varepsilon_l/\partial t_i\}_j = -[T]_j [e_1][R]^{-1} [\partial R/\partial t_i]\{\varepsilon_{pl}\} - [T]_j z_j [e_2][R]^{-1} [\partial R/\partial t_i]\{\varepsilon_{pl}\} \quad (4.3.7)$$

Now differentiatng eqn. (4.3.5) with repect to the lamina ply angle θ gives, for $j \neq i$

$$\{\partial \varepsilon_l/\partial \theta_i\}_j = [T]_j [e_1]\{\partial \varepsilon_{pl}/\partial \theta_i\} + [T]_j z_j [e_2]\{\partial \varepsilon_{pl}/\partial \theta_i\} \quad (4.3.8)$$

and for $j = i$,

$$\{\partial \varepsilon_l/\partial \theta_i\}_j = [\partial T/\partial \theta_i]_j [e_1]\{\varepsilon_{pl}\} + [T]_j [e_1]\{\partial \varepsilon_{pl}/\partial \theta_i\}_j + [\partial T/\partial \theta_i]_j z_j [e_2]\{\varepsilon_{pl}\} + [T]_j z_j [e_2]\{\partial \varepsilon_{pl}/\partial \theta_i\}_j \quad (4.3.9)$$

Expressions similar to eqn. (4.3.7) for $\{\partial \varepsilon_l/\partial t_i\}$ can be obtained for $\{\partial \varepsilon_l/\partial \theta_i\}$ by substituting eqn. (4.3.3) into eqns. (4.3.8) and (4.3.9).

The above equations can thus be used to evaluate the Taylor series expansion (to first order) of the strain expressions, as given below.

$$\{\varepsilon_l\}_j = [[T]_j [e_1]\{\varepsilon_{pl}\} + [T]_j z_j [e_2]\{\varepsilon_{pl}\}]_a + \sum_{j=1}^{L} (t - t_a)_j (\partial \varepsilon_l/\partial t_j)_a + \sum_{j=1}^{L} (\theta - \theta_a)_j (\partial \varepsilon_l/\partial \theta_j)_a \quad (4.3.10)$$

and

$$(\varepsilon_L)_j = [1 \quad 0 \quad 0]\{\varepsilon_l\}_j$$
$$(\varepsilon_T)_j = [0 \quad 1 \quad 0]\{\varepsilon_l\}_j \qquad (4.3.11)$$
$$(\varepsilon_{LT})_j = [0 \quad 0 \quad 1]\{\varepsilon_l\}_j$$

Equations (4.3.10) and (4.3.11) can be combined to give the linearized form of the strain constraints with bounds placed on ε_L, ε_T and ε_{LT} as required.

4.4 Linearization Of The Buckling Constraint Equations

The buckling equations in section 3.2.1 define the critical buckling load in the x-direction as (eqn. (3.2.1.7))

$$(F_x)_{crit} = (\pi a)^2 [D_{11} m^2/a^4 + 2(D_{12} + 2D_{33})/(ab)^2 + D_{22}/(m^2 b^4)] \qquad (4.4.1)$$

where $m = a/b(D_{22}/D_{11})^{0.25}$, or the next higher integer, and is the number of half wave-lengths into which the plate will buckle.

Now if it is assumed that the number of half wave-lengths will not vary during any one iteration (m can be recalculated at every iteration of the recursive LP optimization process), the derivatives of F can be evaluated as

$$\partial F_x/\partial t_j = (\pi a)^2 [(m^2/a^4)(\partial D_{11}/\partial t_j) + (2/(ab)^2)((\partial D_{12}/\partial t_j) + 2(\partial D_{33}/\partial t_j)) + (\partial D_{22}/\partial t_j)/(m^2 b^4)] \qquad (4.4.2)$$

where $\partial D_{mn}/\partial t_j$ are defined in Appendix B.

The constraint on buckling in the x-direction can now be linearized using a Taylor expansion and can be written as

$$(F_x)_{crit} = (\pi a)^2 [D_{11} m^2/a^4 + 2(D_{12} + 2D_{33})/(ab)^2 + D_{22}/(m^2 b^4)] + \sum_{j=1}^{L} (t-t_a)_j (\partial F_x/\partial t_j) + \sum_{j=1}^{L} (\theta-\theta_a)_j (\partial F_x/\partial \theta_j) \quad (4.4.3)$$

In a similar manner the linearized expression for the critical buckling load in the y-direction can be derived, giving

$$(F_y)_{crit} = (\pi b)^2 [D_{11}/(n^2 a^4) + 2(D_{12} + 2D_{33})/(ab)^2 + D_{22}(n^2/b^4)] + \sum_{j=1}^{L} (t-t_a)_j (\partial F_y/\partial t_j) + \sum_{j=1}^{L} (\theta-\theta_a)_j (\partial F_y/\partial \theta_j) \quad (4.4.4)$$

where $\partial F_y/\partial t_j$ and $\partial F_y/\partial \theta_j$ will be similar in form to eqn. (4.4.2), but derived from the expression for $(F_y)_{crit}$ given in section 3.2.1.

The critical shear buckling load $(F_{xy})_{crit}$ is dependent on the parameter C, (see section 3.2.1), where

$$C = (D_{11} D_{22})^{0.5}/(D_{12} + 2D_{33})$$

If $C \geqslant 1$, then

$$(F_{xy})_{crit} = (2/b)^2 (D_{11} D_{22}^3)^{0.25} (8.125 + 5.05/C)$$

or if $C < 1$, then

$$(F_{xy})_{crit} = (2/b)^2 (D_{22}(D_{12}+2D_{33}))^{0.5}(11.7+0.532C+0.938C^2)$$

Parameter C is not related to the number of half wave-lengths of the buckle and hence has to be included in the equation for (F_{xy}) before the derivatives are taken.

Thus for $C \geqslant 1$ (at the point of linearization)

$$\begin{aligned}(F_{xy})_{crit} &= (2/b)^2 (D_{11} D_{22}^3)^{0.25} (8.125+5.05(D_{12}+2D_{33})/(D_{11} D_{22})^{0.5}) \\ &= (2/b)^2 (D_{22}/D_{11})^{0.25} (8.125(D_{11} D_{22})^{0.5} + 5.05(D_{12}+2D_{33})) \end{aligned} \quad (4.4.5)$$

Thus

$$\begin{aligned}(\partial F_{xy}/\partial t_j) = {} & (2/b)^2 (D_{22}/D_{11})^{0.25} (8.125(\partial/\partial t_j (D_{11} D_{22})^{0.5}) + \\ & 5.05(\partial D_{12}/\partial t_j + 2(\partial D_{33}/\partial t_j)) + (2/b)^2 (\partial/\partial t_j) \\ & (D_{22}/D_{11})^{0.25})(8.125(D_{11} D_{22})^{0.5} + 5.05(D_{12}+2D_{33}))\end{aligned} \quad (4.4.6)$$

where

$$\partial/\partial t_j (D_{11} D_{22})^{0.5} = 0.5((D_{11}/D_{22})^{0.5}(\partial D_{22}/\partial t_j) + (D_{22}/D_{11})^{0.5} (\partial D_{11}/\partial t_j))$$

$$\partial/\partial t_j (D_{22}/D_{11})^{0.25} = 0.25(D_{22}/D_{11})^{0.25} ((\partial D_{22}/\partial t_j)/D_{22} - (\partial D_{11}/\partial t_j)/D_{11})$$

where $\partial D_{mn}/\partial t_j$ is given in Appendix B.

An equation similar to eqn. (4.4.6) can be written for $\partial F_{xy}/\partial \theta_j$.

The linearized form of eqn.(4.4.5) can thus be written (by Taylor expansion) as

$$(F_{xy})_{crit} = [(2/b)^2 (D_{22}/D_{11})^{0.25} (8.125(D_{11} D_{22})^{0.5} + 5.05(D_{12} + 2D_{33}))]_a + \sum_{j=1}^{L} (t-t_a)_j (\partial F_{xy}/\partial t_j) + \sum_{j=1}^{L} (\theta - \theta_j)(\partial F_{xy}/\partial \theta_j) \quad (4.4.7)$$

Now if $C < 1$ (at the point of linearization)

$$(F_{xy})_{crit} = (2/b)^2 (D_{22})^{0.5} (D_{12} + 2D_{33})^{-1.5} [11.7(D_{12} + 2D_{33})^2 + 0.532(D_{11} D_{22})^{0.5} (D_{12} + 2D_{33}) + 0.938(D_{11} D_{22})] \quad (4.4.8)$$

Thus

$$(\partial F_{xy}/\partial t_j) = (2/b)^2 [0.5(D_{22})^{-0.5} (\partial D_{22}/\partial t_j) (D_{12} + 2D_{33})^{-1.5} (11.7(D_{12} + 2D_{33})^2 + 0.532(D_{11} D_{22})^{0.5} (D_{12} + 2D_{33}) + 0.938(D_{11} D_{22})) - 3/2(D_{22}^{0.5}((\partial D_{12}/\partial t_j) + 2 (\partial D_{33}/\partial t_j)))(D_{12} + 2D_{33})^{-2.5} (11.7(D_{12} + 2D_{33})^2 + 0.532(D_{11} D_{22})^{0.5} (D_{12} + 2D_{33}) + 0.938(D_{11} D_{22}))) + (D_{22})^{0.5} (D_{12} + 2D_{33})^{-1.5} (11.7(2(\partial D_{12}/\partial t_j + 2\partial D_{33}/\partial t_j) (D_{12} + 2D_{33}) + 0.532(\partial/\partial t_j (D_{11} D_{22})^{0.5})(D_{12} + 2D_{33}) + (D_{11} D_{22})^{0.5} ((\partial D_{12}/\partial t_j) + 2(\partial D_{33}/\partial t_j)) + 0.938 (D_{11} (\partial D_{22}/\partial t_j) + D_{22}(\partial D_{11}/\partial t_j))))] \quad (4.4.9)$$

where $\partial/\partial t_j (D_{11} D_{22})^{0.5}$ is given above and $\partial D_{mn}/\partial t_j$ is given in Appendix B.

Again an equation similar to eqn. (4.4.9) can be written for $\partial F_{xy}/\partial \theta_j$.

The linearized form of equation (4.4.8) can be written as

$$(F_{xy})_{crit} = [(2/b)^2 (D_{22})^{0.5} (D_{12}+2D_{33})^{-1.5} (11.7(D_{12}+2D_{33})^2 + 0.532(D_{11} D_{22})^{0.5} (D_{12}+2D_{33})+0.938(D_{11} D_{22}))] + \sum_{j=1}^{L} (t-t_a)_j (\partial F_{xy}/\partial t_j) + \sum_{j=1}^{L} (\theta-\theta_a)_j (\partial F_{xy}/\partial \theta_j) \qquad (4.4.10)$$

These linearized forms of the buckling (critical load) equations are then used in the form of the constraint given in section 3.2..

4.5 Move Limit Strategy

The linearization techniques used in sections 4.3 and 4.4 provide constraint equations which only approximate the original (non-linear) constraint expressions in a small region around the point of linearization. There is thus the risk that as the design is changed the error in the approximated constraints would become large, and the design may move into an infeasible region i.e. where the actual constraints are violated. The most common method of limiting the risk is to prescribe move limits for the design variables, thereby limiting the extent of change allowed in the design at each iteration.

Computational efficiency requires that these move limits be kept as large as possible whereas the smaller the move limit the more stable the convergence is likely to be. Compromise schemes have been developed where the move limits are large in the early stages of the optimization and become tighter as the optimization proceeds. A typical example of this type of strategy is given in Ref. [36], where the upper and lower move limits are of the form

$$x^L \leqslant x \leqslant x^u$$

where

$$x_k^L = (1 - b(c^{k-1}))x_{k-1}$$
$$x_k^u = (1 + u(c^{k-1}))x_{k-1}$$

and

b and u are lower and upper limits (typically 0.6)

c is a progressive shrinkage factor (typically 0.9–0.95)

k is the iteration number

x is the initial design variable

The strategy employed in this work is very similar but involves the use of slightly different formulae for the lamina thickness and ply-angle variables.

The move limits for the lamina thickness variables are defined (using similar notation to that given above) by

$$t^L \leqslant t \leqslant t^u$$

where

$$t_k^L = (1 - bc^{k-1})t_{k-1}$$
$$t_k^u = (1 + bc^{k-1})t_{k-1} \qquad (4.5.1)$$

Experience in using the program developed indicated that values of 0.5 and 0.95 for b and c generally provide a satisfactory compromise of speed and stability of convergence. (Ref [36] suggests that values of 0.6 and 0.95 generally provide satisfactory results when dealing with isotropic structures).

The allowable movement of the ply-angle variables is limited by expressions of a slighty different form;

where

$$\theta_k^L = \theta_{k-1} - bc^{k-1}$$
$$\theta_k^u = \theta_{k-1} + bc^{k-1} \qquad (4.5.2)$$

The ply-angle change is expressed as an absolute value rather than a proportion of the initial value so that the allowable variations in lamina stiffness (and so the strain variations) are directly controlled and progressively decreased. If expressed as a proportion of the initial value the variations allowed in lamina stiffness would change dramatically as the ply-angle varied from 0 to 90 . Experience proved that a maximum move limit value of b = 15 (degrees) and a shrinkage factor of c = 0.9 provided favourable convergence characteristics. The shrinkage factor needed to be smaller than that associated with the lamina thickness because of the particularly non-linear constraint behaviour associated with changes in ply-angle.

CHAPTER 5

5 ILLUSTRATIVE EXAMPLES OF ELEMENT LEVEL OPTIMIZATION

A FORTRAN program (LAMOPT - described in Appendix F) was written in order to substantiate the theory developed in the previous chapters, using actual numerical problems. Four problems, solved using LAMOPT, are presented to illustrate the suitability of the method for weight optimization problems. A futher two examples are given to demonstrate both the suitability of the form of the multi-criteria objective function (given is section 3.1) and the effect on the optimum of varying the weighting coefficients in the objective function.

The weight optimization examples are all based on the plate shown in Figure 5.1 and initial laminate design given below. The same plate and layup is also used for the first of the problems illustrating the effect of varying the objective function weighting coefficients.

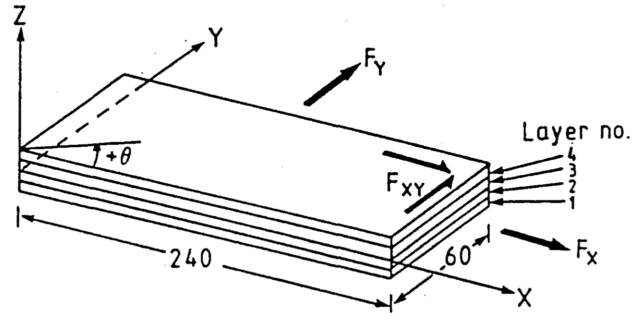

Figure 5.1 Test plate (simply supported)

Layer No.	Thickness	Ply angle
	(mm)	(deg)
1	2.5	45.0
2	2.5	0.0
3	2.5	0.0
4	2.5	45.0

where all the layers were assigned the following material properties (representative of a high strength carbon/epoxy composite) and strain limits (same for tension and compression)

E	= 130 000 MPa	ε_L	= 0.004
E	= 9 000 MPa	ε_T	= 0.004
G	= 4 800 MPa	ε_{LT}	= 0.0055
ν	= 0.28		

In all the examples given a design variable linking option was employed to ensure that the design remained symmetric about the midplane. It is interesting to note, however, that when this was not included the final (optimum) results did not differ significantly from those presented here.

No consideration was given to strain energy change in the first four examples i.e. only the weight was minimized. These results are summarized in Tables 5.1 - 5.4 which also contain information on the loading condition used (for reference axes see Appendix A), the final result and the percentage weight decrease achieved. In cases where compression or shear loads were considered, buckling constraints were included, and the calculations for these were based on plate dimensions of 240mm (x-direction) by 60mm (y-direction). The convergence criteria used in all the examples was that the design was deemed to have converged if the weight change in subsequent iterations was less than 1 percent and the sum of the ply-angle changes less than 10 degrees.

TABLE 5.1 - EXAMPLE CASE 1

Load Condition (N/mm and Nmm/mm)

F_X	F_Y	F_{XY}	M_X	M_Y	M_{XY}
-150.	0.	0.	0.	0.	0.

Final design

Layer No.	Thickness (mm)	Ply-angle (deg)
1	0.631	33.1
2	0.081	-6.8
3	0.081	-6.8
4	0.631	33.1

Percentage of original mass = 14.2%
((final mass/initial mass)x100)

Number of iterations to convergence = 12

TABLE 5.2 - EXAMPLE CASE 2

Load Condition (N/mm and Nmm/mm)

F_x	F_y	F_{xy}	M_x	M_y	M_{xy}
150.	-150.	0.	100.	100.	0.

Final design

Layer No.	Thickness (mm)	Ply-angle (deg)
1	1.762	68.4
2	0.146	2.1
3	0.146	2.1
4	1.762	68.4

Percentage of original mass = 38.3%
((final mass/initial mass)x100)

Number of iterations to convergence = 9

TABLE 5.3 - EXAMPLE CASE 3

Load Condition (N/mm and Nmm/mm)

F_x	F_y	F_{xy}	M_x	M_y	M_{xy}
150.	0.	0.	0.	0.	0.
150.	-150.	100.	0.	0.	0.

Final design

Layer No.	Thickness (mm)	Ply-angle (deg)
1	1.976	57.0
2	0.286	19.7
3	0.286	19.7
4	1.976	57.0

Percentage of original mass = 45.2%
((final mass/initial mass)x100)

Number of iterations to convergence = 12

TABLE 5.4 - EXAMPLE CASE 4

Load Condition (N/mm and Nmm/mm)

F_x	F_y	F_{xy}	M_x	M_y	M_{xy}
150.	-150.	100.	0.	0.	0.
150.	-150.	0.	100.	100.	0.

Final design

Layer No.	Thickness (mm)	Ply-angle (deg)
1	1.965	55.1
2	0.302	23.9
3	0.302	23.9
4	1.965	55.1

Percentage of original mass = 45.3%
((final mass/initial mass)x100)

Number of iterations to convergence = 14

The results demonstrate the effectiveness of the method in producing a minimum weight design for a laminated composite plate subject to strain and buckling constraints, and numerous load conditions. The optimization algorithm is also shown to be relatively efficient in that all the test cases satisfied the stringent convergence criteria in 14 or less iterations.

The two examples given below demonstrate the effect of varying the weighting coefficients in the multi-criteria objective function. The curves presented are plots of the percentage strain energy change against the final design mass as a percentage of the original mass. The points are marked with the associated weighting coefficients, the first value being that assigned to the weight part of the objective function and the second that assigned to the strain energy change part.

The results obtained when optimizing the flat plate (Figure 5.1) with various weighting coefficients are shown below in Figure 5.2.

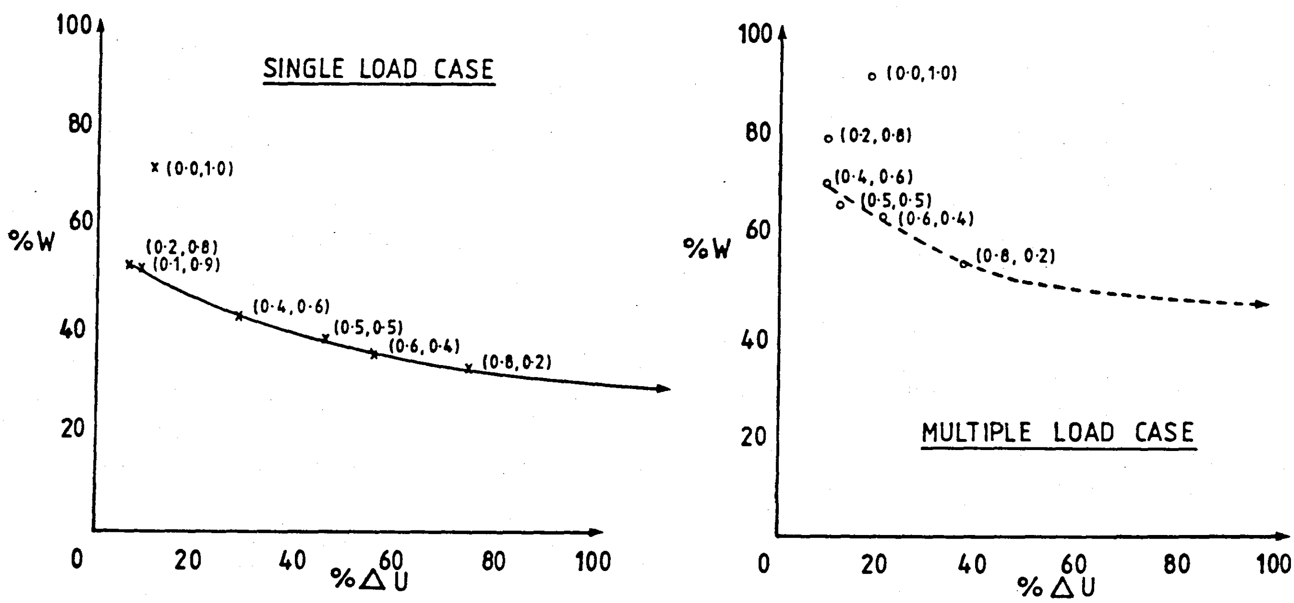

Figure 5.2 Influence of weighting coefficients (1)

The solid line (points marked with x) in Figure 5.2 represents the results of a test case where a load of 150 N/mm was applied in the x-direction, while the broken line (points marked with o) represents the results of a multiple load, test case.

These loads were as follows:-

	F_x	F_y	F_{xy}	M_x	M_y	M_{xy}
1.	150.	-150.	100.	0.	0.	0.
2.	150.	-150.	0.	100.	100.	0.
3.	-150.	0.	0.	0.	0.	0.

Consider first the curve representing the single load case (solid line). This curve is nearly linear over the region (0.2,0.8) to (0.8,0.2) and thus in this range the weighting coefficients can be said to accurately represent the relative importance of the two parts of the objective function. This is also the range of coefficients most likely to be used in order to achieve a satisfactory compromise between strain energy change and weight minimization, when switching between upper and lower levels of optimization. Outside this range, as the weighting coefficients become biased more in favour of weight reduction, the strain energy change increases rapidly to about 130 percent at (0.9,0.1) and 1200 percent at (1.0,0.0). At the other end of the scale the changes are less dramatic but slightly less consistent. This is to be expected, however, because as the coefficients are biased more heavily in favour of minimizing the strain energy change, the number of alternative solutions (local minima) increases. In practical terms this can readily be explained by the fact that there are numerous combinations of ply thicknesses and angles that will give very similar plate strains (for a given set of loads) and stiffnesses (rigidities). The end result is that variations of the weighting coefficients in the region (0.2,0.8) to (0.0,1.0) produce a cluster of points around the (0.2,0.8) mark, which have no definite pattern. This phenomena was found in all the (single load) test cases run, and the location of these points was apparently only dependent on the initial design chosen. They are, however, all perfectly acceptable points in that all the constraints are satisfied and the strain energy change is minimal (as required).

A similar distribution of the points was obtained when multiple load cases were considered. The range of the weighting coefficients associated with the linear distribution of the points did, however, vary to some degree depending on the relative magnitude, type and orientation of the applied loads. If the loads considered contained a dominant load case the results produced were very similar to those for the single load case. At the other extreme, when two or more load cases of similar magnitude, but different sign and/or orientation were included then the linear distribution of points in some cases only extended as far as the point associated with the weighting coefficients (0.4,0.6), as shown by the broken line in Figure 5.2. In these cases, weighting coefficients biased futher in favour of minimizing strain energy change produced an irregular distribtion of points in the region of the (0.4,0.6) mark (for the same reasons as mentioned above). Although the exact degree of compromise between minimization of strain energy change and weight could therefore not be accurately predicted in this region, the designs produced were still quite acceptable in that the strain energy change was minimal, the weight had been decreased and all the constraints were satisfied.

The effectiveness of varying the weighting coefficients in the multi-criteria objective function when considering larger, slightly more complex structures is illustrated below using a rectangular box section, which can be considered to be representative of a wing box. The layout and dimensions of the box section are shown in Figure 5.3.

The laminate construction of all the elements in the bottom skin was defined to be of laminate type 1 (i.e. design variable linking was used), all the elemnts in the top skin of laminate type 2 and all the elements in the webs and ribs of laminate type 3.These various laminate types are defined below.

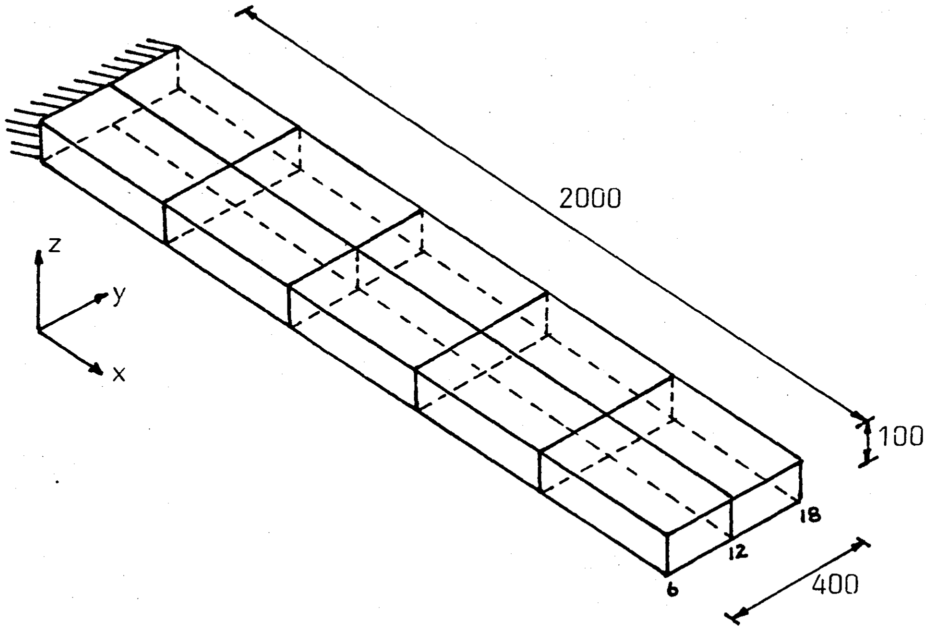

Figure 5.3 Rectangular box beam

Laminate type 1 - Bottom skin

Layer no.	Thickness (mm)	Ply angle (degrees)
1	2.5	0.0
2	1.25	-45.0
3	1.25	45.0
4	1.25	45.0
5	1.25	-45.0
6	2.5	0.0

Laminate type 2 - Top skin

Layer no.	Thickness (mm)	Ply angle (degrees)
1	2.0	0.0
2	2.0	-45.0
3	2.0	45.0
4	2.0	45.0
5	2.0	-45.0
6	2.0	0.0

Laminate type 3 - Webs and ribs

Layer no.	Thickness (mm)	Ply angle (degrees)
1	1.0	-45.0
2	1.0	45.0
3	1.0	45.0
4	1.0	-45.0

All the layers were assigned the same material properties as those in the plate examples shown above.

This structure was subjected to two loads applied at the tip nodes, and these were as follows:-

	Load 1			Load 2		
Node no.	6	12	18	6	12	18
Force (N)	10000	20000	10000	10000	15000	20000

The section was then optimized for this multiple load case using varying weighting coefficients in the objective function and the results are presented in Figure 5.4.

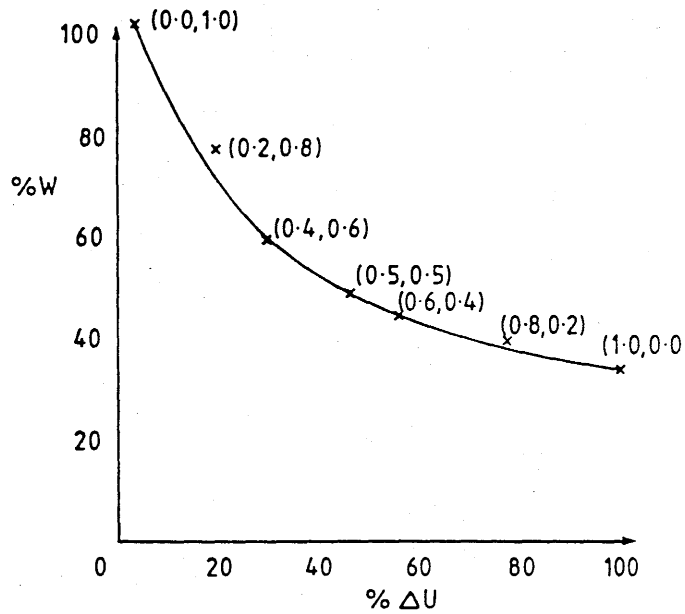

Figure 5.4 Influence of weighting coefficients (2)

The strain energy change in Figure 5.4 was calculated for the entire structure (rather than element by element) by multipling the applied loads by the displacements at the nodes where the loads were applied in the direction of the load. Since this was a multiple load case the strain energy change was evaluated as (see eqn. (4.2.8))

$$\Delta U = \sum_{n=1}^{2} (U_n - U_n^*)$$

Although the curve shown in Figure 5.4 does not have any linear, or nearly linear, sections in it, it does represent a smooth progression from a design dominated by the strain enegy change considerations at the one end to another where weight minimization is the only objective at the other end. The points between these extremes fall neatly on the curve shown and thus quite effectively represent the relative importance of the two parts of the objective function.

Inspection of the nodal displacements of the structure prior and subsequent to the optimization process also provides good insight into the effect that varying the weighting coefficients has on the overall structural stiffness. In Table 5.5 below the displacements of the nodes where the loads are applied are given in the direction of the applied load. Results are presented for the two load cases given above, with the terms W1 and W2 denoting the weighting coefficients assigned to the weight and strain energy change parts of the objective function respectively.

TABLE 5.5 - NODAL DISPLACEMENTS

				Load 1			
W1	1.0	0.8	0.6	0.5	0.4	0.2	0.0
W2	0.0	0.2	0.4	0.5	0.6	0.8	1.0
δ_6	149.7	133.8	116.3	111.5	97.7	86.9	67.0
δ_{12}	149.6	133.4	116.9	110.5	96.3	85.4	69.4
δ_{18}	146.4	129.5	113.7	106.3	95.5	84.8	70.9
				Load 2			
W1	1.0	0.8	0.6	0.5	0.4	0.2	0.0
W2	0.0	0.2	0.4	0.5	0.6	0.8	1.0
δ_6	135.5	120.1	104.6	100.6	92.5	83.1	62.4
δ_{12}	139.4	124.1	108.7	102.6	94.7	84.4	65.4
δ_{18}	141.1	125.8	110.3	102.4	95.3	85.7	67.7

These results show how effectively the stiffness change of the structure can be controlled by minimizing the strain energy change in the various laminate types. This capability combined with the smooth, progressive transition to the other extreme (pure weight minimization) for all the intermediate weighting coefficients (Figure 5.4) demonstrates the viability, and flexibility, of the form of objective function developed in section 3.1.

The examples above demonstrate the viability of the method developed for the element level optimization and its suitability for inclusion in the multilevel optimization system.

CHAPTER 6

6 SYSTEM LEVEL OPTIMIZATION

6.1 Objective Function At System Level

A single criteria objective function is used at the system level (as opposed to the multi-criteria objective function at the element level), which is that of minimizing total structural weight. This is commonly used as the objective fuction in structural optimization problems since it not only has an intrinsic merit of it's own, but in many cases also indirectly reflects the cost associated with the structure. This is especially true in aircraft structures where the cost penalties associated with excessive weight can be severe. Futhermore, in composite strutures the weight function can frequently be more directly related to cost than say, in aluminium structures, since the final product cost is generally more closely related to the raw material volume cost, as there is little material wasted in machining processes.

The system level objective function can thus be simply written as

$$W(t) = \sum_{j=1}^{NEL} \sum_{l=1}^{L} (\rho A t)_{lj} \qquad (6.1.1)$$

where NEL is the total number of elements in the finite element model

L is the number of layers in element j

A is the surface area of element j

ρ is the density of layer i in element j

t is the thickness of layer i in element j

6.2 Constraints At The System Level

The constraints considered at the system level of optimization are buckling (to be prevented), strain (with upper (tension) and lower (compression) bounds), displacement limits on the structure and bounds on lamina thicknesses. The buckling, strain and geometric constraints can be written in a similar manner to the element level constraints as:-

Buckling:-

$$(F_x)_{crit}/F_x \geq 1/C_1$$
$$(F_y)_{crit}/F_y \geq 1/C_2 \qquad (6.2.1)$$
$$(F_{xy})_{crit}/F_{xy} \geq 1/C_3$$

where $F_x + F_y + F_{xy} = F_{TOT}$

and $F_x/F_{TOT} = C_1$; $F_y/F_{TOT} = C_2$; $F_{xy}/F_{TOT} = C_3$

Strain:-

(per layer)

$$\varepsilon_L^L \leq \varepsilon_L \leq \varepsilon_L^u$$
$$\varepsilon_T^L \leq \varepsilon_T \leq \varepsilon_T^u \qquad (6.2.2)$$
$$\varepsilon_{LT}^L \leq \varepsilon_{LT} \leq \varepsilon_{LT}^u$$

Thickness:-

$$t^L \leq t \leq t^u \qquad (6.2.3)$$

and the deflection constraints are written in the following form,

$$\text{Deflection:-} \quad \delta_{np}^{L} \leqslant \delta_{np} \leqslant \delta_{np}^{u} \qquad (6.2.4)$$

The constraints (6.2.1) apply to each element as a whole, whereas the constraints (6.2.2) and (6.2.3) are applicable to the individual laminae of the elements.

The buckling constraint equations (6.2.1) are exactly the same format as those for the element level buckling constraint. The arguments used to derive the buckling constraint equations in section 3.2 hold for any plate, regardless of its stiffness or dimensions. These parameters (stiffness and dimensions) only affect the actual numerical value of $(F_x)_{crit}$, $(F_y)_{crit}$ and $(F_{xy})_{crit}$ (see section 3.2.1), and not the form of the constraint equations. The use of these equations at both system and element level is thus justified.

It is worth remembering that eqns. (6.2.1) only approximate (albeit very closely) the well known form of buckling equation, eqn. (3.2.5). This equation is in itself an approximation to the real solution, but one that works well for flat, reasonably proportioned plates (i.e. a ratio of side lengths of less than about 6:1 and a side length to thickness ratio greater than 10). If the finite element model used in the analysis phase has any areas of very complex geometry or substantial curvature, more accurate buckling analyses would have to be done using eigen solutions. It may not be necessary to do this at each iteration since eqns. (6.2.1) may provide accurate enough approximations (at decidedly less computational cost) to proceed for a few iterations. The exact compromise of the two buckling calculation methods would naturally be problem dependent and only experience in using each method would provide a guide for future problems.

This argument can be extended to the case of panels made of elements of various stiffnesses i.e. laminate types, where again some compromise would have to be made between the accuracy of eigen solutions and the rather less costly (in terms of computational time) option of using an equivalent, smeared stiffness to evaluate the buckling loads. (In this work this problem has not been addressed and only panels made up of elements of the same stiffness (layup) are considered).

The relevant detail on the strain constraints and the reason for their choice can be found in section 3.2 and will not be repeated here. Suffice it to say that using the same type of "strength" constraint at system and element levels greatly facilitates the interpretation of the results especially when switching from one level to another.

A limit may be placed on displacements, in the x, y and z directions, of any node of the finite element model. These displacements (with upper and lower bounds) are written as

δ_{np} (eqn. (6.2.4)), where the subscripts n and p define the node number and degree of freedom (x, y and z) respectively of the displacement to be constrained.

CHAPTER 7

7 OPTIMIZATION METHOD AT THE SYSTEM LEVEL

7.1 Optimization Algorithm

The arguments put forward in favour of a sequential linear programming (LP) method for the optimization algorithm in section 4.1 hold whatever problem is considered. One of the possible disadvantages of this technique, however, (as mentioned in section 4.1) is that the linearizations are only approximations of the original constraint functions, and thus the step size needs to be controlled by move limits to ensure that the design stays in or near the feasible region. The more non-linear the objective function or constraints are, in terms of the design variables, the tighter these move limits must be and thus the slower the convergence of the solution. The system level optimization problem is, if anything, not as highly non-linear as the element level problem due to the exclusion of the ply-angle variables, and is thus even better suited to the use of a sequential LP method.

The move limit strategy applied at the system level is identical to that at the element level (see section 4.5).

7.2 Linearization Of The Objective Function

In section 6.1 the form of the objective function was given (eqn. 6.1.1) as

$$W(t) = \sum_{j=1}^{NEL} \sum_{i=1}^{L} (\rho A t)_{ij}$$

This is a linear function of the design variables t_{ij} and thus is suitable in the above form for use in the LP algorithm.

7.3 Linearization Of The Lamina Strain Constraints

The strain constraint functions are linearized at the system level, as at the element level, by using a Taylor series expansion (to first order) giving,

$$\{\varepsilon_l\}_{km} = (\{\varepsilon_l\}_{km})_a + \sum_{j=1}^{NEL} \sum_{i=1}^{L} (t-t_a)_{ij} \ (\{\partial\varepsilon_l/\partial t_{ij}\}_{km})_a \quad (7.3.1)$$

where NEL is the number of elements in the finite element model

L is the number of layers in element j

t is the thickness of layer i in element j

$\{\partial\varepsilon_l/\partial t_{ij}\}_{km}$ is the derivative of the strain vector for layer k of element m with respect to the thickness of layer i of element j.

The evaluation of the strain derivatives is explained in sections 7.5 and 7.5.1.

Note that eqn. (7.3.1) has a slightly different form to the equivalent equation (eqn. (4.3.10)) for the element level linearized strain function. This is due to the fact that at the system level the strain in any layer is considered to be a function of all the design variables in the structure i.e. layer thicknesses in all elements. At the element level only the layers in the laminate under consideration are used in the calculation of the derivatives and the linearized constraint function.

7.4 Linearization Of The Deflection Constraints

The linearized form of the deflection constraints is very similar to that of the strain constraints, and can be written as,

$$\delta_{np} = (\delta_{np})_a + \sum_{j=1}^{NEL} \sum_{i=1}^{L} (t-t_a)_{ij} \; (\partial \delta_{np} / \partial t_{ij})_a \qquad (7.4.1)$$

where δ_{np} is the displacement at node n in the direction p (x, y or z directions)

$(\partial \delta_{np} / \partial t_{ij})$ is the derivative of displacement δ_{np} with respect to thickness t_{ij}

The remaining notation is the same as that explained above for eqn. (7.3.1).

The method used for evaluating the derivatives ($\partial \delta_{np} / \partial t_{ij}$) is given in sections 7.5 and 7.5.2.

7.5 Constraint Derivative Evaluation Using The Finite Difference Technique

There are numerous methods for evaluating derivatives of the constraints with respect to the design variables. The most widely used of these are

(i) the behaviour space method

(ii) the design space method

(iii) the virtual load method

(iv) the finite difference method

The first three methods are briefly described in Appendix D and their various advantages highlighted. The finite difference method is explained below in more detail since it the method chosen for this work.

The various pro's and con's of the finite difference technique, as applied to structural optimization, can be explained using the following mathematical description. The derivative, or gradient, of any function at a given point can be approximated by (see figure 7.5.1),

$$\partial f/\partial x = (f(x+\Delta x) - f(x-\Delta x))/2\Delta x \qquad (7.5.1)$$

$$\partial f/\partial x = (f(x+\Delta x) - f(x))/\Delta x \qquad (7.5.2)$$

$$\partial f/\partial x = (f(x) - f(x-\Delta x))/\Delta x \qquad (7.5.3)$$

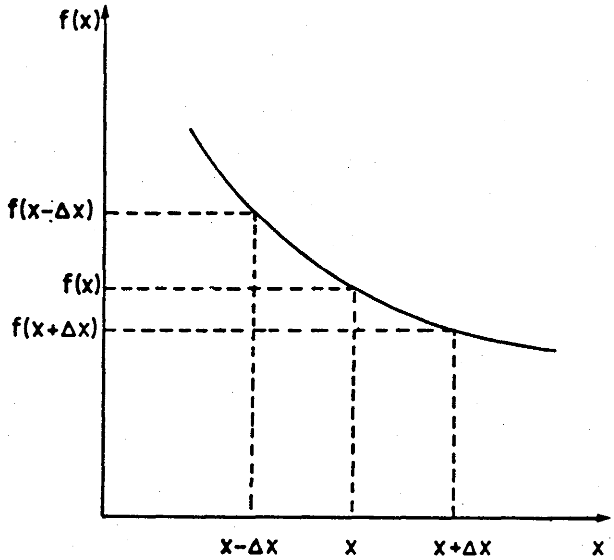

Figure 7.5.1 Finite difference methods

Eqn. (7.5.1) uses central differencing, eqn. (7.5.2) forward differencing and eqn. (7.5.3) backward differencing to obtain approximate derivatives of the function f(x).

The accuracy of the approximation is obviously dependent on the degree of non-linearity of the function f(x), the step size Δx at the point in question, and the differencing method chosen. In most cases central differencing will yield the best estimates of the derivatives, although numerical evidence indicates that eqns. (7.5.2) and (7.5.3) will generally also give a good approximation (Ref. [34]) and the variation in the results produced by eqns. (7.5.1) - (7.5.3) will be small.

Stuctural optimization problems typically include displacement and strain (or stress) constraints so these are used here to illustrate the application of finite differences in the evaluation of constraint derivatives.

In the upper level of optimization, the lamina thicknesses are the design variables, so the nodal displacements of the finite element model of the structure, can be written as

$$\delta_n = f(t_{ij}) \qquad (7.5.4)$$

where δ_n is the displacement of node n, and t_{ij} is the thickness of layer i in laminate type j.

Using equation (7.5.3) the derivatives of the displacement constraints with respect to t_{ij} can be written as below. The reason for the choice of backward differencing will become apparent later.

$$\partial\delta_n/\partial t_{ij} = (\delta_n(t_{ij}) - \delta_n(t_{ij} - \Delta t_{ij}))/\Delta t_{ij} \qquad (7.5.5)$$

Similarly the derivatives of the strain constraints can be written as

$$\partial\varepsilon/\partial t_{ij} = (\varepsilon(t_{ij}) - \varepsilon(t_{ij} - \Delta t_{ij}))/\Delta t_{ij} \qquad (7.5.6)$$

The nodal displacements in eqn. (7.5.6) are evaluated using the standard finite element equilibrium equation

$$\{F\} = [K]\{\delta\}$$

giving

$$\{\delta\} = [K]^{-1}\{F\} \qquad (7.5.7)$$

where $\{\delta\}$ is the nodal displacement vector containing all the δ_n values, and [K] is the stiffness matrix which is a function of the t_{ij} values.

The evaluation of the displacement derivatives (eqn. (7.5.5)) for all n design variables (t_{ij}) thus requires the solution of eqn. (7.5.7) n+1 times (since the displacement values associated with design variables t_{ij} and those associated with the incremented values ($t_{ij} - \Delta t_{ij}$) of all the design variables are required).

It should be noted that if a central differencing method was used that the number of finite element solutions required (eqn. (7.5.7)) required then rises to 2n+1 i.e. the computational effort involved in the analysis stages is practically doubled, since eqn. (7.5.7) needs to be solved for all ($t_{ij} - \Delta t_{ij}$) and ($t_{ij} + \Delta t_{ij}$). Any slight gain in the accuracy of approximation of the derivatives by this method is heavily outweighed by the additional computational effort required.

Since forward and backward differencing involve the same computational effort and neither method is sure to consistently give better results than the other, the choice was made, somewhat arbitrarily, to use backward differencing in this work.

The fact that even backward differencing calls for n+1 finite element solutions (n design variables) for each iteration of the design optimization procedure, is the major drawback of using differencing methods to evaluate constraint derivatives. Although this certainly implies more computational effort than is associated with, say, the design space, behaviour space or virtual load methods mentioned above, the difference becomes less marked as the number of (active) constraints becomes large (as may frequently happen if stress, displacement and buckling constraints are considered). It also has a slight advantage in that the number of solutions required is fixed, and so the computational effort required is always a known quantity, irrespective of the number of constraints.

The greatest advantage of finite differencing though, is its ease of use and adaptibility. The design space and behaviour space methods require detail knowledge of the finite element formulations (shape functions etc) of the elements used, and access to the finite element global stiffness matrix ([K]) (or another must be created outside of the finite element program). These methods are thus frequently limited to use with only one specific finite element package. In contrast, finite difference methods can be used with any element and any finite element program, with no need for detail knowledge of their internal workings. This makes them particularly attractive for use in development work so that new elements may be included in the design process with very little extra programming effort, and even changes to other finite element systems can be made quite easily.

7.5.1 Evaluation Of The Lamina Strain Constraint Derivatives

In order to evaluate the individual lamina strains in a plate or shell by classical lamination theory, information is needed concerning the midsurface strains and flexure (curvature) induced in the element. This information is frequently obtainable directly from the output of the finite element program used for the structural analysis (as is the case with the program LUSAS used in this work). Some programs may, however, only give top and bottom surface strains, in which case a little simple manipulation (using basic elasticity formulae) of the results is required to get them into the form needed.

The information extracted from the finite element analysis is thus $\varepsilon_x^\circ, \varepsilon_y^\circ, \varepsilon_{xy}^\circ, \kappa_x, \kappa_y$ and κ_{xy} where ε° and κ denote the midsurface strains and curvatures respectively. These are obtained for all n+1 analyses i.e. for all analyses using t_{ij} and $(t_{ij} - \Delta t_{ij})$. Using these results the derivatives of the plate strains can be obtained by the finite difference method. Thus

$$(\partial \varepsilon_x^\circ / \partial t_{ij})_m = (\varepsilon_x^\circ(t_{ij}) - \varepsilon_x^\circ(t_{ij} - \Delta t_{ij}))_m / \Delta t_{ij} \qquad (7.5.1.1)$$

where m (subscript) denotes element (or plate) m, and t_{ij} the thickness of layer i in laminate type j.

Similar expressions can be written for the other components of midsurface strain and curvature.

Now, in section 3.2.2 it was shown that individual lamina strains can be written as (using the element/plate axes)

$$\{\varepsilon_l\}_i = \begin{Bmatrix} \varepsilon_x \\ \varepsilon_y \\ \varepsilon_{xy} \end{Bmatrix}_i = \begin{Bmatrix} \varepsilon^\circ_x + \chi_x z_i \\ \varepsilon^\circ_y + \chi_y z_i \\ \varepsilon^\circ_{xy} + \chi_{xy} z_i \end{Bmatrix} \qquad (7.5.1.2)$$

(eqn. (3.2.2.9))

or

$$\{\varepsilon_l\}_i = \{\varepsilon^\circ\} + \{\chi\}\, z_i \qquad (7.5.1.3)$$

where z_i is the distance of the centre of the lamina from the plate midsurface, and $\{\varepsilon^\circ\}$ and $\{\chi\}$ are the vectors of the midsurface strains and curvatures respectively (obtained from the finite element analysis).

Thus the derivatives of the strain in layer k of element m with respect to the design variable t_{ij} is given by

$$\{\partial\varepsilon_l/\partial t_{ij}\}_{km} = \{\partial\varepsilon^\circ/\partial t_{ij}\}_m + \{\partial\chi/\partial t_{ij}\}_m z_{km} + \{\chi_m\}(\partial z_{km}/\partial t_{ij}) \qquad (7.5.1.4)$$

and thus

$$\{\partial\varepsilon_l/\partial t_{ij}\}_{km} = \{\partial\varepsilon^\circ/\partial t_{ij}\}_m + \{\partial\chi/\partial t_{ij}\}_m z_{km} \qquad (7.5.1.5)$$

except where $i \neq k$ and the i and k being considered are in the same element, in which case

$$\{\partial\varepsilon_l/\partial t_{ij}\} = \{\partial\varepsilon^\circ/\partial t_{ij}\}_m + \{\partial\chi/\partial t_{ij}\}_m z_{km} + \{\chi/2\} \qquad (7.5.1.6)$$

since

$$z_k = 1/2\left(\sum_{n=1}^{k-1} t_n - \sum_{n=k+1}^{L} t_n\right) \qquad \text{(eqn. C.7)}$$

giving

$$\partial z_{km}/\partial t_{ij} = 1/2 \qquad \text{for } i \neq k$$
$$= 0 \qquad \text{for } i = k$$

The components of the vectors $\{\partial \varepsilon^{\circ}/\partial t_{ij}\}_m$ and $\{\partial \chi/\partial t_{ij}\}_m$ are evaluated using equations such as eqn. (7.5.1.1) and so $\{\partial \varepsilon_{\ell}/\partial t_{ij}\}_{km}$ is easily calculated.

Strain constraints are, however, generally expressed in terms of the lamina longitudinal (L) (with respect to fibre direction), transverse (T) and shear (LT) strains. These strains can be obtained using the transformation matrix derived in section 3.2.2 and eqns. (7.5.1.3) - (7.5.1.5), to give

$$\{\varepsilon'_{\ell}\}_{km} = [T]\{\varepsilon_{\ell}\}_{km} \qquad (7.5.1.6)$$

which leads to

$$\{\partial \varepsilon'_{\ell}/\partial t_{ij}\}_{km} = [T]_{km}\{\partial \varepsilon_{\ell}/\partial t_{ij}\}_{km} \qquad (7.5.1.7)$$

where

$$\{\varepsilon'_{\ell}\}_{km} = \{\varepsilon_L \quad \varepsilon_T \quad \varepsilon_{LT}\}^T_{km}$$

Eqn. (7.5.1.7) can be written in a slightly expanded, more explicit, form as

$$\begin{Bmatrix} \partial \varepsilon_L/\partial t_{ij} \\ \partial \varepsilon_T/\partial t_{ij} \\ \partial \varepsilon_{LT}/\partial t_{ij} \end{Bmatrix}_{km} = [T]_{km} \begin{Bmatrix} \partial \varepsilon_x/\partial t_{ij} \\ \partial \varepsilon_y/\partial t_{ij} \\ \partial \varepsilon_{xy}/\partial t_{ij} \end{Bmatrix}_{km} \qquad (7.5.1.8)$$

Thus eqns. (7.5.1.1),(7.5.1.4),(7.5.1.5) and (7.5.1.8) can be used to evaluate the derivatives of the strain constraints.

7.5.2 Evaluation Of The Deflection Constraint Derivatives

The results of the n+1 finite element analyses are again used to obtain an approximate constraint derivative value by using finite differences. The information required from the finite element analyses is the actual displacement of the constrained nodes in the direction specified eg. $(\delta_4)_x$ being the displacement of node 4 in the global x-direction.

Having obtained all the required displacement values for all cases of t_{ij} and the incremented values $(t_{ij} - \Delta t_{ij})$ the following equation is used to evaluate the constraint derivative

$$\partial \delta_{np} / \partial t_{ij} = (\delta_{np}(t_{ij}) - \delta_{np}(t_{ij} - \Delta t_{ij}))/\Delta t_{ij} \qquad (7.5.2.1)$$

where δ_{np} is the displacement of node n in the direction p (p being used to define the x, y or z directions)

Displacement constraints are thus readily evaluated using finite differences.

7.6 Linearization Of The Buckling Constraint Equations

As stated in section 6.2 the buckling loads and associated constraints are evaluated in exactly the same way at element level and system level. The linearization of the buckling constraints is thus achieved in a manner similar to that in section 4.4 (the linearization of the buckling constraint equations at the element level). The only difference is that the derivatives of the buckling loads with respect to the various lamina ply angles are not considered since the lamina orientations are not considered as variables at the system level. The linearized equation for the buckling load $(F_x)_{crit}$ to be used in the constraint equation (6.2.1) can thus be written as

$$(F_x)_{crit} = (\pi a)^2 [D_{11} m^2/a^4 + 2(D_{12} + 2D_{33})/(ab)^2 + D_{22}/(m^2 b^4)] + \sum_{j=1}^{L} (t-t_a)_j (\partial F_x/\partial t_j)_a \qquad (7.6.1)$$

The meaning of all the terms is explained in sections 3.2.1 and 4.4, and the method of evaluating the derivatives $\partial F_x/\partial t_{ij}$ can be found in section 4.4 as well.

The linearized form of the equations for evaluating $(F_y)_{crit}$ and $(F_{xy})_{crit}$ will be similar in form i.e. they will be the same as eqns. (4.4.4) and (4.4.5) (or (4.4.10)) respectively, but with all the $\partial F_y/\partial\theta_j$ and $\partial F_{xy}/\partial\theta_j$ terms zero.

CHAPTER 8

8 ILLUSTRATIVE EXAMPLES OF SYSTEM LEVEL OPTIMIZATION

A FORTRAN program (UPOPT - described in Appendix G) was developed in order to substantiate the theory developed in chapters 6 - 8. Four problems, solved using this program, are presented to illustrate the effectiveness of the method developed.

8.1 Flat Panel

The first example considered is the optimization of a flat panel (figure 8.1) made of two laminate types and subjected to multiple loading (32000 N in tension and 32000 N in shear - distributed over nodes 7, 14 and 21). Buckling and strain constraints were applied with the same strain limits imposed as those given in chater 5.

Design variable linking was used to define that elements 1 to 6 were all of laminate type 1 and elements 7 to 12 are all of laminate type 2. Futher linking is used to ensure that both the laminate types remain symmetric about their midplane. The two initial laminate designs are defined in Table 8.1, with only one half of the symmetric layup being given (layer 1 is the uppermost layer).

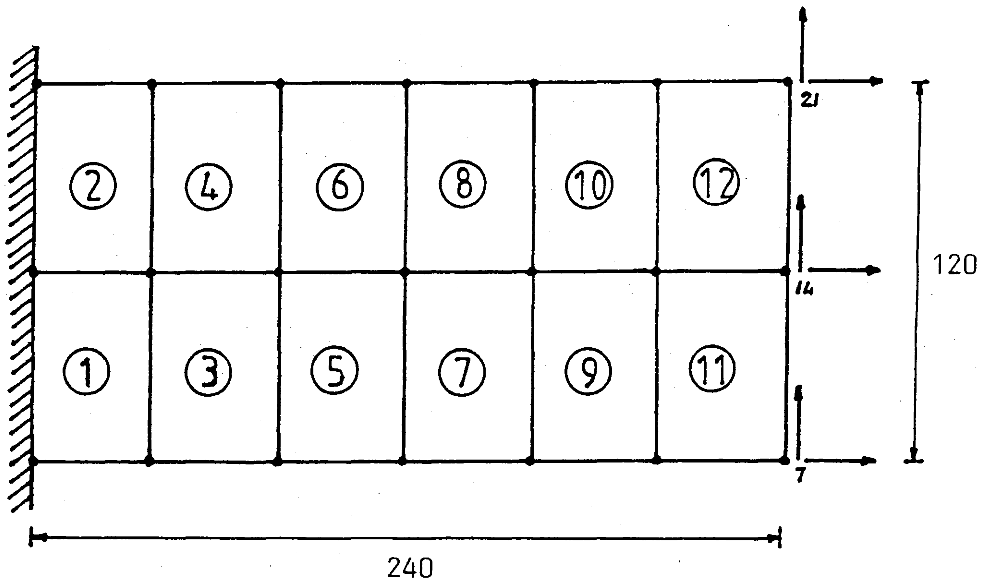

Figure 8.1 Flat panel

The optimization process converged (with the weight change in consecutive iterations being less than 2%) after 8 iterations and the final results are summarized in Table 8.1.

Table 8.1 - Flat panel example

Laminate type	Initial design (symmetric) t (mm)	Final design (symmetric) t (mm)	Ply angle (deg)
1. Layer 1	2.5	0.610	0.0
2	1.25	0.935	-45.0
3	1.25	0.143	45.0
2. Layer 1	2.0	0.478	0.0
2	2.0	0.726	-45.0
3	2.0	0.094	45.0
Weight (kg)	5.10	1.82	

The results are very much as could be expected with the two load cases considered. The $\pm 45^{\circ}$ material component is the largest as this provides optimal resistance to the shear load and so keeps the strains induced within the prescribed limits. There is also a substantial component of material in the 0° direction. These fibres would provide most of the resistance to the tension load, reduce the shear strain in the $\pm 45^{\circ}$ layers for this load case and provide some of the bending resistance required to react the shear load on the end.

8.2 Rectangular Box Beam

The next two examples are based on the 34 element rectangular box structure shown in figure 8.2

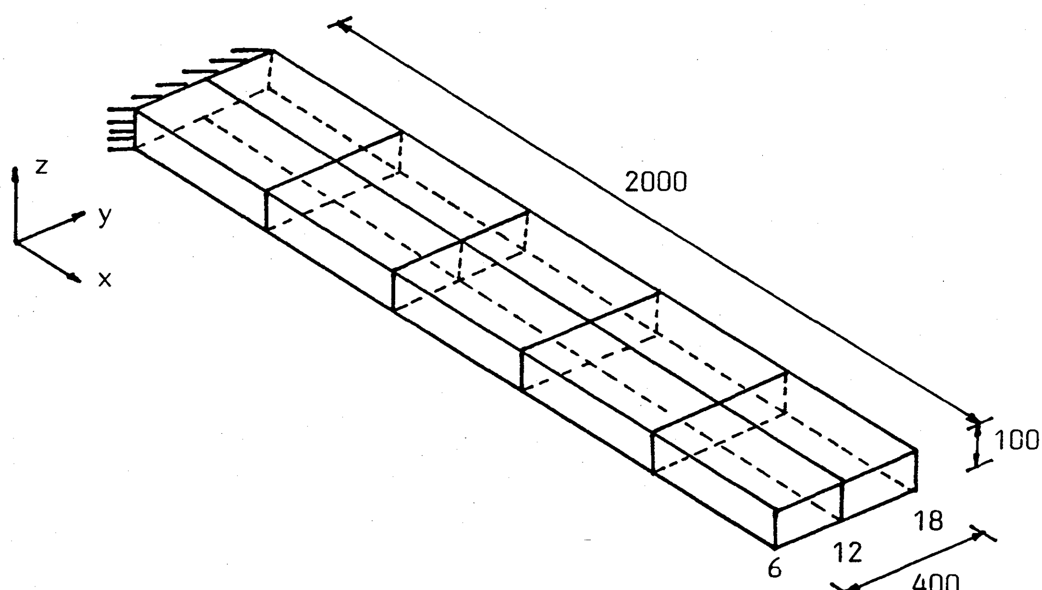

Figure 8.2 Rectangular box structure

The structure for these two problems was defined to be made up of the three laminate types given in Table 8.2. The four elements in the top skin nearest to the fixed end of the box were defined to be of laminate type 1, as were the corresponding elements in the lower skin. The remaining skin elements were defined to be of laminate type 2 and the webs and ribs all of laminate type 3. Strain, buckling and displacement constraints ($\pm$80 mm maximum deflection at the tip) were considered for the first problem. Buckling constraints were not included in the second problem which was otherwise identical. The strain limits imposed were 0.004 in the longitudinal and transverse fibre directions and 0.0055 on the shear strain. The multiple load cases given below were selected to ensure that all the three types of constraints were active in some region of the structure.

Load case	No. 1 (twist)		No. 2 (comp.)		No. 3 (bend)	
	Force	DOF	Force	DOF	Force	DOF
Node no. 6	-15000	z	-15000	x	12000	z
12	0	-	-30000	x	24000	z
18	15000	z	-15000	x	12000	z

The initial and final converged designs for the both problems (achieved after 5 iterations in both cases) are given in Table 8.2 below. Note that the designs were constrained to remain symmetric about the midplane and thus the layup for only one half of the laminate types are given, with layer 1 being the uppermost in the laminate.

Table 8.2 - Rectangular box structure

Laminate type	Initial design t (mm)	Final design (buckling constraint) t (mm)	Final design t (mm)	Ply angle (deg)
1. Layer 1	2.5	2.052	2.102	0.0
2	1.25	0.413	0.294	-45.0
3	1.25	0.912	0.294	45.0
2. Layer 1	2.0	1.772	1.971	0.0
2	2.0	0.319	0.325	-45.0
3	2.0	1.317	1.256	45.0
3. Layer 1	1.0	0.876	0.221	-45.0
2	1.0	0.672	0.221	45.0
Weight (kg)	324.6	203.8	173.2	

The final designs satisfy all the constraints imposed on the structure and on inspection can be seen to be similar to those which might have been obtained using traditional design and sizing methods.

All the elements at the root end (fixed end) of the rectangular box are of laminate type 1 and, as can be expected, the layup in this region for both problems is predominantly in the 0° degree direction to provide the necessary strength and stiffness to satisfy the bending loads. There is some material retained in the $\pm 45^{\circ}$ direction to provide additional resistance to the torsional load but in the problem with buckling constraints there is significantly more material in the 45° direction to help satisfy those constraints.

The outer elements (laminate type 2) also contain a large component of the 0° ply to assist the design in satisfying the displacement constraints under the bending load. The thickness of the 45° ply may initially seem surprising but there are logical explanations for this. Considering the buckling constrained problem first, a larger component of 45° layers is required in laminate type 2 than in laminate type 1 to prevent buckling under the direct compressive load since the thickness of the 0° ply is less in the former laminate type. It is also well known that to increase the torsional stiffness of a cantilever type structure such as the one under consideration (ie. so that the constraints are satisfied) material should be added at the tip rather than at the root end. The greatest torsional resistance is provided by the $\pm 45^{\circ}$ layers and thus the thickness of this layer(s) has been increased in both problems.

These results demonstrate the ability of the optimization method at the upper level to satisfy the buckling constraints on the structure while keeping the strain and displacement constraints within the prescribed limits.

The preferred ply orientations and thicknesses for satisfaction of the buckling constraints can in many structures differ significantly from those needed to satisfy only strain and displacement constraints (eg. the case of shear webs and shear buckling). When all the constraint types are considered simultaneously it can thus be difficult to interpret what the contribution of each ply is in satisfying the various constraints. Since the feasibility of the method for problems with buckling constraints has been shown in the examples above only strain and displacement constraints will be considered in the remaining example so that interpretation of the results and comparison with "tradtional" design method results is made easier.

8.3 Multilaminate Rectangular Box Beam

The final example given in this chapter is a refinement of the above rectangular box problems in that a greater number of laminate types (ie. design variables) is considered. These are defined in Table 8.3. Design variable linking was used to define that the four root end elements in the bottom skin were of laminate type 1, the four root end elements in the top skin of laminate type 2, the remaining bottom skin of laminate 3 and the remaining top skin elements of laminate type 4. The shear webs (spars) and ribs were all defined to be of laminate type 5.

Linking was again used to ensure laminate symmetry about the midplane and the layups given in Table 8.3 thus only define the one half of the laminate (layer 1 being the furthest from the midplane).

The strain limits used were 0.004 for the longitudinal and transverse strains and 0.0055 for the shear strain, and a limit of $\pm$120 mm was put on the displacements of all the tip nodes while the load cases considered were:-

Load case	No. 1		No. 2	
	Force	DOF	Force	DOF
Node no. 6	12000	z	10000	z
12	24000	z	15000	z
18	12000	z	20000	z

The initial and final converged designs are given in Table 8.3 below. The convergence criteria was a weight change of less than 2% and this was achieved after 5 iterations.

Table 8.3 - Multiple laminate rectangular box

Laminate type	Initial design t (mm)	Final design t (mm)	Ply angle (deg)
1. Layer 1	2.5	1.169	0.0
2	1.25	0.218	-45.0
3	1.25	0.218	45.0
2. Layer 1	2.5	1.150	0.0
2	1.25	0.154	-45.0
3	1.25	0.154	45.0
3. Layer 1	2.0	0.376	0.0
2	2.0	0.204	-45.0
3	2.0	0.204	45.0
4. Layer 1	2.0	0.307	0.0
2	2.0	0.203	-45.0
3	2.0	0.506	45.0
5. Layer 1	1.0	1.529	-45.0
2	1.0	1.529	45.0

These results show that a large quantity of material has been put into the shear webs compared to the top and bottom skins. This unexpected solution is the result of a problem with the elements used in the finite element model rather than a problem with the optimization procedure. The QS4 4-node shell elements in LUSAS, which were used in these problems, were shown to give inaccurate results when used to model a cantilever beam with an end load (seen as a shear load by the elements). The finite element model produced end deflections much smaller than the analytical results, indicating an effective stiffness much greater than the true stiffness. Since the spars in the rectangular box are essentially such cantilevers, their effective stiffness was much greater proportionately than the material in the skins. This enhanced stiffness thus made the spars the most "attractive" place to put extra material in terms of satisfying the constraints in the optimization procedure.

This problem was not really noticeable in the two previous examples as the limited number of design variables (laminate types) allowed less freedom for the redistribution of material.

Bearing the modelling inaccuracies in mind, the results shown in Table 8.3 can be regarded as realistic and accurate. The material in the skins also shows a distribution of material similar to that that would be obtained using conventional design methods. The root end elements (laminate type 1 and 2) contain predominately 0° fibres to resist the bending load and to provide the required stiffness to meet the displacement requirements. Some additional torsional resistance is supplied by the 45° layers, and these plies also help to reduce the shear strains induced in the 0° degree fibres by the torsion component of the second load case.

The outer elements (laminate types 3 and 4) contain only just enough material to resist the bending load and to satisfy the tip displacement constraints for the first load case. Both laminate types (3 and 4) contain a large proportion of 45 fibres as they provide the most effective resistance (in terms of weight) to the torsion component of the second load case. Again the optimization routine has placed the torsionally stiffer elements at the tip in preference to other parts in accordance with well established minimum weight design rules for wing type structures.

If the finite element model had been more accurate (ie. less tendency to put material in the spars) it is expected that the proportions of the material in all the layers of the various laminate types would be very similar but with all the thicknesses of the skins suitably increased to take the bending and torsion loads, presently taken by the spars.

These examples demonstrate the effectiveness and viability of the method developed for the system level of optimization. It can therefore be concluded that the method is entirely suitable for use in the multilevel optimization system.

CHAPTER 9

9 RESULTS OF MULTILEVEL OPTIMIZATION

The examples given in this chapter show that the final result (in terms of weight and the design variable values) and the speed of convergence of the multilevel optimization is relatively insensitive to the weighting coefficients used in the element level objective function. They also show that the results obtained are feasible and realistic and can readily be explained using simple design logic.

9.1 Influence Of The Weighting Coefficients

The first point is illustrated using two structures which were optimized using three different sets of weighting coefficients. The structures considered were cantilever box sections representative of forwrd swept and delta wing boxes, shown in figures 9.1 and 9.2 respectively. A vertical load (ie. in the +z direction) of 60000N, distributed over the tip nodes of the lower skin, was the load case considered for both the structures and strain and displacement constraints were imposed. The strain limits used were 0.004 for the longitudinal and transverse ply strains and 0.0055 for the shear strains throughout, while the displacement limits were ±80mm at the tip nodes of the forward swept wing and ±60mm for the delta wing. These problems were run using weighting coefficients (0.8,0.2), (0.5,0.5) and (0.2,0.8) where the first value is the coefficient associated with the weight part of the element level objective function and the second part is that associated with the strain energy change part of the function.

9.1.1 Forward Swept Wing

The results of the swept wing (figure 9.1) are discussed first.

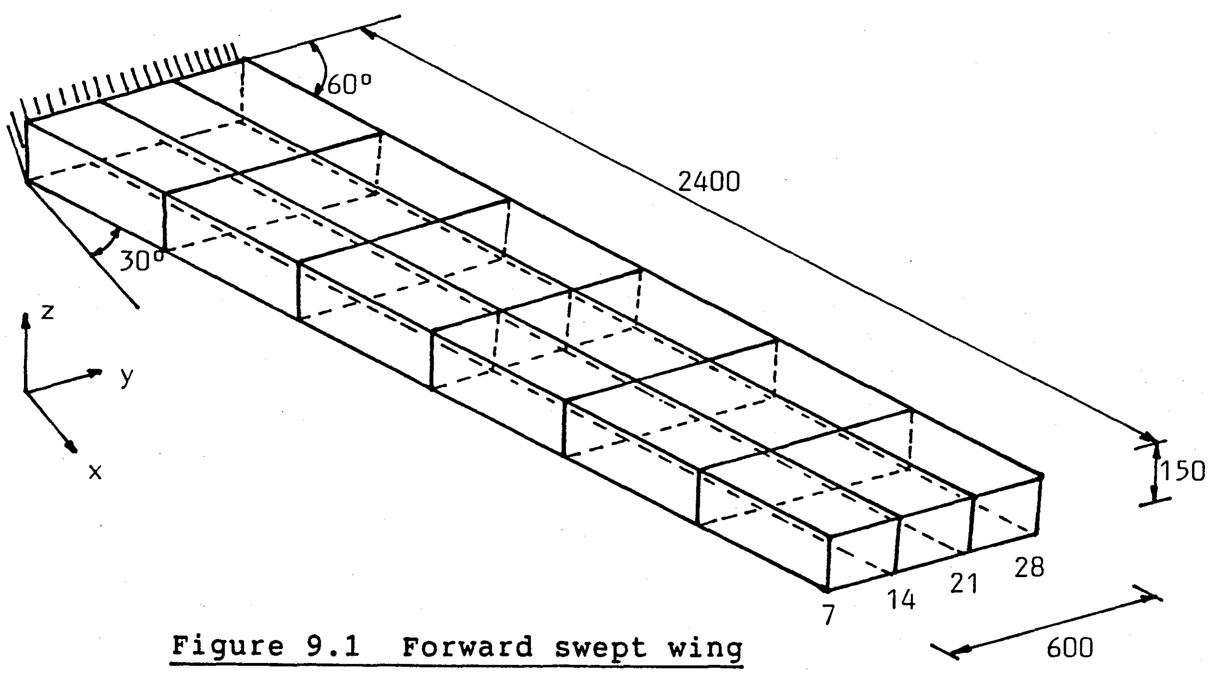

Figure 9.1 Forward swept wing

Design variable linking was used to define that all the elements in the top skin were of laminate type 1, all those in the bottom skin of laminate type 2 and all the spar webs and ribs of laminate type 3. All three laminate types were constrained to remain symmetric about their midplane. The starting designs for these laminates as well as the optimized values for the various weighting coefficients are given in Table 9.1 below, with only the upper half of the symmetric layups being given (layer 1 is uppermost). It should be noted that the ply orientations are given relative to the element x-axes which are all parallel to the wing leading and trailing edges.

Table 9.1 - Swept wing results (I)

Lam. type	Initial design		Final design					
			WC1 = 0.8 WC2 = 0.2		WC1 = 0.5 WC2 = 0.5		WC1 = 0.2 WC2 = 0.8	
	t	θ	t	θ	t	θ	t	θ
1.Ply 1	2.5	0.0	3.21	-14.7	3.21	-12.2	3.34	-15.3
2	1.25	-45.0	0.10	-18.4	0.04	33.3	0.02	-10.6
3	1.25	45.0	2.15	29.6	2.44	34.3	2.22	25.5
2.Ply 1	2.0	0.0	4.58	11.2	3.02	16.3	4.74	17.1
2	2.0	-45.0	1.31	-28.6	1.93	-23.1	1.56	-23.9
3	2.0	45.0	0.48	60.2	0.91	49.8	0.45	66.0
3.Ply 1	1.0	-45.0	0.98	-45.0	1.60	-41.7	0.83	-39.0
2	1.0	45.0	0.87	46.9	0.92	46.9	1.12	49.0
Weight	556.4		604.3		608.2		624.2	
Displ.								
Node 7	87.7		77.6		76.4		76.4	
14	94.1		83.6		79.1		82.0	
21	99.5		89.0		83.2		86.8	
28	105.4		93.8		87.8		91.1	

The ply thicknesses and the nodal displacements are given in mm, the ply angle in degrees and the weights in kg.

The multilevel system, in all the cases shown, converged after 4 iterations, with the convergence criteria having been taken to be a weight change in consecutive iterations of less than 2%. The weight of the structure was evaluated in each iteration after the upper level optimization had been performed. Each multilevel iteration included 5 iterations at the upper level and 8-10 iterations per laminate type at the lower level.

On inspection it can be seen that the final results obtained when using the different weighting coefficients are remarkably similar in terms of the design variables (particularly the ply orientations) and the final weight. Where there are large differences in the final ply angles chosen (eg. layer 2 of laminate type 1) the related thicknesses are generally small relative to the entire laminate and so their effect on the overall laminate stiffness is small. Any differences in ply orientation in these cases thus have a very small effect indeed on the laminate rigidity values used in the finite element analysis.

Since the final design variables for each test case were similar, the displacements of the loaded structure were, as could be expected, very similar as well. The slightly lower values of displacements associated with the case with equal weighting coefficients are probably due to the proportionately higher thickness variable values assigned to the spar webs (laminate type 3). As explained in chapter 8 the elements used in this work perform poorly in a cantilever type situation (as the spar webs can be regarded) and appear, in terms of the finite element model, to have a stffness greater than the true value. As a result any additional material added to these elements has the effect of increasing the stiffness by a larger amount than it should (and hence the smaller displacements at the tip).

The displacements of the tip nodes, shown in Table 9.1, are all, with the exception of those at node 7, greater than the 80mm prescribed limit and yet were accepted as a feasible solution by the optimization routine. The explanation for this lies in the fact that sequential linear programming was used as the optimization algorithm. The constraints, which are all non-linear, thus had to be converted to linear approximations. The boundaries of the linearized feasible design region thus only coincide with those of the true feasible region at the point of linearization. Futhermore the solution to a linear programming problem always lies at a vertex of the feasible region and these generally lie outside the feasible region of the non-linear design space. The optimum found in these cases was thus the feasible solution in terms of the linearized design space which here obviously lay outside the true, non-linear feasible region.

9.1.2 Delta Wing

The delta wing structure that was optimized is shown in figure 9.2 below.

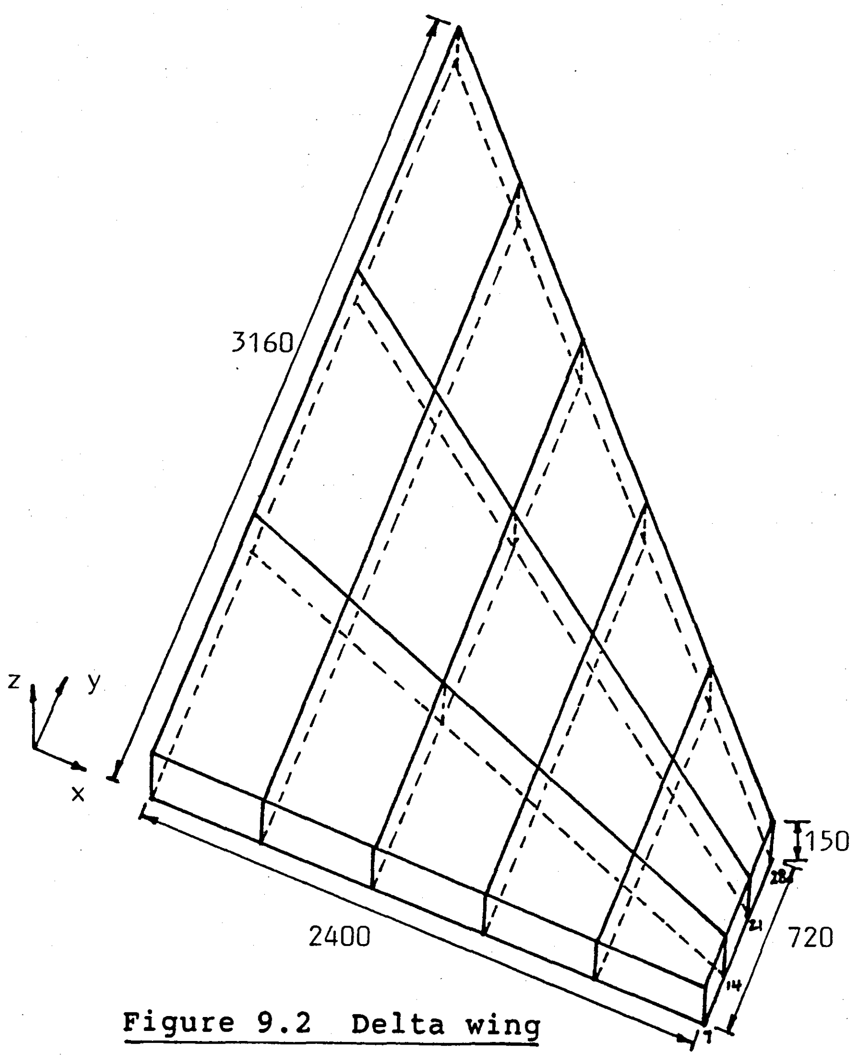

Figure 9.2 Delta wing

Design variable linking was used here to define that all the trailing edge elements in the top and bottom skins were of laminate type 1, the leading edge elements in top and bottom skins of laminate type 3 and the remaining skin elements of laminate type 2. The spar webs and ribs were all of laminate type 4. Futher variable linking was used to ensure that all these laminates remained symmetric about their midplane. The initial designs for all 4 lamiante types, as well as their optimized values are given in Table 9.2, with only the upper half of the symmetric layups being given (layer 1 is the uppermost). In this case the ply orienatations are also given with respect to the element x-axes which are here taken to be parallel to the spanwise lines in the finite element model immediately behind, but adjacent to, the elements being considered ie. the trailing edge is the local x-axis for all the trailing edge elements but the leading edge does not form an x-axis for any elements.

Table 9.2 - Delta wing results

Lam. type	Initial design		Final design					
			WC1 = 0.8 WC2 = 0.2		WC1 = 0.5 WC2 = 0.5		WC1 = 0.2 WC2 = 0.8	
	t	θ	t	θ	t	θ	t	θ
1.Ply 1	2.5	0.0	2.18	-13.4	1.83	-11.9	2.48	-10.3
2	1.25	-45.0	0.78	-13.1	0.05	-8.1	0.28	-3.3
3	1.25	45.0	0.05	29.2	0.03	26.8	0.02	83.2
2.Ply 1	2.0	0.0	0.40	1.0	0.57	3.1	0.53	6.3
2	2.0	-45.0	0.21	-72.4	0.21	-73.5	0.11	-83.2
3	2.0	45.0	0.22	56.9	0.17	55.1	0.10	42.9
3.Ply 1	1.0	0.0	0.20	19.1	0.41	24.7	0.57	38.4
2	1.0	-45.0	0.44	-57.0	0.31	-64.0	0.47	-57.5
3	1.0	45.0	0.41	51.5	0.41	64.3	0.15	45.6
4.Ply 1	1.0	-45.0	1.25	-45.8	2.12	-46.9	0.82	-42.8
2	1.0	45.0	0.62	47.8	1.37	49.6	1.21	45.8
Weight	777.8		279.9		288.2		279.6	
Displ.								
Node 7	34.5		62.3		60.4		58.8	
14	35.7		64.1		62.3		60.5	
21	35.9		64.4		62.9		62.0	
28	35.0		63.0		61.9		61.1	

The ply thicknesses and the nodal displacements are given in mm, the ply angle in degrees and the weights in kg.

Convergence of the multilevel system, defined by a weight change of less than 2% in consecutive iterations, was achieved in 4 iterations for all the cases above.

As for the swept wing examples above it can be seen that the final design variables and structural weights for the delta wing optimized with the three combinations of weighting coefficients, are all very similar. Since the same trends exhibited by the swept wing results (Table 9.1) are apparent in the delta wing results (Table 9.2) suffice it to say that the discussion above, on the swept wing, applies directly to the delta wing as well.

9.1.3 Concluding Discussion

The swept and delta wing examples given above show that the final design results and the speed of convergence of the multilevel system are thus not very sensitive to the weighting coefficients chosen for use in the element level optimization. The most likely explanation for this is that although the thickness variables can change quite significantly when changing from one level to the other the ply orientations get close to their final, optimal values in the very first entry to the element level optimization (this happens irrespective of which weighting coefficient was chosen). The resultant effect is that only the ply thicknesses are being altered significantly in subsequent iterations at the element level and thus much the same type of function is being performed as at the system level. Thus in the case of the weighting coefficients being biased if favour of the weight part of the element level objective function, the displacement constraints will be violated after the element level optimization, and the system level thus has to scale the design before starting its optimization process. The greater the weighting coefficient WC1 (weight part of the objective function) relative to the weighting coefficient WC2 (strain energy change part) the greater the scaling factor is likely to be. Since the ply angles selected in all the cases is similar, however, it is to be expected that the system level optimization should converge to optimal points with similar thickness variable values even if the starting points are slightly different. The results show that this is indeed the case, bearing in mind the problem of the zig-zaging (of the solutions) associated with sequential LP solutions (which may to some extent account for the slight differences in the results).

Inspection of the results given in Tables 9.1 and 9.2 shows that the final solutions are quite feasible and can be explained using simple design logic. The effectiveness of the multilevel optimization system, in terms of producing optimal results is, however, better illustrated in the following two examples where a greater number design variables were used.

9.2 Multilaminate Forward Swept Wing

The first example is a forward swept wing box type structure of the same general arrangement as that shown in figure 9.1. For this problem, however, the elements were defined to be of different laminate types as follows:- the 9 root end elements of the lower skin were of laminate type 1, the 9 root end elements of the top skin of laminate type 2, the remaining bottom and top skins of laminate types 3 and 4 respectively and the spar webs and ribs of laminate type 5. As in previous examples the designs were constrained to remain symmetric about their midplane. The initial designs are defined in Table 9.3 with only the upper half of the laminates being given (layer 1 being the uppermost). The loading used was the same as the previous swept wing examples (ie. 60 000N distributed over the lower skin tip nodes) and a displacement limit of 80mm was placed on the tip nodes of the structure. The strain limits imposed were, as before, 0.004 on the allowable longitudinal and transverse strains and 0.0055 on the allowable shear strain. The structure was optimized using weighting coefficients of 0.5 for both parts of the element level objective function. In view of the discussion above on the influence of the weighting coefficients it is not expected that the results would be significantly different if some other coefficients had been used.

The design converged in 4 iterations (with a weight change of less than 2%) and the results are given below in Table 9.3.

Table 9.3 - Multilaminate swept wing results

Laminate type	Initial design		Final design	
	t	θ	t	θ
1. Layer 1	2.5	0.0	2.41	3.1
2	1.25	-45.0	0.15	83.1
3	1.25	45.0	3.08	35.4
2. Layer 1	2.5	0.0	6.14	13.6
2	1.25	-45.0	1.26	-24.5
3	1.25	45.0	0.90	53.0
3. Layer 1	2.0	0.0	0.77	0.4
2	2.0	-45.0	0.04	-44.4
3	2.0	45.0	0.12	45.6
4. Layer 1	2.0	0.0	0.76	0.2
2	2.0	-45.0	0.05	-44.0
3	2.0	45.0	0.14	44.0
5. Layer 1	1.0	-45.0	2.40	-32.7
2	1.0	45.0	1.64	40.0
Weight (kg)	556.4		460.2	
δ_z node 7	87.7		80.6	
14	94.1		84.4	
21	99.4		87.5	
28	105.4		90.0	

The ply thicknesses and the nodal displacements are given in mm, the ply angle in degrees and the weights in kg. The ply orientations are again given with respect to the element local x-axes which all lie parallel to the spanwise lines shown in the finite element grid in figure 9.1.

The final design is feasible in that all the constraints have been satisfied with respect to the linearized problem (a sequential LP is used as the optimization algorithm). The displacements at the tip nodes are, however, greater than the prescribed limits due to the inaccuracies involved in making linear approximations to the non-linear constraints, and thus the design is not truly feasible with respect to the non-linear design space. This problem was addressed in more detail in the discussion on the swept wing optimization earlier in this chapter.

The final values assigned to the various design variables are quite realistic with the exception of the unduly heavy spar webs and ribs (laminate type 5). The reason for this phenomenon was poor element behaviour in the finite element model, which is discussed at length in chapter 9. Notwithstanding this, the values assigned to the other design variables can be quite easily explained.

Considering first laminate type 2 (root end elements of the top skin), a very large proportion of the material has been orientated at an angle of 13.6° ahead of the spanwise lines.

This would produce a favourable shear coupling effect when the laminate is loaded in compression (as it is under the applied bending load) which would tend to twist the wing leading edge down. These effects can be used to achieve a minimum weight design whilst satisfying the displacement constraints ie. under a given bending load the wing leading edge will twist up less than for the 0° or isotropic material case. This characteristic has already been applied to aircraft with forward swept wings to avoid divergence problems eg. the Grumman X-29 wing is made of composites with the major material axis 9° ahead of the 25% chord line. The other components in this laminate can be seen to be at just about $\pm 40^\circ$ on either side of the major material direction (13.6) which is close to the optimal orientation for torsional resistance (bending induced torsion is found in swept wings) and for relief of the shear strains induced in the major material component.

The solution given for laminate type 1 (root end elements of the bottom skin) is not quite as easily explained. Layers 1 and 3 contain nearly all the material in this laminate - layer 2 can almost be ignored except for the small contribution it makes to reducing shear and transverse stresses in the other layers. They are both angled ahead of the spanwise lines and hence would produce some advantageous shear coupling effects. While each of these layers assists in this role, layer 1, being near to 0° offers substantial bending stiffness and layer 3, being closer to the 45° position offers good torsional resistance. The angle between them is sufficient to ensure that they provide some measure of relief to each other in terms of shear and transverse strains.

The reason for laminate types 1 and 2 being so different is not apparent, but can perhaps be explained by there being two or more local optima near to each other, to which the designs may be driven. The exact one that is found may be dependent on the loads imposed on and the stress state induced in the various laminates.

In contrast to laminates 1 and 2, the final designs for laminate type 3 and 4 (outer skin elements of the bottom and top skins respectively) are very similar indeed - so similar in fact that a discussion of one set of results will suffice for the other. This similarity between top and bottom skins could be expected since the allowable strains in tension and compression are the same and no buckling constraints have been included. There is sufficient material in layer 1 of these laminates orientated at 0° (or just about 0°) to resist the tension/compression induced in them by the bending load on the wing. A lesser quantity of material has been placed near a 45° orientation (layer 3) to resist the bending induced torsion in the wing. This $0^\circ/45^\circ$ also provides a reasonably favourable shear coupling effect. The remaining plys at -44° are negligably small.

The final design of the forward swept wing is thus realistic and readily explained using simple design logic.

9.3 Multilaminate Rectangular Box Beam

As a final illustration of the methods capabilities the example of a rectangular box cantilever with multiple loading and subject to strain, displacement and buckling constraints is presented.

The general layout of the structure is as shown in figure 9.3 below (same as figure 8.2) and the laminate arrangement, applied loads and strain limits are exactly the same as those described for the last example in chapter 8.

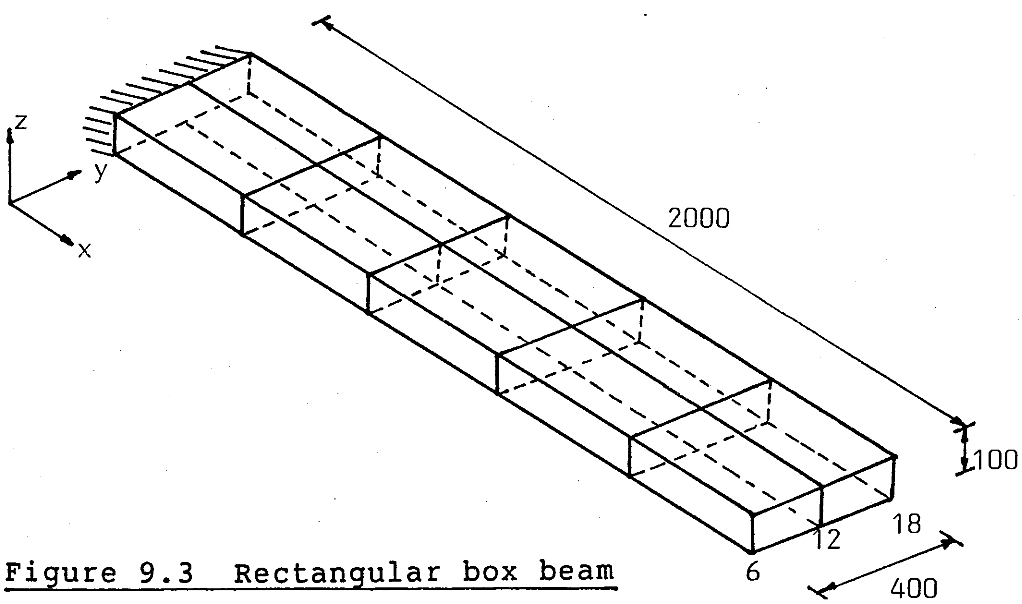

Figure 9.3 Rectangular box beam

Displacement limits were $\pm$120mm at the tip nodes of the lower skin. This limit ensured that the buckling constraints would be active. As with previous examples the initial and final designs are presented in tabular form (Table 9.4) with only the upper half of the laminates (all symmetric) being given.

Table 9.4 - Multilaminate rectangular box results (II)

Laminate type	Initial design		Final design	
	t	θ	t	θ
1. Layer 1	2.5	0.0	1.98	-4.2
2	1.25	-45.0	0.83	-50.1
3	1.25	45.0	0.02	47.1
2. Layer 1	2.5	0.0	2.07	-1.9
2	1.25	-45.0	1.31	-40.4
3	1.25	45.0	0.05	59.7
3. Layer 1	2.0	0.0	0.60	21.2
2	2.0	-45.0	1.71	-55.0
3	2.0	45.0	0.01	32.2
4. Layer 1	2.0	0.0	0.29	30.9
2	2.0	-45.0	1.95	-53.8
3	2.0	45.0	0.01	27.8
5. Layer 1	1.0	-45.0	1.41	-47.4
2	1.0	45.0	1.30	41.4
Weight (kg)	329.7		183.6	

The ply thicknesses and the nodal displacements are given in mm, the ply angle in degrees and the weights in kg. The ply orientations are again given with respect to the element local x-axes which all lie parallel to the spanwise lines shown in the finite element grid in figure 9.3.

The design in this case converged after 3 iterations.

Laminates 1 and 2 (root end bottom and top skins respectively) show similar tendencies in their material distribution having the largest component in approximately the 0° degree direction to offer the necessary bending stiffness. Both have significant components in the region of -45° offering resistance to the torsion component of the second load case. However, the top skin, which is in compression, has distinctly more material in this region than the bottom skin so that the panels do not buckle ($\pm 45^{\circ}$ material offers optimum resistance to buckling for square plates).

Laminates 3 and 4 (tip elements in the bottom and top skin respectively) both have large components of material in approximately the 54° direction, with proportionately more being found in laminate 4 (top skin - under compression). Although not at quite the optimum angle, this material provides near optimal torsional stiffness to resist the torsion load component of the second load case, and also provides very good resistance to buckling (for lamiante type

4). The material in layer 1 in both laminates is orientated at $20^\circ - 30^\circ$ where it provides a good compromise between additional torsional rigidity and bending stiffness.

9.4 Concluding Comment

The multilevel optimization system thus produces logical and feasible results and does not seem to be very sensitive to the weighting coefficients used at the element level, in terms of the final design variable values and speed of convergence.

CHAPTER 10

10 CONCLUSIONS AND RECOMMENDATIONS

10.1 Aim Of This Work

Published literature indicates that very few researchers have broached the subject of developing synthesis systems capable of optimizing composite structures in which full design variable freedom is allowed. This was thus identified as an area in which a contribution could be made to the knowledge in the field of structural optimization.

In view of this the aim of the work was defined, rather broadly, as the development of a structural synthesis system for laminated composite structures that would ensure the most efficient use of the material in the structure. More specifically, a general method for the optimal design of composite structures, that avoided all the problems and limitations associated with previously published work, was to be developed.

10.2 Objectives Achieved And Conclusions Drawn

It can reasonably be said that the objectives set out at the begining of this work have been achieved. A general method has been developed for the optimal design of laminated composite structures which allows full design variable freedom (ply thickness and orientation). The method includes the ability to link design variables and to keep ply angles and/or thicknesses fixed as an option, rather than a limitation. Although the present system (used for the test cases) was limited to using shell elements to model the structure, and to the consideration of strain, displacement and buckling constraints there is nothing in the formulation which prevents the inclusion of futher element types or constraints.

The test cases used for evaluating the performance of the method were essentially all aircraft type structures. They were, however, selected specifically for being good compromises between complex structures (and thus complex load paths) and being test cases with relatively predictable results (so that the validity of the optimized values could be assessed). The multilevel optimization method performed well on all these test cases, converging reliably and reasonably quickly and producing very plausible results.

The general conclusions that can be drawn from this work can be summarized in point form as:-

1. General optimization methods for composite materials capable of using full design variable freedom, can be developed for, and successfully implemented on, the present generation of computers.

2. The multilevel optimization scheme seems to work well and is an effective way of reducing the number of design variables and constraints under consideration at any given time in the optimization process. This makes it feasible to optimize large composite structures on existing computers.

3. The two levels of optimization, in the multilevel optimization system, are very effectively decoupled using the dual criteria objective function at the lower level. This means that the lower (element) level optimization part of the system could easily be coupled to some other optimization package which effectively performs the upper (system) level of optimization ie. some package which is capable of optimizing composite structures using only layer thicknesses as variables and keeping ply angles fixed.

4. If classical lamination theory is used as a basis for evaluating element stiffnesses then one general optimization method can be developed for a wide range of elements (as long as they conform to the theoretical formulation).

5. The multilevel system developed in this work would seem to be a sound basic method for the optimization of composite structures and warrants futher development to fully exploit its potential.

10.3 Recommendations

A number of recommendations are made below for improvements which could be made to the existing system. These are followed by a brief discussion on some futher development areas which could be pursued as part of the continuing research effort toward developing a comprehensive composite structural optimization system.

1. A sequential linear programming method is used in this work as the optimization algorithm. Although it proved to be quite suitable for the purposes of this work it does suffer from some problems which would make it unacceptable if the present system is to be developed futher and is to be made more "user friendly". The first of these is the well-known problem of zig-zaging of the solution. This makes it difficult to check for convergence and also poses problems for the less experienced user trying to identify any trends in the behaviour of variables etc. The second problem associated with the sequential LP is rather more complex. Having to make linear approximations to the highly non-linear constraints means that the solutions generally lie in the infeasible region (of the non-linear design space). Re-linearizing the constraints about these infeasible points does in some cases lead to a linearized design space with no feasible region. A fairly reliable cure for this was to scale the design back into the (non-linear) feasible region before linearization. This

particular problem is addressed in more detail in Appendix E and will not be discussed futher here. The efficiency and reliability of the present method could thus be enhanced somewhat by using some non-linear programming method in place of the sequential LP method. This would have the added benefit of avoiding the zig-zaging problem and result in interim designs being feasible, or at least near feasible, rather than consistently infeasible.

2. At present no active set strategy is included in the system. This was intentionally done so that the optimization process could be checked under the most rigorous conditions. Having established that it works well under these conditions, however, it is recommended that some active set strategy is employed to enhance the efficiency of the solution procedure. Reducing the number of constraints under consideration in any given iteration in this way may also help to partially alleviate the second problem explained in point abve.

3. The maximum strain failure criteria is used in this work. While being useful in that it concurs well with existing composite design methodology it does suffer from two problems. The first of these is that it is not an accurate gauge of material reserve factors when multiple stress states are considered. This could be especially critical in an optimized structure which frequently has simultaneous modes of failure. The second problem

associated with this failure criteria is that it leads to 3 strength constraints per layer, which means that the number of constraints grows very rapidly as the number of layers (variables) in the problem increases. Both of these problems can be solved by using one of the more complex failure criteria such as the Tsai-Hill or Tsai-Wu criteria which consider the interaction of the stresses and results in a single value (constraint) for each layer.

4. Finite difference techniques were used to evaluate the constraint derivatives at the system level of optimization. While this proved to be the best method in the existing circumstances (where it was not possible to access the finite element stiffness matrix) and gave very plausible results, it is very inefficient. It is recommended that if the system is to be developed futher and is to be used on problems with many design variables that one of the analytical methods described in Appendix D, or a semi-analytical method, is used for the derivative evaluation.

Some recommendations are now made for areas in which futher research and development could take place to follow-up on this work.

1. The present system is only capable of dealing with shell elements. An extended range of elements is required to conclusively prove the generality and usefulness of the

method. Both plate and membrane elements could be very easily included as all the mathematics and required manipulations thereof already exist in the formulation. The full rigidity matrix is evaluated in the laminate analysis and all the rigidity derivatives are evaluated in the system so the required values are all readily accessible. It is thus merely a matter of selecting the relevant values for use in membrane, plate or shell elements.

2. Futher constraints should be added to the system to improve its capabilities and usefulness. Most of the additional constraints that are likely to be required will basically be an extension of the existng constraints (eg. twist can be expressed as relative deflections) or involve just a slight change of form (eg. buckling and vibration constraints require very similar information) and thus should be relatively easy to install. The similarity in form should also ensure that no unexpected problems arise in terms of incompatibility of the constraint type and the optimization method developed.

3. The possibilty of using some form of linear design variable linking between laminate types should be investigated. This could be used to limit the differences in the design variable values between adjacent laminate groups so that greater continuity in the structure is obtained (and hence less interference at the laminate type boundaries) and so lead to designs closer to the

manufacuturable item.

4. The method developed is based on the assumption that all the constraints, with the exception of local element buckling, can be satisfied at the upper level of optimization. While this is not a particularly limiting assumption it does mean that the designs produced at the upper level may not always be as efficient (optimal) as desired. This implies that the load paths may also be "non-optimal". The lower level of optimization essentially uses the load paths generated at the upper level (via the force distribution on the element) to decide on the optimal ply oreintations and thicknesses for each element/laminate type. Thus the system could find itself optimizing the plys for non-optimal load paths. The situation is not as bad as it seems at first, however, since the stiffness change of the element (and hence to some extent the change of the loads on it) is not constrained to zero, but is written as part of the function to be minimized. This does allow a certain degree of flexibility in terms of redistribution of the load paths. In this way the multilevel system does, after several iterations between the two levels, converge to an optimal solution. It is suggested that the convergence could be speeded up (particularly in the cases with potentially awkward constraints such as twist constraints) by slight changes to the upper level optimization process. The change recommended is to include the overall laminate

orientations of each laminate type as variables at the system (upper) level ie. the laminate would be free to change its general orientation while keeping the relative angles between all the layers of that laminate fixed. This would not greatly increase the number of variables at the system level but would significantly improve its flexibility in terms of satisfying the constraints in an optimum manner. If the multilevel optimization system can get nearer the optimum in the system level process in this way it will reduce the number of switches required from one level to the other before overall convergence is achieved.

10.4 Concluding Comment

The immediate objectives of this work have been achieved, and in that sense the work can be said to have been successfully completed. The ultimate success of the project must, however, be judged on the contribution it has made to knowledge in the field of optimal design of composite structures. In this context it is also felt that the project was successful in that a small, but hopefully significant, contribution has been made both in the field of optimization of composite structures and mutilevel optimization schemes.

REFERENCES

1. JAMES, A.M., HARVILL, W.E. — Advanced composites, Lockheed Horizons, 17, Feb. 1985, pp 30-43.
2. WADDOUPS, M.D., McCULLERS, L.A., OLSON, F.O., ASHTON, J.E. — Advanced composite wing box structural synthesis development, FZM-5265, General Dynamics Fort Worth Division, 1969.
3. KICHER, T.P., CHAO, T., — Minimum weight design of stiffened fibre composite cylinders, J. Aircraft, Vol. 8, 1971, p 562.
4. KHOT, N.S., VENKAYYA, V.B., JOHNSON, C.D., TISCHLER, V.A. — Optimization of fibre reinforced composite structures, Int. J. Solids and Structures, Vol. 9, 1973, pp 1225-1236.
5. SCHMIT, L.A., FARSHI, B. — Optimum laminate design for strength and stiffness, Int. J. Num. Methods in Engng., Vol. 7, 1973, pp 519-536
6. MASSARD, T.N. — Computer sizing of composite laminates for strength, J. Reinf. Plastics and Comps., Vol 3, 1984, pp 300-345.
7. FLANAGAN, G.N. — Development and application of optimization techniques for composite laminates, M.S. Thesis, AFIT/GAE/AA/83S-4, Air Force Institue of Technology, Wright

Patterson AFB, 1983.

8. PARK, W.J. — An optimal design of simple symmetric laminates under first ply failure criterion, J. Composite Materials, Vol. 16, 1982, pp 341-345

9. SCHMIT, L.A., FARSHI, B. — Optimum design of laminated composite plates, Int. J. Num. Methods in Engng., Vol. 11, 1977, pp 623-640.

10. TAUCHERT, T.R., ADIBHATLA, S. — Design of laminated plates for maximum stiffness, J. Composite Materials, Vol.18(1), 1984, pp 58-69

11. TAUCHERT, T.R., ADIBHATLA, S. — Design of laminated plates for maximum bending strength, Engng. Optimization, Vol. 8(4), 1985, pp 253-263.

12. STROUD, W.J., AGRANOFF, N. — Minimum-mass design of filamentary composite panels under combined loads: Design procedure based on simplified buckling equations, NASA TN D-8257, Oct. 1976.

13. STROUD, W.J., AGRANOFF, N., ANDERSON, M.S. — Minimum-mass design of filamentary composite panels under combined loads: Design procedure based on a rigorous buckling analysis, NASA TN D-8257, Oct. 1976.

14. McKEOWN, J.J. — A fixed upper bound on the number

of layers in optimal composite sheets, Int. J. Solids and Struct., Vol. 14, 1978, pp 113-119.

15. ADALI, S. Design sensitivity analysis of an antisymmetric angle-ply laminate, TWISK 318, National Institute for Mathematical Sciences, CSIR, 1983.

16. ADALI, S. Multiobjective design of an antisymmetric angle-ply laminate by non-linear programming, ASME J. of Mechanisms, Trans. and Automation in Design, Vol. 105(2) 1983, pp 214-219.

17. KHOT, N.S. Computer program (OPTCOMP) for optimization of composite structures for minimum weight design, AFFDL TR-76-149, Air Force Flight Dynamics Laboratory, Wright Patterson AFB, 1977.

18. KHOT, N.S., VENKAYYA, V.B., BERKE, L. Optimum design of composite structures with stress and displacement constraints,Proceedings of the AIAA 13th Aerospace Sciences Meeting, Pasadena, California, Jan. 1975.

19. KHOT, N.S., VENKAYYA, V.B., Optimum design of composite wing structures with twist constraint for

BERKE, L., SCHRADER, K. — aeroelastic tailoring, AFFDL TR-76-117, Air Force Flight Dynamics Laboratory, Wright Patterson AFB, Dec. 1976.

20. McKEOWN, J.J., — A quasi-linear programming algorithm for optimizing fibre reinforced structures of fixed stiffness, Comp. Meth. in App. Mech. and Engng., Vol. 6, 1975, pp 123-154.

21. McKEOWN, J.J., — Optimal composite structures by deflection variable programming, Comp. Meth. in App. Mech. and Engng, Vol. 12, 1977, pp 155-179.

22. STARNES, J.H., HAFTKA, R.T. — Preliminary design of composite wings for buckling, strength and displacement constraints, Proceedings of 19th AIAA, ASME Structures, Structural Dynamics and Materials Conference, Bethesda, Md., April 1978.

23. SOBIESKI, J. — An integrated computer procedure for sizing composite airframe structures, NASA TP 1300, Feb. 1979.

24. SCHMIT, L.A., MEHRINFAR, M. — Mutilevel optimum design of structures with fibre-composite stiffened-panel components, AIAA Journal, Vol. 20, 1982, pp 138-147.

25. STROUD, W.J. — Optimization of composite structures, Proceedings of the IUTAM Symposium on Mechanics of Composite Materials, Blacksburg, Virginia, August 1982.

26. SCHMIT, L.A., RAMANATHAN, R.K. — Multilevel approach to minimum weight design including buckling constraints, AIAA Journal, Vol. 16, Feb. 1978, pp 97-104.

27. OSYCZKA, A. — Multicriterion optimization in engineering : With Fortran programs, Ellis Horwood Ltd., Chichester,1984.

28. HWANG, C.L., PAIDY, S.R., YOON, K., MASUD, A.M. — Mathematical programming with multiple objectives : A tutorial, Compt. and Ops. Res., Vol. 7, 1980, pp 5-31.

29. COHON, J.L. — Multiobjective programming and planning, Academic Press, New York, 1978.

30. LEKHNITSKII, S.G. (S.W. TSAI and T. CHERON, translaters) — Anisotropic plates, Gordon and Breach Science Publishers, New York, 1968.

31. TIMOSHENKO, S. — Theory of elastic stability, McGraw-Hill, New York, 1936.

32. ALLEN, H.G. BULSON, P.S. — Background to buckling, McGraw-Hill Book Co., Maidenhead,

1980.

33. JONES, R.M. — Mechanics of composite materials, Mcgraw-Hill Kogakusha Ltd., Tokyo, 1975.

34. MORRIS, A.J. (editor) — Foundations of structural optimization : A unified approach, John Wiley and Sons, Chichester, 1982.

35. KIRSCH, U. — Optimum structural design, McGraw - Hill, New York, 1981.

36. HAFTKA, R.T., KAMAT, M.P. — Elements of structural optimization, Martinus Nijhoff, The Hague, 1985.

37. STEWART, G.W. — A modification of Davidson's minimization method to accept difference approximations of derivatives, J. Assoc. Comp. Mach., Vol 14(1), Jan. 1967, pp 72-83.

38. ARORA, J.S., HAUG, E.J. — Efficient optimal design of structures by generalized steepest descent programming, Int. J. Num. Meth. Eng., Vol 10(4), 1976, pp 747-766.

39. HAUG, E.J., ARORA, J.S. — Design sensitivity analysis of elastic mechanical systems, Comput. Meth. Appl. Mech. Eng., Vol. 15, 1978, pp 35-62.

40. ARORA, J.S., — Methods of design sensitivity

HAUG, E.J. analysis in structural optimization, AIAA Journal, Vol 17, Sept. 1979, pp 970-974.

41. BROWN, R.T., NACHLAS, J.A. Structural optimization of laminated conical shells, AIAA Journal, Vol 23(5), 1985, pp 781-787

42. SOBIESKI, J., JAMES, B.B., DOVI, A.R. Structural optimization by multilevel decomposition, AIAA Journal, Vol 23(11), 1985, pp 1775-1782.

43. REKLAITIS, G.V., RAVINDRAN, A., RAGSDELL, K.M. Engineering optimization : Methods and applications, John Wiley and Sons Inc., New York, 1983.

44. BALDUR, R. Structural optimization by inscribed hyperspheres, ASCE, J. Eng Mech., Vol 98, 1972, pp 503-518.

45. HERMANN, L.R., WELCH,K.R., LIM,C.K. Composite FEM analysis for layered systems, ASCE, J. Eng. Mech., Vol 110(9), 1984, pp 1284-1302.

46. TSAI, S.W., HAHN,H.T. Introduction to composite materials Technomic Publishing, Westport, 1980

47. BELL, W.W. Matrices for scientists and engineers, van Nostrand Reinhold, New York, 1975.

48. DAHLQUIST, G., BJORCK, A. Numerical methods, Prentice Hall Inc., New Jersey, 1974.

49. SHANLEY, F.R. Weight - strength analysis of

aircraft structures, McGraw-Hill, New York, 1952.

50. GALLGHER, R.H., ZIENKIEWICZ, O.C. (Editors) Optimum structural design, John Wiley and Sons, London, 1973.

51. HAUG, E.J., ARORA, J.S. Applied optimal design : Mechanical and structural systems, John Wiley and Sons, New York, 1979.

52. AVRIEL, M. Nonlinear programming : Analysis and methods, Prentice Hall Inc., New Jersey, 1976.

53. ARORA, J.S., GOVIL, A.K. Design sensitivity analysis with substructuring, ASCE, J. Eng. Mech., Vol. 103, 1977, pp 537-548.

54. VANDERPLAATS, G.N. Numerical optimization techniques in engineering design : with applications, McGraw-Hill, New York, 1984.

APPENDIX A

Derivation of a laminated composite plate rigidity matrix.

For a single lamina of orthotropic material (figure A1) a plane stress state is defined as $\sigma_3 = 0$, $\tau_{13} = 0$ and $\tau_{23} = 0$.

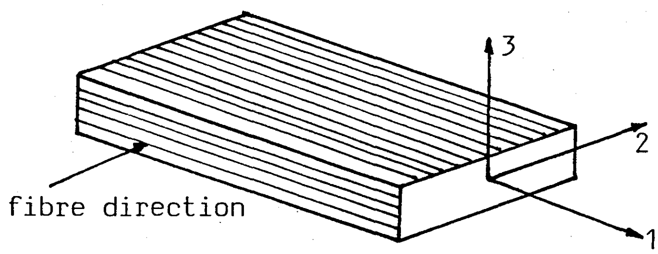

Figure A.1 Unidirectionally reinforced lamina

The stress-strain relations for such a lamina can be written as (Ref. [33])

$$\begin{Bmatrix} \sigma_1 \\ \sigma_2 \\ \tau_{12} \end{Bmatrix} = \begin{bmatrix} \bar{Q}_{11} & \bar{Q}_{12} & 0 \\ \bar{Q}_{12} & \bar{Q}_{22} & 0 \\ 0 & 0 & \bar{Q}_{66} \end{bmatrix} \begin{Bmatrix} \varepsilon_1 \\ \varepsilon_2 \\ \gamma_{12} \end{Bmatrix} \qquad (A.1)$$

where the Q are called the reduced stiffnesses, and are

$$\bar{Q}_{11} = E_1/(1 - \nu_{12}\nu_{21})$$
$$\bar{Q}_{12} = \nu_{12}E_2/(1 - \nu_{12}\nu_{21})$$
$$\bar{Q}_{22} = E_2/(1 - \nu_{12}\nu_{21})$$
$$\bar{Q}_{66} = G_{12}$$

Note that eqn. (A.1) is derived for the special case of plane stress from the stress-strain relation given in Ref. [33] for an orthotropic material.

Futhermore, if this lamina were to be arbitrarily orientated, at some angle θ relative to a reference (or global) axis system (figure A.2),

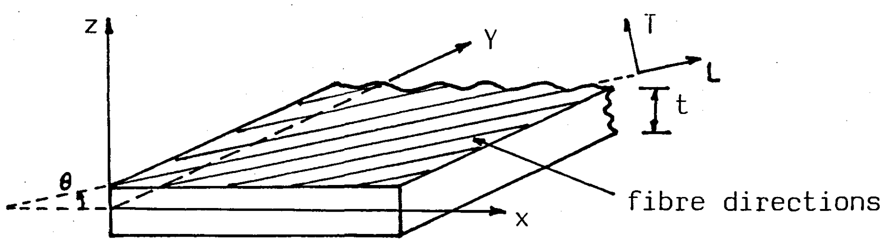

Figure A.2 Reference axis system

then by using suitable transformations (Ref. [33]) the stress-strain relations can be written as

$$\begin{Bmatrix} \sigma_x \\ \sigma_y \\ \tau_{xy} \end{Bmatrix} = \begin{bmatrix} Q_{11} & Q_{12} & Q_{13} \\ Q_{12} & Q_{22} & Q_{23} \\ Q_{13} & Q_{23} & Q_{33} \end{bmatrix} \begin{Bmatrix} \varepsilon_x \\ \varepsilon_y \\ \gamma_{xy} \end{Bmatrix} \qquad (A.2)$$

where

$$\begin{aligned} Q_{11} &= U_1 + U_2 \cos 2\theta + U_3 \cos 4\theta \\ Q_{12} &= U_4 - U_3 \cos 4\theta \\ Q_{22} &= U_1 - U_2 \cos 2\theta + U_3 \cos 4\theta \\ Q_{13} &= 1/2\ (U_2 \sin 2\theta) + U_3 \sin 4\theta \\ Q_{23} &= 1/2\ (U_2 \sin 2\theta) - U_3 \sin 4\theta \\ Q_{33} &= U_5 - U_3 \cos 4\theta \end{aligned} \qquad (A.3)$$

and

$$\begin{aligned} U_1 &= 1/8\ (3\bar{Q}_{11} + 3\bar{Q}_{22} + 2\bar{Q}_{12} + 4\bar{Q}_{66}) \\ U_2 &= 1/2\ (\bar{Q}_{11} - \bar{Q}_{22}) \\ U_3 &= 1/8\ (\bar{Q}_{11} + \bar{Q}_{22} - 2\bar{Q}_{12} - 4\bar{Q}_{66}) \\ U_4 &= 1/8\ (\bar{Q}_{11} + \bar{Q}_{22} + 6\bar{Q}_{12} - 4\bar{Q}_{66}) \\ U_5 &= 1/8\ (\bar{Q}_{11} + \bar{Q}_{22} - 2\bar{Q}_{12} + 4\bar{Q}_{66}) \end{aligned} \qquad (A.4)$$

Note that eqns. (A.4) are known as the invariant properties of a lamina, as they are dependent only on the material properties and not fibre angle or lamina thickness.

It is also occassionally convenient to write the [Q] matrix of eqn. (A.2) in the form

$$[Q] = [r_0]+[r_1]\cos 4\theta+[r_2]\sin 4\theta+[r_3]\cos 2\theta+[r_4]\sin 2\theta \qquad (A.5)$$

where

$$[r_0] = \begin{bmatrix} U_1 & U_4 & 0 \\ U_4 & U_1 & 0 \\ 0 & 0 & U_5 \end{bmatrix} \quad ; \quad [r_1] = \begin{bmatrix} U_3 & -U_3 & 0 \\ -U_3 & U_3 & 0 \\ 0 & 0 & -U_3 \end{bmatrix}$$

$$[r_2] = \begin{bmatrix} 0 & 0 & U_3 \\ 0 & 0 & -U_3 \\ U_3 & -U_3 & 0 \end{bmatrix} \quad ; \quad [r_3] = \begin{bmatrix} U_2 & 0 & 0 \\ 0 & -U_2 & 0 \\ 0 & 0 & 0 \end{bmatrix}$$

$$[r_4] = \begin{bmatrix} 0 & 0 & U_2/2 \\ 0 & 0 & U_2/2 \\ U_2/2 & U_2/2 & 0 \end{bmatrix}$$

Now following from the Kirchoff hypothesis for plates and the Kirchoff-Love hypothesis for shells it can be stated that

$$\begin{Bmatrix} \varepsilon_x \\ \varepsilon_y \\ \varepsilon_{xy} \end{Bmatrix} = \begin{Bmatrix} \varepsilon_x^o \\ \varepsilon_y^o \\ \varepsilon_{xy}^o \end{Bmatrix} + z \begin{Bmatrix} \chi_x \\ \chi_y \\ \chi_{xy} \end{Bmatrix}$$

where

z is the distance from the plate midsurface

χ is the plate midsurface curvature

^{o} (superscript) denotes midsurface strains

and thus eqn. (A.2) can be written as

$$\begin{Bmatrix} \sigma_x \\ \sigma_y \\ \tau_{xy} \end{Bmatrix} = [Q] \begin{Bmatrix} \varepsilon_x^o + \chi_x z \\ \varepsilon_y^o + \chi_y z \\ \varepsilon_{xy}^o + \chi_{xy} z \end{Bmatrix} \tag{A.6}$$

The resultant laminate forces and moments can be obtained by intergration of the stresses in each lamina through the thickness, for example

$$F_x = \int_{-t/2}^{t/2} \sigma_x \, dz$$

$$M_x = \int_{-t/2}^{t/2} \sigma_x \, z dz$$

where F_x and M_x are the loading intensities i.e. per unit width of plate.

Expanding this to matrix form, and summing over the L layers of the laminate, gives

$$\begin{Bmatrix} F_x \\ F_y \\ F_{xy} \end{Bmatrix} = \int_{-t/2}^{t/2} \begin{Bmatrix} \sigma_x \\ \sigma_y \\ \tau_{xy} \end{Bmatrix} dz = \sum_{j=1}^{L} \int_{z_{j-1}}^{z_j} \begin{Bmatrix} \sigma_x \\ \sigma_y \\ \tau_{xy} \end{Bmatrix} dz \tag{A.7}$$

and

$$\begin{Bmatrix} M_x \\ M_y \\ M_{xy} \end{Bmatrix} = \int_{-t/2}^{t/2} \begin{Bmatrix} \sigma_x \\ \sigma_y \\ \tau_{xy} \end{Bmatrix} zdz = \sum_{j=1}^{L} \int_{z_{j-1}}^{z_j} \begin{Bmatrix} \sigma_x \\ \sigma_y \\ \tau_{xy} \end{Bmatrix} zdz \tag{A.8}$$

where z_j, z_{j-1} represent the distance from the midsurface to the top and bottom of the laminate respectively.

Substituting eqn. (A.6) into eqns. (A.7) and (A.8) and remembering that $\varepsilon_x^\circ, \varepsilon_y^\circ, \gamma_{xy}^\circ, \kappa_x, \kappa_y, \kappa_{xy}$ are the midsurface values, and so independent of z, and can thus be removed from under the summation signs, gives

$$\begin{Bmatrix} F_x \\ F_y \\ F_{xy} \end{Bmatrix} = \begin{bmatrix} A_{11} & A_{12} & A_{13} \\ A_{12} & A_{22} & A_{23} \\ A_{13} & A_{23} & A_{33} \end{bmatrix} \begin{Bmatrix} \varepsilon_x^\circ \\ \varepsilon_y^\circ \\ \gamma_{xy}^\circ \end{Bmatrix} + \begin{bmatrix} B_{11} & B_{12} & B_{13} \\ B_{12} & B_{22} & B_{23} \\ B_{13} & B_{23} & B_{33} \end{bmatrix} \begin{Bmatrix} \kappa_x \\ \kappa_y \\ \kappa_{xy} \end{Bmatrix} \tag{A.9}$$

$$\begin{Bmatrix} M_x \\ M_y \\ M_{xy} \end{Bmatrix} = \begin{bmatrix} B_{11} & B_{12} & B_{13} \\ B_{12} & B_{22} & B_{23} \\ B_{13} & B_{23} & B_{33} \end{bmatrix} \begin{Bmatrix} \varepsilon_x^\circ \\ \varepsilon_y^\circ \\ \gamma_{xy}^\circ \end{Bmatrix} + \begin{bmatrix} D_{11} & D_{12} & D_{13} \\ D_{12} & D_{22} & D_{23} \\ D_{13} & D_{23} & D_{33} \end{bmatrix} \begin{Bmatrix} \kappa_x \\ \kappa_y \\ \kappa_{xy} \end{Bmatrix} \tag{A.10}$$

where

$$A_{mn} = \sum_{j=1}^{L} (Q_{mn})_j (z_j - z_{j-1}) = \sum_{j=1}^{L} (Q_{mn})_j t_j$$

$$B_{mn} = \sum_{j=1}^{L} (Q_{mn})_j (z_j^2 - z_{j-1}^2) = \sum_{j=1}^{L} (Q_{mn})_j \bar{z}_j t_j$$

$$D_{mn} = \sum_{j=1}^{L} (Q_{mn})_j (z_j^3 - z_{j-1}^3) = \sum_{j=1}^{L} (Q_{mn})_j (\bar{z}_j^2 t_j + t_j^3/12)$$

where

$\bar{z}_j$ is the distance from the midsurface to the centroid of the j-th lamina

t is the thickness of the j-th lamina

Now eqns. (A.9) and (A.10) can be combined to write the following

$$\begin{Bmatrix} F_x \\ F_y \\ F_{xy} \\ M_x \\ M_y \\ M_{xy} \end{Bmatrix} = \left[\begin{array}{c|c} A & B \\ \hline B & D \end{array}\right] \begin{Bmatrix} \varepsilon_x \\ \varepsilon_y \\ \varepsilon_{xy} \\ \kappa_x \\ \kappa_y \\ \kappa_{xy} \end{Bmatrix} \qquad (A.11)$$

where the 3x3 submatrices A,B and D are defined by eqns. (A.11) and the complete 6x6 A,B,D matrix is known as the rigidity matrix.

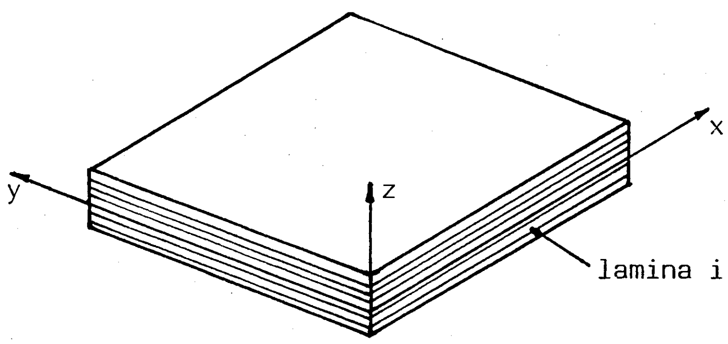

Figure A.3 Lamina stacking sequence

Definitions.

(Refer to figure A3)

1) A specially orthtropic laminate has symmetry of its lamina (with regard to thickness and fibre angle) about both the x-y plane (element midsurface) and the y-z plane i.e. for each lamina at $+\theta$ there must be an equivalent one at $-\theta$, and for each lamina above the midsurface there must be an identical one below the midsurface. For these layups the components A_{13}, A_{23}, D_{13} and D_{23} are zero (note

that the A,B and D matrices are symmetric) and the entire B matrix is zero.

2) A balanced symmetric laminate only has symmetry about the midsurface (x-y plane). In this case only the B matrix is zero.

3) A general laminate, or an unbalanced unsymmetric laminate has no zero terms in the rigidity matrix.

APPENDIX B

Derivatives of the rigidity matrix.

The rigidity matrix [R] is a 6x6 matrix which can be partitioned as (see Appendix A, eqn,(A.11)),

$$[R] = \left[\begin{array}{c|c} A & B \\ \hline B & D \end{array}\right] \qquad (B.1)$$

where A,B and D are 3x3 matrices and

$$A_{mn} = \sum_{j=1}^{L} (Q_{mn})_j \, t_j \qquad (B.2)$$

$$B_{mn} = \sum_{j=1}^{L} (Q_{mn})_j \, z_j \, t_j \qquad (B.3)$$

$$D = \sum_{j=1}^{L} (Q_{mn})(z_j^2 t_j + t_j^3/12) \qquad (B.4)$$

where

Q_{mn} is defined in Appendix A, eqns. (A.3)

m,n indicate the matrix row and column number

j indicates the lamina/layer number

The derivation of eqns. (B.2) - (B.4) can be found in Appendix A.

Using the form of eqn. (B.1) the derivatives of [R] with respect to the design variables can be written as

$$[\partial R/\partial t_j] = \left[\begin{array}{c|c} \partial A/\partial t_j & \partial B/\partial t_j \\ \hline \partial B/\partial t_j & \partial D/\partial t_j \end{array}\right]$$

and

$$[\partial R/\partial \theta_j] = \left[\begin{array}{c|c} \partial A/\partial \theta_j & \partial B/\partial \theta_j \\ \hline \partial B/\partial \theta_j & \partial D/\partial \theta_j \end{array}\right]$$

where

$$\partial A_{mn}/\partial \theta_j = (\partial Q_{mn}/\partial \theta_j)t_j \quad (B.5)$$

$$\partial B_{mn}/\partial \theta_j = (\partial Q_{mn}/\partial \theta_j)z_j t_j \quad (B.6)$$

$$\partial D_{mn}/\partial \theta_j = (\partial Q_{mn}/\partial \theta_j)(z_j^2 t_j + t_j^3/12) \quad (B.7)$$

where the $\partial Q_{mn}/\partial \theta_j$ are given by

$$\left.\begin{aligned} \partial Q_{11}/\partial \theta_j &= -(2U_2 \sin 2\theta_j + 4U_3 \sin 4\theta_j) \\ \partial Q_{12}/\partial \theta_j &= 4U_3 \sin 4\theta_j \\ \partial Q_{22}/\partial \theta_j &= 2U_2 \sin 2\theta_j - 4U_3 \sin 4\theta_j \\ \partial Q_{13}/\partial \theta_j &= U_2 \cos 2\theta_j + 4U_3 \cos 4\theta_j \\ \partial Q_{23}/\partial \theta_j &= U_2 \cos 2\theta_j - 4U_3 \cos 4\theta_j \\ \partial Q_{33}/\partial \theta_j &= 4U_3 \sin 4\theta_j \end{aligned}\right\} \quad (B.8)$$

and

$$\partial A_{mn}/\partial t_j = (Q_{mn})_j \quad (B.9)$$

$$\partial B_{mn}/\partial t_j = (Q_{mn})_j z_j \quad (B.10)$$

$$\partial D_{mn}/\partial t_j = (Q_{mn})_j (z_j^2 + t_j^2/4) \quad (B.11)$$

APPENDIX C

Upper bound on the number of layers in optimal composite plates

In Ref. [14] a fixed upper limit is established for the number of layers required in an optimal plane-stress linear composite structure. It is also shown in that paper that the limit is independent of the complexity of the finite elements in terms of which the structure is idealized, the number of alternative loading conditions or the number or form of constraints, except that they must be expressible as functions of the deflections and fibre angles only.

In this section it will be shown (in a similar manner to Ref. [14]) that the same upper limit can be established for plate elements.

In Appendix A the following relationship is established for a lamina:-

$$\{\sigma\} = ([r_0]+[r_1]\cos 4\theta+[r_2]\sin 4\theta+[r_3]\cos 2\theta+[r_4]\sin 2\theta)\{\varepsilon\} \tag{C.1}$$

where

$[r_0]$, $[r_1]$, $[r_2]$, $[r_3]$ and $[r_4]$ are 3x3 matrices dependent on material constants only (as defined in Appendix A)

θ is the fibre angle

The stiffness matrix of any lamina is linear in the stiffness coefficients of the material (eqn. (C.1)). A lamina of thickness t_j and fibre angle θ_j will thus have a stiffness matrix of the general form

$$k_j(\theta_j)=[k_0]_j+[k_1]_j\cos 4\theta_j+[k_2]_j\sin 4\theta_j+[k_3]_j\cos 2\theta_j$$
$$+[k_4]_j\sin 2\theta_j \qquad (C.2)$$

where $k_j(\theta_j)$ is expressed in terms of unit thickness.

The bending stiffness is then given by

$$[K] = \sum_{j=1}^{L} (k_j(\theta_j))(\bar{z}_j^2 t_j + t_j^3/12) \qquad (C.3)$$

where

L is the number of lamina

$\bar{z}$ is the distance from the plate midsurface to the centroid of the lamina.

Now if linear elastic behaviour of the plate is assumed (which is quite reasonable for most composites) then the following familiar equation holds

$$[K].\{\delta\} = \{P\} \qquad (C.4)$$

where

[K] is the stiffness matrix

$\{\delta\}$ is the deflection vector

{P} is the load vector

Substituting eqn. (C.3) into eqn. (C.4) gives

$$\sum_{j=1}^{L} [k_j(\theta_j)].\{\delta\}.(\bar{z}_j^2 t_j + t_j^3/12) = \{P\}$$

or in expanded form

$$\sum_{j=1}^{L}([k_0]_j\{\delta\}+[k_1]_j\{\delta\}\cos4\theta_j+[k_2]_j\{\delta\}\sin4\theta_j+[k_3]_j\{\delta\}\cos2\theta_j$$

$$+ [k_4]_j\{\delta\}\sin2\theta_j).(\bar{z}_j^2 t_j+t_j^3/12) = \{P\}$$

This equation can now be written as

$$\sum_{j=1}^{L} [M]_j \{\Phi\}_j (\bar{z}_j^2 t_j+t_j^3/12) = \{P\} \qquad (C.5)$$

where

$[M]_j = [[k_0]_j\{\delta\} , [k_1]_j\{\delta\} , \ldots\ldots ,[k_4]_j\{\delta\}]$

- a 3x5 matrix

$\{\Phi\}_j = \{1 , \cos4\theta_j , \sin4\theta_j , \cos2\theta_j , \sin2\theta_j \}$

- a 5x1 vector

Eliminating the summation and writing eqn. (C.5) in full matrix form gives

$$[M][\Phi]\{\bar{z}^2 t+t^3/12\} = \{P\} \qquad (C.6)$$

where $[M]$ is a 3x5 matrix

$[\Phi]$ is a 5xL matrix (L = no. of lamina)

$\{\bar{z}^2 t+t^3/12\}$ is a Lx1 vector

Now if there is an upper bound on the number of layers in an optimum element then $\bar{z}_j$ can be expressed in terms of t_j as

$$\bar{z}_j = 1/2(\sum_{n=1}^{j-1} t_n - \sum_{n=j+1}^{L} t_n) \qquad (C.7)$$

Note that eqn. (C.7) is correct only if z = 0 at the plate midsurface and layer 1 (of consecutively numbered layers) is in the negative z direction.

Eqn. (C.6) can thus now be written as

$$[M][\Phi]\{(1/2(\sum_{n=1}^{j-1} t_n - \sum_{n=j+1}^{L} t_n))^2 t + t^3/12\} = \{P\}$$

or

$$[M][\Phi]\{At + t^3/12\} = \{P\}$$

$$\text{where } A = (1/2(\sum_{n=1}^{j-1} t_n - \sum_{n=j+1}^{L} t_n))^2$$

or

$$[M][\Phi]\{Y\} = \{P\} \qquad (C.8)$$

where

$$Y_j = A_j t_j + t_j^3/12$$

The t_j are always non-negative, as is A_j, which is also independent of t_j, and thus there is a one to one correspondence of t_j and Y_j.

Now the optimization problem can be stated as

$$\min W(t_j) = \sum_{j=1}^{L} c(t_j)$$

subject to:- $[K]\{\delta\} = \{P\}$ (eqn. (C.4))

i.e. $[M][\Phi]\{Y\} = \{P\}$ (eqn. (C.8))

and $t_j \geqslant 0$ $j=1,2,\ldots,L$

This is a linear programming problem in the Y_j (with its one to one correspondence with t_j) subject to N_d equality constraints (eqn. (C.8)), where N_d is the number of deformation modes of the plate.

The constraints are not generally all independent, so a reduced set can be defined by eliminating all the equations corresponding to the linearly dependent rows of [M], giving

$$[M'][\Phi]\{Y\} = \{P'\}$$

where [M'] and {P'} define the reduced set.

The rank of these remaining equations is equal to the rank of $[\Phi]$ or [M'], whichever is the less (Ref. [14]).

Now [M'] has 5 columns and $[\Phi]$ has 5 rows and the maximum rank of either is thus 5. The rank of [M'], however, cannot exceed N_d since that is the rank of $k_j(\theta_j)$, and so the number of independent equality constraints of the linear programming problem is $\min(5, N_d)$.

The effect of increasing the number of load cases is now considered. For each additional load a set of equations of equilibrium are added:-

$$[K]\{\delta\}^k = \{P\}^k$$

The principal of virtual work, however, requires that for deflection and load sets

$$\{P\}^r \{\delta\}^s = \{\delta\}^r \{P\}^s$$

Hence, N_p load cases imply at most $N_p(N_d-(N_p-1)/2)$ independent rows of $[M']$, and $[\Phi]$ is obviously unaltered. The maximum rank of the equations thus becomes $\min(5,N_p(N_d-(N_p-1)/2)) = R$.

The vector $\{Y\}$ thus solves a linear programming problem with R equality constraints. By the fundamental theory of Linear Programming, therefore, not more than R values of Y_j may be non-zero. Since there is a one to one correspondence of Y_j and t_j this implies that there can be no more than R non-zero values of t_j.

Now let a balanced layup be defined as a double layer (lamina), with one half-thickness containing fibre at angle θ and the other at $-\theta$ relative to the datum axis. For this form of layup, terms in the odd functions in the expression for $k_j(\theta_j)$ (eqn. (C.2)) vanish, and so the expansion has only three terms left. The same reasoning as above can then be applied to obtain a maximum rank of $\min\{3,N_p(N_d-(N_p-1)/2)\} = R$. This implies a maximum of 3 "balanced layup" lamina i.e. a total of 6 layers.

These results are thus exactly the same as those derived in Ref. [14] for membrane action finite elements i.e. plane-stress elements, and so it can be concluded that the maximum number of layers in an optimum composite plate (subjected to in-plane and bending loads) is equal to R, where $R = \min\{6, N_p(N_d-(N_p-1)/2)\}$. In general N_p is greater than 1 and N_d will be at least 3 (for plate bending elements) and may be 5 (shell elements) and thus the value of R will normally be 6. This is the value used in this work as it is then the uppermost bound on the number of lamina in an optimum composite plate.

APPENDIX D

Methods for constraint derivative evaluation.

The calculation of the derivatives of the constraint functions with respect to the design variables (often called design sensitivity analysis) is required when using most of the efficient optimization methods. It is also necessary to evaluate these derivatives when applying explicit approximations of the constraint functions, such as the Taylor series, used in this work.

In most structural optimization problems the object is usually to find the derivatives of the displacements $\{\delta\}$ (eqn. (D.1)) when using a displacement analysis (finite element) method. The equations for the displacement analysis are

$$[K]\{\delta\} = \{F\} \qquad (D.1)$$

Derivatives of stresses and strains can then be obtained by differentiation of the strain-displacement or stress-displacement equations,

$$\{\sigma\} = [S]\{\delta\} \qquad (D.2)$$

where the system stress-displacement, or stress transformation, matrix [S] is constant.

For an optimization problem with n design variables x_i (i=1,....,n), the calculation of the derivatives of the displacements with respect to the design variables by the finite difference method would require the analysis (eqn. (D.1)) to be repeated for each of (n+1) different stiffness matrices. The derivatives can, however, often be calculated more efficiently using analytical means, so avoiding the large number of analyses associated with finite difference calculations.

Some of the more common approaches used for such analytical evaluation of the derivatives are descibed below and their relative merits discussed.

D.1 Behaviour Space Method

This method for evaluating the constraint derivatives was proposed by Haug and Arora (Refs. [38]-[40]), who originally called it the state space method. It has, however, recently become more commonly (and appropriately) reffered to as the behaviour space approach.

In this method the displacements $\{\delta\}$ are treated as independent variables, and an adjoint relationship is then introduced to express the effect of a variation in $\{\delta\}$ in terms of a variation in the design variables.

Treating $\{\delta\}$ and $\{x\}$ as the independent variables, the first variation of any constraint function $g(\{x\},\{\delta\})$ can be written as

$$\Delta g_j = \{\partial g_j/\partial x\}^T \{\Delta x\} + \{\partial g_j/\partial \delta\}^T \{\Delta \delta\} \qquad (D.1.1)$$

where $\{\partial g_j/\partial x\}$ and $\{\partial g_j/\partial \delta\}$ are the partial derivatives of the constraint j with respect to $\{x\}$ and $\{\delta\}$ respectively (evaluated at a given point $\{x^*\}$ and the corresponding $\{\delta^*\}$), while $\{\Delta x\}$ and $\{\Delta\delta\}$ represent small variations in $\{x\}$ and $\{\delta\}$ respectively.

The constraint variation must, however, finally be written only as a function of the design variables $\{x\}$ i.e. as

$$\{\Delta g_j\} = \{dg_j/dx_1 \ , \ \ldots\ldots \ , \ dg_j/dx_n\}\{\Delta x\} \qquad (D.1.2)$$

where dg_j/dx_i are the total derivatives.

The term $\{\partial g_j/\partial\delta\}\{\Delta\delta\}$ in eqn. (D.1.1) must therefore be expressed as a function of $\{\Delta x\}$. In order to do this an adjoint variable vector $\{\phi_j\}$, associated with the constraint function g_j, is defined such that

$$[K]\{\phi_j\} = \{\partial g_j/\partial\delta\} \qquad (D.1.3)$$

If the j-th constraint g_j is actually the displacement δ_j then $\{\partial g_j/\partial\delta\} = \{I_j\}$, which is a vector with a unit value in the j-th position and zeroes elsewhere. Thus eqn. (D.1.3) becomes

$$[K]\{\phi_j\} = [I_j] \qquad (D.1.4)$$

Now taking the first variation of eqn. (D.1) with respact to x_i gives

$$[K]\{\Delta\delta\} + \sum_{i=1}^{n} [\partial K/\partial x_i]\{\delta\}\Delta x_i = \sum_{i=1}^{n} \{\partial F/\partial x_i\}\Delta x_i \qquad (D.1.5)$$

Defining matrix [H] as

$$[H] = [\{\partial F/\partial x_1\}, \ldots ,\{\partial F/\partial x_n\}] - [[\partial K/\partial x_1]\{\delta\}, \ldots ,[\partial K/\partial x_n]\{\delta\}] \qquad (D.1.6)$$

eqn. (D.1.5) can be written as

$$[K]\{\Delta\delta\} = [H]\{\Delta x\} \qquad (D.1.7)$$

Premultipling eqn. (D.1.7) by the adjoint variable vector $\{\phi_j\}^T$ and substituting eqn. (D.1.3) into the resulting equation gives

$$\{\partial g_j/\partial\delta\}^T\{\Delta\delta\} = \{\phi_j\}^T[H]\{\Delta x\} \qquad (D.1.8)$$

and thus eqn. (D.1.1) can now be written purely as a function of $\{\Delta x\}$ by substituting eqn. (D.1.8) into eqn. (D.1.1), giving

$$\{\Delta g_j\} = (\{\partial g_j/\partial x\} + \{\phi_j\}^T[H])\{\Delta x\} \qquad (D.1.9)$$

From eqns. (D.1.9) and (D.1.2), the following expression for $\{\nabla g_j\}$ is obtained

$$\{\nabla g_j\} = \{\partial g_j/\partial x\}^T + \{\phi_j\}^T[H] \qquad (D.1.10)$$

and again if $g_j \equiv \delta_j$ then $\{\partial g_j/\partial x\} = \{0\}$ and eqn. (D.1.10) becomes

$$\{\nabla\delta_j\}^T = \{\phi_j\}^T[H] \qquad (D.1.11)$$

The desired derivative vector is thus computed using eqns. (D.1.4), (D.1.6) and (D.1.11).

D.2 Design Space Method

The behaviour variables $\{\delta\}$ are taken to be dependent variables is this approach and can be expressed in terms of the independent design variables $\{x\}$, as

$$\{\Delta\delta\} = [\partial\delta/\partial x]\{\Delta x\} \tag{D.2.1}$$

where

$$[\partial\delta/\partial x] = \begin{bmatrix} \partial\delta_1/\partial x_1 & \ldots\ldots & \partial\delta_1/\partial x_n \\ \ldots\ldots & \ldots\ldots & \ldots\ldots \\ \ldots\ldots & \ldots\ldots & \ldots\ldots \\ \ldots\ldots & \ldots\ldots & \ldots\ldots \\ \partial\delta_m/\partial x_1 & \ldots\ldots & \partial\delta_m/\partial x_n \end{bmatrix} \tag{D.2.2}$$

Substituting eqn. (D.2.1) into eqn. (D.1.1) gives

$$\Delta g_j = (\{\partial g_j/\partial x\}^T + \{\partial g_j/\partial\delta\}^T [\partial\delta/\partial x])\{\Delta x\}$$

so leading to

$$\{\nabla g_j\}^T = \{\partial g_j/\partial x\} + \{\partial g_j/\partial\delta\} [\partial\delta/\partial x] \tag{D.2.3}$$

The matrix $[\partial\delta/\partial x]$ is obtained by differentiation of eqn. (D.1), giving

$$[\partial K/\partial x]\{\delta\} + [K]\{\partial\delta/\partial x\} = \{\partial F/\partial x\}$$

which can be re-written as

$$[K]\{\partial\delta/\partial x\} = [H] \tag{D.2.4}$$

where [H] is defined by eqn. (D.1.6)

Note that in problems where {F} is assumed to be independent of the design variables (as in the element level optimization) eqn. (D.2.4) reduces to

$$[K]\{\partial\delta/\partial x_i\} = -[\partial K/\partial x_i]\{\delta\} \qquad i = 1, \ldots, n$$

or

$$\{\partial\delta/\partial x_i\} = -[K]^{-1}[\partial K/\partial x_i]\{\delta\} \qquad (D.2.5)$$

Again assuming $g_j \equiv \delta_j$ then $\{\partial g_j/\partial x\} = \{0\}$ and $\{\partial g_j/\partial\delta\} = \{I_j\}$, so eqn. (D.2.3) becomes

$$\{\nabla\delta_j\}^T = \{I_j\}[\partial\delta/\partial x] \qquad (D.2.6)$$

The derivative vector $\{\nabla\delta_j\}^T$ of the displacement constraints is evaluated using eqn. (D.2.4) (to solve for the set of $\{\partial\delta/\partial x_i\}$) and eqn. (D.2.6).

D.3 Virtual Load Method

In this approach it is also assumed that the $\{\delta\}$ are the dependent variables which can be expressed in terms of the independent design variables $\{x\}$. The equations (D.2.1) - (D.2.3) of the design space approach therefore hold for the virtual load method.

Any desired displacement δ_j can be expressed as

$$\delta_j = \{Q_j\}^T\{\delta\} \qquad (D.3.1)$$

where $\{Q_j\}^T$ is a virtual load vector which has a unit value in the j-th location and zeroes elsewhere. Differentiating eqn. (D.3.1) with respect to $\{x\}$ gives

$$\{\partial\delta_j/\partial x\}^T = \{\nabla\delta_j\}^T = \{Q_j\}^T[\partial\delta/\partial x] \qquad (D.3.2)$$

The virtual displacement vector $\{\delta_j^Q\}$ corresponding to the virtual load vector $\{Q_j\}$ is evaluated by

$$[K]\{\delta_j^Q\} = \{Q_j\} \qquad (D.3.3)$$

which can be sustituted into eqn. (D.3.2) giving

$$\{\nabla\delta_j\}^T = \{\delta_j^Q\}^T [K][\partial\delta/\partial x] \qquad (D.3.4)$$

Now using the expression derived for $\{\partial\delta/\partial x\}$ in the design space method (eqn. (D.2.4)), eqn. (D.3.4) can be written as

$$\{\nabla\delta_j\}^T = \{\delta_j^Q\}[H] \qquad (D.3.5)$$

where [H] is defined in eqn. (D.1.6).

The derivative vector $\{\nabla\delta_j\}$ is then evaluated using eqns. (D.3.3) (to solve for $\{\delta_j^Q\}$) and (D.3.5)

D.4 Comparison of the Methods

These three different approaches to design sensitivity analysis have been analysed and shown to give the same results (Ref. [40]). There are, however, differences to be found in the generality and efficiency of the individual methods. The behaviour space and design space methods are more general than the virtual load approach and can be extended to include other behaviour constraints which may not be readily expressed in terms of the displacement vector.

The relative efficiency of the methods is dependent on the number of constraints under consideration. The behaviour space and virtual load methods require the same number of operations for a given number of active constraints J. The behaviour space method requires the calculation of J adjoint variables $\{\phi_j\}$ (eqn. (D.1.4)), while the virtual load method requires the evaluation of J virtual displacement vectors $\{\delta_j^Q\}$ (eqn. (D.3.3)). This is followed by the solution of eqn. (D.1.11), and eqn. (D.3.5) respectively. In the design space method, the number of vectors $\{\partial\delta/\partial x_i\}$ (from eqn. (D.2.4)) that must be determined is $n \times N_p$, where n is the number of design variables x_i and N_p is the number of loading conditions. This is followed in turn by the solution of eqn. (D.2.6).

Since very similar computational effort is involved in solving eqns. (D.1.11), (D.2.6) and (D.3.5) the final choice of method depends on the relative values of J and nN_p. Thus if $J < nN_p$ the design space method is less efficient than the other two methods.

In many real design problems, however, stress constraints are also included and in these cases the number of active constraints often becomes large. The choice of method then becomes less obvious and indeed the differences in efficiency of the various methods in such a situation is probably insignificant in terms of the total computational effort required for the structural optimization task.

APPENDIX E

Implementation experience with derivative evaluation and scaling of variables

While developing programs LAMOPT and UPOPT (for descriptions see Appendices F and G respectively) certain problems were encountered with regard to the evaluation of the derivatives with respect to the lamina ply angles, the design space produced by linearization of the constraint functions and with the scaling of certain laminates. The reasons for these problems, the methods used to overcome them and their effectivness is described below.

E.1 Derivatives with respect to lamina ply angle

These derivatives are only evaluated in the element level optimization where the lamina ply angles are considered to be variables. The problem stems from the fact that the derivatives of the laminate rigidity matrix are zero when ply angles of 0° and 90° are considered. The buckling and strain constraints are functions of the laminate rigidity matrix and thus if the derivatives of the rigidity matrix are zero, then the constraint derivatives will also be zero (see sections 4.3 and 4.4). This in turn implies that the design variable coefficients in the linear programming (LP) problem are zero and so do not influence the LP solution.

This may well lead to an incorrect (non-optimal) solution since the lamina ply angle will not then be changed from it's 0° or 90° position to a nearer optimal orientation.

The solution to this was to evaluate the derivatives of the constraints assuming the ply angles to be at 1 or 89 , in place of the 0° or 90° respectively. Experience has shown this to be a very effective solution, which is very easy to implement. It provides a good approximate derivative value which is non-zero, thereby allowing the ply-angle to be changed when solving the LP problem, and so move to a solution nearer the optimum. If the optimal solution is actually 0° or 90° this result is returned by the LP solution even when the derivatives are evaluated assuming 1° and 89° ply orientations.

E.2 Infeasible designs and scaling of the variables

One of the problems of using a sequential linear programming method for solving non-linear problems is that the solutions generated are frequently infeasible i.e. they lie outside the true feasible region defined by the non-linear constraint boundaries. The extent to which the constraints are violated is largely dependent on the degree of non-linearity of the constraint functions and the size of the move limits applied.

There is no intrinsic reason why the design should not be allowed to progress from one infeasible (or nearly feasible) solution to another since the solutions should, after a number of iterations, tend to converge on the true (non-linear) optimum. The degree of infeasibility of the design is also tightly controlled in the later stages by the progressively decreasing move limits. Most standard LP solvers, such as the NAG routine H01BAF used in this work, will also find an initial design that lies in the feasible design region (defined by the linearized constraints), and hence it is expected that a sequential LP method would be quite satisfactory for this work.

The fact that the constraints are linearized about an infeasible (or nearly feasible) point, however, proved to be the source of a problem encountered in applying the sequential LP algorithm. The combination of an infeasible starting point and highly non-linear constraints (especially the buckling constraints) resulted, in numerous cases, in a design space (with the linearized functions) with no feasible region at all. The problem encountered is graphically illustrated below in Figures E.2.1 and E.2.2 which show respectively a design space with a feasible region and one without a feasible region.

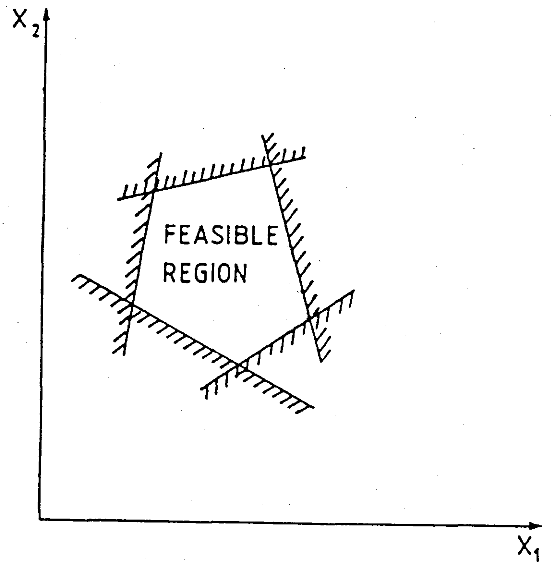

Figure E.2.1 Feasible design region

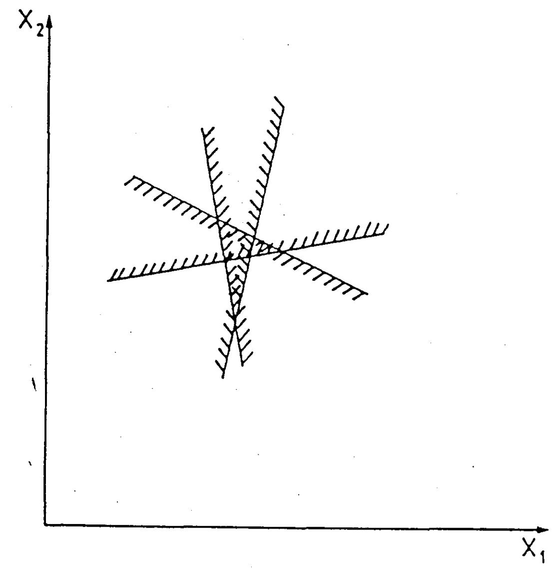

Figure E.2.2 No feasible design region

It was found that the easiest and most efficient way of avoiding this problem was by scaling the design into the (non-linear) feasible region, if the design produced by the the previous LP was infeasible. This new feasible solution was then used as the linearization point for the constraints and objective function for the next iteration.

Traditionally, for isotropic structures, a scaling parameter λ is caluclated from the violated constraints by

$$\lambda = \delta_{np}/\delta_{np}^{b} \qquad \text{for displacement constraints} \qquad (E.2.1)$$

or

$$\lambda = \varepsilon_i/\varepsilon_i^{b} \qquad \text{for strain constraints} \qquad (E.2.2)$$

where

b (superscript) indicates the constraint limit value

δ_{np} is the displacement of node n in the direction p

ε_i is the strain in element i

The value λ is thus the ratio of the actual value and the constraint limit value.

In the case of a displacement constraint being violated the entire set of variables (typically plate thicknesses) is scaled by this parameter such that

$$\{x'\} = \lambda\{x\} \tag{E.2.3}$$

where the superscript ′ denotes the scaled variable values. It can be easily shown (Ref. [34]) that this leads to

$$\delta_{np}' = \lambda\,\delta_{np} \tag{E.2.4}$$

if the structure stiffness matrix is a linear function of $\{x\}$.

Similarly, strain constraint violations can be satisfied in the same manner ($\{x'\} = \lambda\{x\}$) to give

$$\varepsilon_i' = \lambda\,\varepsilon_i \tag{E.2.5}$$

The actual design variable values that will ensure that all the constraints are satisfied can thus be calculated by eqn. (E.2.3), where λ is determined for the most severely violated constraint.

This simple scaling procedure can only be used effectively when the structure stiffness matrix is a linear function of the design variables. In the case of composites the stiffness matrix is not a linear function of the design variables and hence procedures other than those described above are required. The method used in this work is different for each type of constraint. In order to satisfy any violated displacement constraints an iterative version of the method described above has been adopted. The eqns. (E.2.1) and (E.2.3) are used to scale the design if any constraints are violated, after which it is reanalysed and the constraints re-evaluated. If any constraints are still violated this operation is performed again and these iterations are continued until a feasible design, with respect to the displacement constraints, is found.

When all the displacement constraints are satisfied the strains are evaluated. The strength criteria used (see section 3.2) requires that the longituduinal, transverse and shear strains of each layer individually be kept within the prescribed limits. Using the method above the entire structure would thus be scaled to satisfy any violated strain constraint in any single layer of a single laminate type. The process may require a few iterations before the constraint is satisfied (as for the displacement constraints) and may in this way lead to a grossly overdesigned structure in areas where the strain constraints were not active. The approach adopted was thus to scale only the layers in the laminate type in which the constraint was violated. It may be argued that this changes the stiffness of only those elements which are of that laminate type, and thereby changes the stiffness distribution and resultant load paths in the structure. This may lead to relative changes in the displacement field, hence requiring a reanalysis and re-evaluation of the constraint values. While this is undoubtedly true, experience has shown that due to the move limits imposed on the LP solution (see section 4.5), the constraints are never violated in any gross manner and thus the resultant scaling factors are relatively small. The change in element stiffness is therefore relatively small and so the load paths are not disturbed significantly. Should any problem arise where the structure stiffness distribution is substantially altered by the scaling operation, the problem can be re-run using tighter move limits in the LP problem, and thereby limit the degree of violation of the constraint(s) and the associated scaling factor(s).

This same logic may be used to argue in favour of scaling only the layer in which the strain constraint is violated. This approach was tried but found to be very inefficient as very many iterations were required, in certain cases, to satisfy the constraint. The number of iterations required is dependent on the relative angle between the lamina fibres under consideration and the load on that laminate. This can be illustrated using a flat plate made of a $0^\circ, \pm 45^\circ$ laminate which is loaded in plane along the 0° (or x) axis (F_X). The critical strains in the layers for this loading case will be the longitudinal strain (ε_L) for the 0° layer and the shear strain (ε_{LT}) for the $\pm 45^\circ$ layers. These strains can be directly related to the magnitude of the plate strain $\mathcal{E}_x$ induced by F_x i.e. in order to reduce any of the layer strains the plate strain $\mathcal{E}_x$ must be reduced. To achieve this the in-plane rigidity of the plate in the x-direction must be increased. This rigidity (see Appendix A) is a linear function of the 0° layer thickness and hence if the strain constraint in this layer is violated only one scaling operation (using eqn. (E.2.5)) is required to get the design feasible again. The rigidity of the plate in the x-direction is, however, non-linearly related to the thickness of the $\pm 45^\circ$ layers and hence numerous iterations of the scaling opertions are required to satisfy the constraints. This also leads to an unnecessary gross scaling up of the 45° layers when in fact it would have been more efficient to scale up the 0° layer by a substantially lesser factor.

The most efficient solution has therefore been found to be the scaling of all layers in the laminate by the ratio λ. Ideally only the layers having the most effect on the violated constraint should be scaled, but this is a rather complex operation to program and is probably not worth the computational effort involved. The scaling of all the layers in the laminate concerned has proved to be an efficient and reliable method which very seldom requires more than one iteration.

In the case of violated buckling constraints the scaling factor λ is evaluated as

$$\lambda = F_x/(F_x)_{crit} + F_y/(F_y)_{crit} + (F_{xy}/(F_{xy})_{crit})^2 \qquad (E.2.6)$$

All the layers in the applicable laminate are then scaled by this factor. Since this is in principle exactly the same opertion as that for the violated strain constraints all the discussion above is applicable in this case. The only difference is that the buckling constraint is a non-linear function of all the design variables (since it is dependent on the laminate bending stiffness which is proportional to t^3 - see Appendix A) and may therefore require a number of iterations of the scaling procedure to obtain a feasible design. The actual number of iterations is highly dependent on the type of loading and lamina orientations and stacking sequence (since bending stiffness is proportional to z^2 - see Appendix A) in the laminate under consideration.

Finally, it is worth noting that although it might be preferable in the interests of efficiency and speed of convergence etc. to use an optimization routine that is able to use infeasible designs as a starting point, it is usually very useful for the designer (i.e. program user) to have interim solutions which are feasible as well. With this information any of the designs along the way can be used if judged to be more suitable than the final "optimum" solution.

APPENDIX F

Description of program LAMOPT developed for the element level optimization.

Program LAMOPT described below is intended primarily for use in the element level optimization part of the multilevel scheme. It is, however, structured in such a way that it could be used as a stand alone program, with a substantial analysis and design capability of its own, in terms of laminated composite panels.

The program has numerous analysis and design options available which are readily selected by setting the three flags at the begining of the data deck. These options, shown in the program flowchart in Figure F.1, are listed below:-

1. Laminate rigidity evaluation only.
2. Lamina strain analyses for any given panel loads (a panel buckling analysis may also be done).
3. Laminate rigidities evaluated and used in the input for a finite element analysis of larger structures made up of various laminates.
4. Same as 3 but followed by a lamina strain analysis and/or buckling analysis for each element.
5. Laminated composite panel optimization.
6. Optimization of all laminate types in a structure modelled by finite elements.

7. Laminate optimization as part of the multi-level optimization scheme.

Program LAMOPT is completely general in that any number of laminates, of any type of construction (with regard to material types, layer thicknesses and orientations, symmetry (or lack of it) and stacking sequence) can be used simultaneously in any of the options listed above. The only limitation in this respect is that the laminate construction and proportions must be such that its behaviour under load is still realistically represented by classical lamination theory (see Appendix A) i.e. it must behave as a membrane, plate or thin shell, otherwise inaccuracies in the resultant strains (stresses) may become significant.

If any of the optimization options are invoked then any, or all, of the following constraints can be applied:-

1. Lamina strain limits
2. Lamina thickness and ply angle bounds
3. Prevention of panel buckling of the laminate

Futhermore, symmetry of the layers about the laminate midplane may also be enforced. The constraint options selected apply to all the laminates under consideration, but the actual limits prescribed can be different for each lamina of each laminate if required. The mathematical formulation of these constraints can be found in section 3.2.

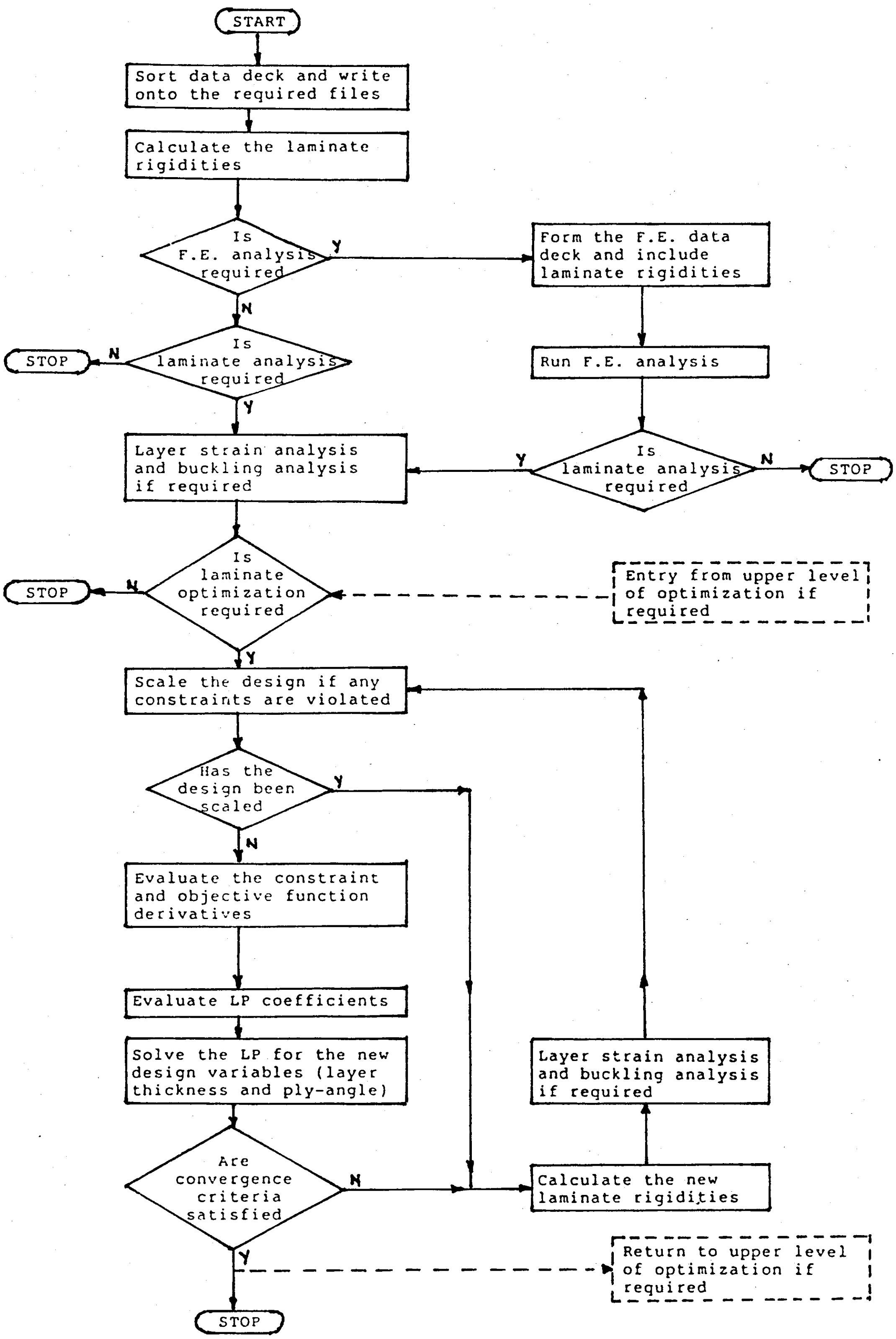

Figure F.1 Program LAMOPT flowchart

A futher "constraint" that can be used in the optimization modes, is the enforcing of a compromise between the minimization of the element/panel weight and minimization of the change of the overall element/panel stiffness (see section 3.1). This is achieved by assigning weighting factors to the two objectives which reflect their relative importance. Although this feature was intended primarily for use in the mutlilevel optimization scheme it could be useful in a few other design cases where it is desirable to keep some control over the stiffness change of the laminate while optimizing it.

An optimum design is achieved in LAMOPT, within the bounds of the constraints, using the individual layer thicknesses and ply orientations as the design variables. If any (or all) of the layer thicknesses or ply angles need to be kept fixed, this can be done by setting both the upper and lower gauge, or ply angle, limits to the same, desired value i.e. effectively making it an equality constraint.

Finally, in the development of LAMOPT, it was decided not to write a new routine for the optimization work but rather to use the existing NAG library routine H01BAF, which is a robust, well proven LP solver.

APPENDIX G

Description of program UPOPT developed for the system level optimization.

Program UPOPT was developed in a similar manner to LAMOPT (see Appendix F) so that it can be used as a stand alone analysis and design system for composite structures, while also fulfilling its role as the upper level optimization part of the multilevel optimization scheme.

The various design and analysis options are shown in the program flowchart in Figure G.1 and also listed below:-

1. Evaluate laminate rigidities only
2. Laminate rigidities evaluated and used in the input for a finite element analysis
3. As for 2 but followed by lamina strain analysis and/or buckling analysis for each element.
4. Laminated composite structure optimization (keeping the ply angles fixed)
5. Laminated composite structure optimization as part of the multilevel optimization scheme.

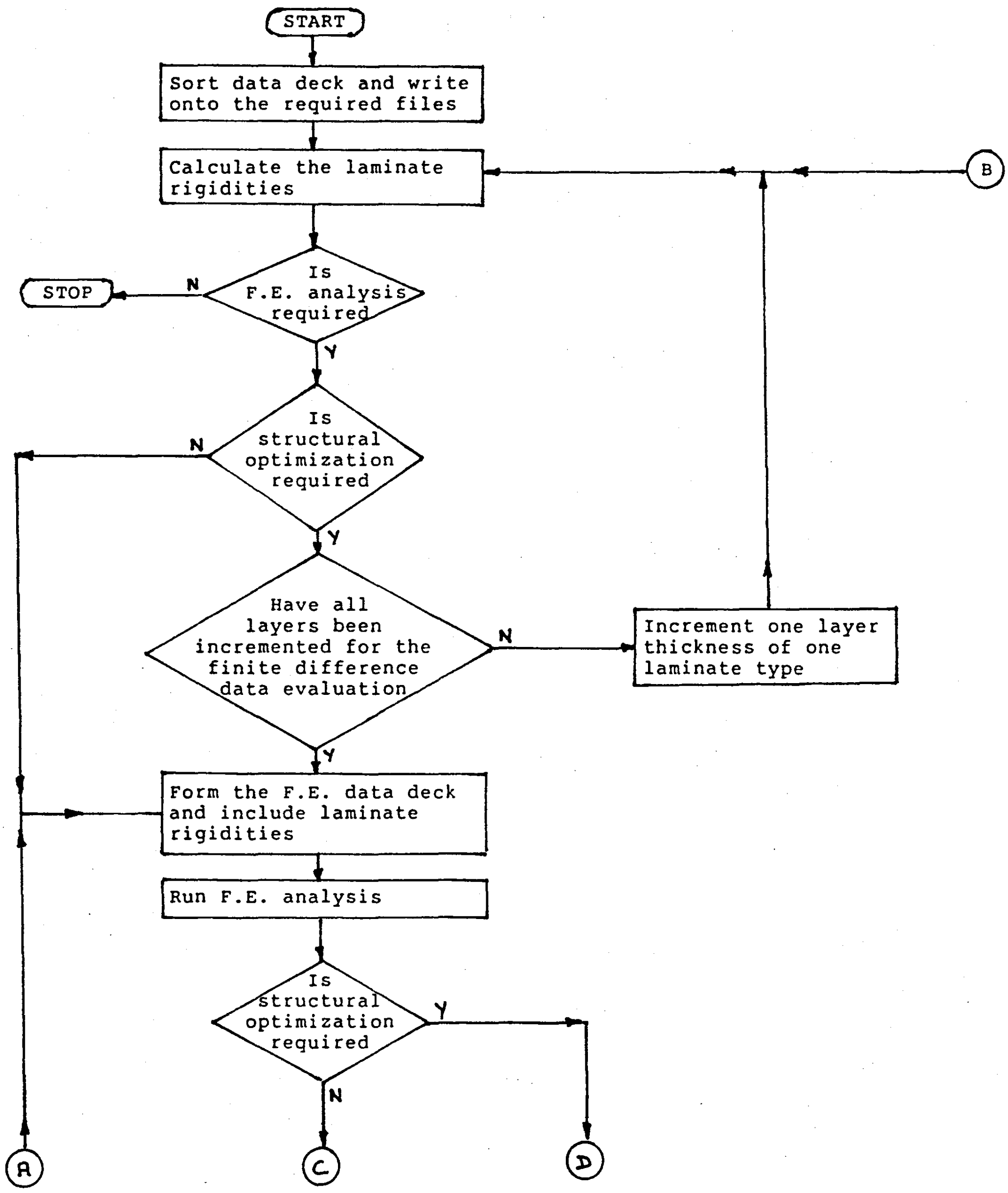

Figure G.1 Program UPOPT flowchart

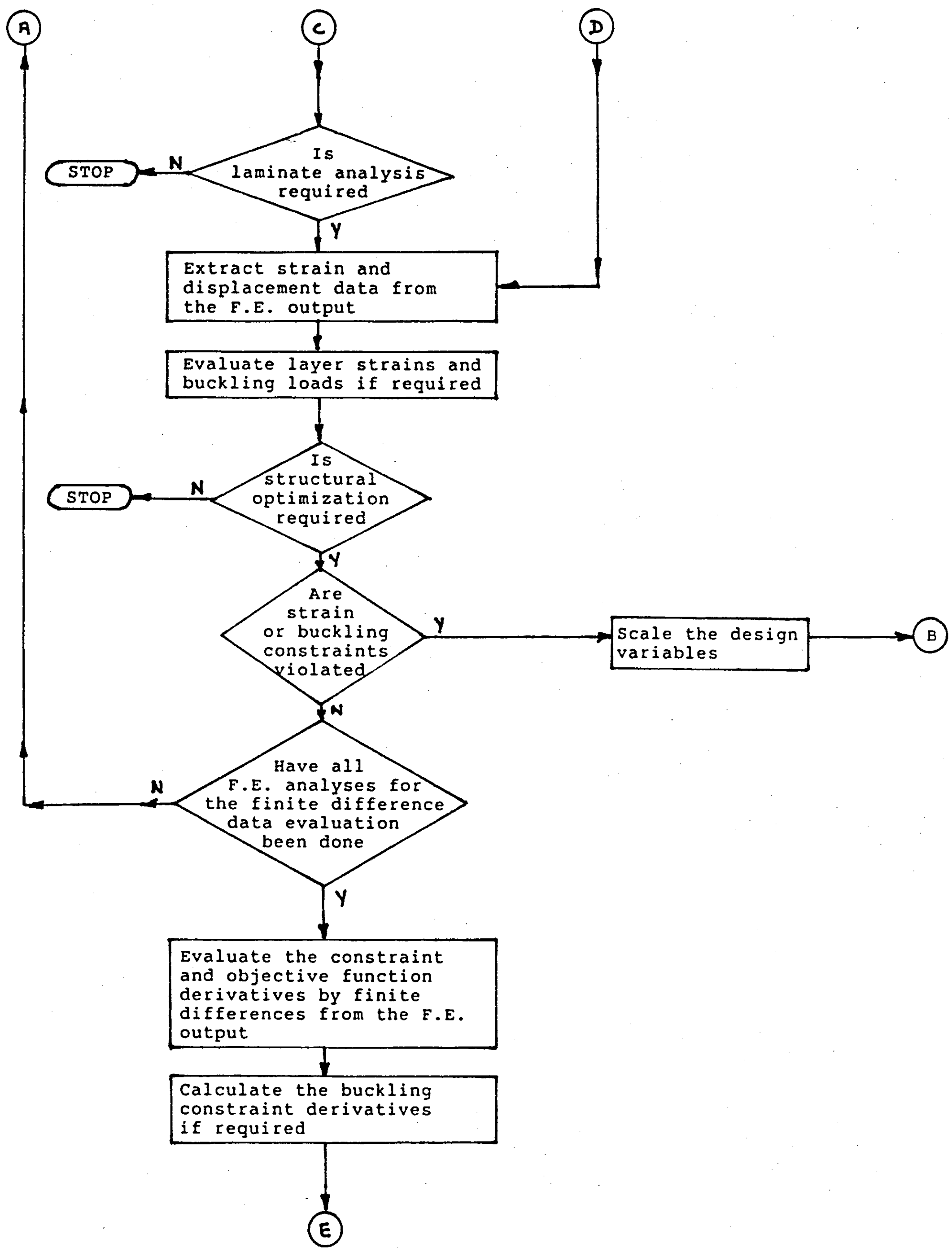

Figure G.1 Program UPOPT flowchart (cont.)

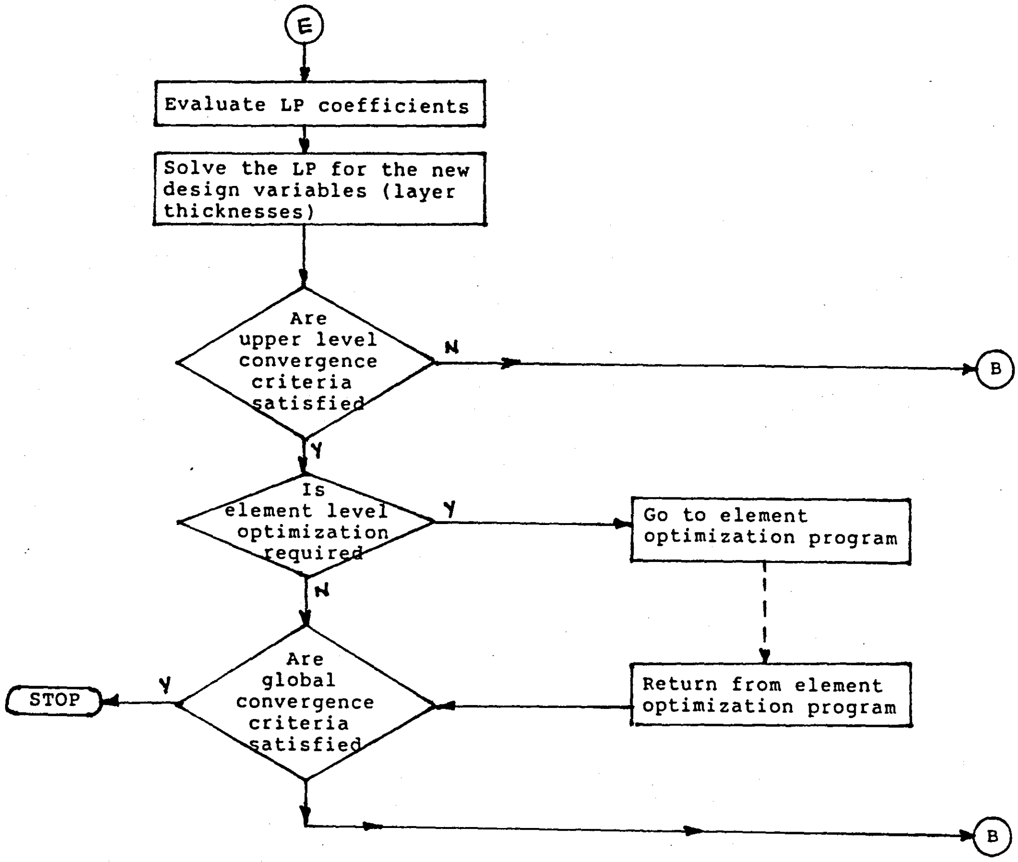

Figure G.1 Program UPOPT flowchart (cont.)

Program UPOPT is completely general, in the same sense as LAMOPT. In any of the options listed above any number of laminates, of any type of construction (with regard to material types, layer thicknesses and orientations, symmetry (or lack of it) and stacking sequence) can be used simultaneously. Again the only limitation in this respect is that the laminate construction and proportions must be such that its behaviour under load is still realistically represented by classical lamination theory (see Appendix A) i.e. it must behave as a membrane, plate or thin shell, otherwise inaccuracies in the resultant strains (stresses) may become significant.

If any of the optimization options are invoked then any, or all, of the following constraints can be applied:-

1. Lamina strain limits
2. Lamina thickness bounds
3. Prevention of panel buckling
4. Nodal displacement limits
5. Twist limits (displacement of two nodes relative to each other)

Futhermore, symmetry of the layers about the laminate midplane may also be enforced. The constraint options selected apply to all the laminates under consideration, but the actual limits prescribed can be different for each lamina of each laminate if required. The mathematical formulation of these constraints can be found in section

6.2.

The lamina thicknesses of the various laminate types are used as the variables in UPOPT (and not ply angles as well as in LAMOPT), to minimize the total weight of the structure while ensuring that all the constraints are satisfied. The NAG library routine H01BAF is also used in UPOPT as the LP solver for the same reasons as given in Appendix F, where program LAMOPT described.